Intracellular self-activation of the TrkB kinase domain causes FAK phosphorylation and disrupts actin filopodia dynamics

Intrazelluläre Selbst-aktivierung der TrkB Kinase induziert FAK Phosphorylierung und verändert die Dynamik von Aktinfilopodien

Doctoral Thesis

for the conferral of the degree

Doctor rerum naturalium (Dr. rer. nat.)

at the Graduate School of Life Sciences,

Julius-Maximilians-Universität Würzburg, Germany

Neuroscience Section

Submitted by

Rohini Gupta

born in Pune, India on 1st September 1990

Würzburg, November 2020

Submitted on:

………………………………………………..……..

Office stamp

Members of the *Promotionskomitee*:

Chairperson: Prof. Dr. Keram Pfeiffer

Primary Supervisor: PD Dr. Robert Blum

Supervisor (Second): Prof. Dr. Svenja Meierjohann

Supervisor (Third): PD Dr. Kurt Bommert

Date of Public Defence: …………………………………………..…………

Date of Receipt of Certificates:………………………………………………..

To my friends & family,

both old & new.

Table of Contents

Abstract

The tropomysin receptor kinase B (TrkB), the receptor for the neurotrophin brain-derived neurotrophic factor (BDNF), plays an important role in neuronal survival, neuronal differentiation, and cellular plasticity. Conventionally, TrkB activation is induced by binding of BDNF at extracellular sites and subsequent dimerization of receptor monomers. Classical Trk signaling concepts have failed to explain ligand-independent signaling of intracellular TrkB or oncogenic *NTRK*-fusion proteins. The intracellular activation domain of TrkB consists of a tyrosine kinase core, with three tyrosine (Y) residues at positions 701, 705 and 706, that catalyzes the phosphorylation reaction between ATPγ and tyrosine. The release of *cis*-autoinhibition of the kinase domain activates the kinase domain and tyrosine residues outside of the catalytic domain become phosphorylated. The aim of this study was to find out how ligand-independent activation of TrkB is brought about. With the help of phosphorylation mutants of TrkB, it has been found that a high, local abundance of the receptor is sufficient to activate TrkB in a ligand-independent manner. This self-activation of TrkB was blocked when either the ATP-binding site or Y^{705} in the core domain was mutated. The vast majority of this self-active TrkB was found at intracellular locations and was preferentially seen in roundish cells, lacking filopodia. Live cell imaging of actin dynamics showed that self-active TrkB changed the cellular morphology by reducing actin filopodia formation. Signaling cascade analysis confirmed that self-active TrkB is a powerful activator of focal adhesion kinase (FAK). This might be the reason why self-active TrkB is able to disrupt actin filopodia formation. The signaling axis from Y^{705} to FAK could be mimicked by expression of the soluble, cytosolic TrkB kinase domain. However, the signaling pathway was inactive, when the TrkB kinase domain was targeted to the plasmamembrane with the help of artificial myristoylation membrane anchors. A cancer-related intracellular *NTRK2*-fusion protein (SQSTM1-NTRK2) also underwent constitutive kinase activation. In glioblastoma-like U87MG cells, self-active TrkB kinase reduced cell migration. These constitutive signaling pathways could be fully blocked within minutes by clinically approved, anti-tumorigenic Trk inhibitors. Moreover, this study found evidences for constitutively active, intracellular TrkB in tissue of human grade IV glioblastoma. In conclusion, the data provide an explanation and biological function for self-active, constitutive TrkB kinase domain signaling, in the absence of a ligand.

Zusammenfassung

Die Rezeptortyrosinkinase TrkB, der Rezeptor für das Neurotrophin *brain-derived neurotrophic factor* (BDNF), spielt eine wichtige Rolle für das neuronale Überleben, die neuronale Differenzierung und die zelluläre Plastizität. Üblicherweise wird TrkB bei der Bindung von BDNF an extrazellulären Domänen durch Dimerisierung von Rezeptormonomeren aktiviert. Klassische Konzepte der Trk Signalübertragung können jedoch die Liganden-unabhängige Signalübertragung von intrazellulären TrkB- oder Onkogen-aktiven *NTRK*-Fusionsproteinen nicht erklären. Die intrazelluläre Aktivierungsdomäne von TrkB besitzt eine Tyrosinkinasedomäne mit drei Tyrosin (Y)-Resten an den Positionen 701, 705 und 706. Diese katalysieren die Phosphorylierungsreaktion zwischen ATPγ und Tyrosin. Durch die Enthemmung der cis-Autoinhibition wird die Kinase-Domäne aktiv und Tyrosinreste außerhalb der katalytischen Domäne werden phosphoryliert. Ziel dieser Arbeit war herauszufinden, wie es zur Liganden-unabhängigen Aktivierung von TrkB kommen kann. Mit Hilfe von TrkB-Phosphorylierungsmutanten wurde gefunden, dass eine hohe, lokale Abundanz des Rezeptors ausreicht, um TrkB Liganden-unabhängig zu aktivieren. Diese Selbstaktivierung von TrkB konnte blockiert werden, wenn entweder die ATP-bindende Domäne oder Y^{705} in der Kinasedomäne mutiert wurden. Die überwiegende Mehrheit dieses selbstaktivierenden TrkB wurde intrazellulär, in rundlichen Zellen ohne Filopodien, gefunden. Live-Zellbildgebung der Aktindynamik zeigte zudem, dass selbstaktives TrkB die Zellmorphologie veränderte, indem es die Bildung von Aktin-Filopodien reduzierte. Die Analyse von Signalkaskaden bestätigte, dass selbstaktives TrkB ein starker Aktivator der *Focal Adhesion Kinase* (FAK) ist. Dies kann der Grund sein, warum selbstaktives TrkB die Bildung von Aktin-Filopodien zerstört. Die Signalkaskade von Y^{705} bis FAK konnte durch Expression der löslichen, zytosolischen TrkB-Kinase-Domäne imitiert werden. Der Signalweg war jedoch inaktiv, wenn die TrkB-Kinase-Domäne durch künstliche Myristoylierung an die Plasmamembran gebunden wurde. Ein intrazelluläres *NTRK2*-Fusionsprotein (SQSTM1-NTRK) zeigte ebenfalls konstitutive Kinaseaktivierung. In Glioblastom-ähnlichen U87MG-Zellen reduzierte die selbstaktive TrkB-Kinase sogar die Zellwanderung. Die konstitutiven Signalwege konnten durch klinisch zugelassene, anti-tumorale Trk-Inhibitoren innerhalb von Minuten vollständig blockiert werden. Darüber hinaus zeigt diese Studie Beweise für konstitutiv-aktives, intrazelluläres TrkB im Gewebe von humanem Glioblastom Grad IV. Die Daten dieser Arbeit geben somit eine Erklärung und eine biologische Funktion für die selbst-aktive, konstitutive Signalübertragung der TrkB-Kinase-Domäne, in Abwesenheit eines Liganden.

1 Introduction

Trk (tropomyosin receptor kinase) receptors belong to the protein family of membrane bound receptor tyrosine kinases (Barbacid, 1994; Klein *et al*, 1991a; Klein *et al*, 1989; Martin-Zanca *et al*, 1986). The three Trk receptors - TrkA, TrkB and TrkC are encoded by the neurotrophin tyrosine kinase receptor (*NTRK*) proto-oncogenes - *NTRK1*, *NTRK2* and *NTRK3* respectively (Barbacid, 1994; Klein *et al.*, 1991a). The Trk receptor was originally discovered as an oncogenic driver in a human colon carcinoma where it became activated by a chromosomal rearrangement thereby forming an *NTRK* gene fusion (Martin-Zanca *et al.*, 1986). All three Trk receptors or pathological *NTRK* gene fusions can act as oncogenic drivers of various adult and pediatric tumor types (Cocco *et al*, 2018). Gene fusions of *NTRK* genes, but also atypical activation of non-mutated Trk receptors, activate protumorigenic signal pathways (Huang & Reichardt, 2003). To treat Trk activity in cancer, membrane-permeable small molecule inhibitors have been developed that reduce or even block Trk kinase activity with high specificity (Cocco *et al.*, 2018). Trk kinase inhibitors such as Larotrectinib (Drilon *et al*, 2018) or Entrectinib (Doebele *et al*, 2020) have become modern pharmaceuticals for precision oncology. Larotrectinib has recently been approved for the treatment of adult and pediatric patients with solid tumors that have a *NTRK* gene fusion. The treatment of patients with *NTRK* fusion-positive cancers with Trk kinase inhibitors are associated with high response rates, regardless of tumor histology (Drilon *et al.*, 2018).

1.1 The Tropomyosin receptor kinase (Trk) family

1.1.1 Trk receptors

In their review, (Cocco *et al.*, 2018) have very nicely summarized a brief history of the discovery of the three Trks. *NTRK1* was first identified as an oncogene in 1982 by Mariano Barbacid and colleagues during gene transfer assays aimed at identifying genes with transforming abilities present in human tumor specimens (in this case, a colon cancer) (Martin-Zanca *et al.*, 1986; Pulciani *et al*, 1982). Specifically, the cDNA of the oncogene identified, contained sequences of a non-muscle tropomyosin fused to sequences of a putative receptor tyrosine kinase. In 1989, the same group isolated the cDNA of the *NTRK1* proto-oncogene and described the gene product, TrkA, as a protein of 790 amino acids with features characteristic of cell surface receptor tyrosine kinases (Martin-Zanca *et al*, 1989). In 1991, two independent groups provided compelling evidence that TrkA was expressed in the nervous system and became phosphorylated in response to stimulation with the neurotrophin nerve growth factor

(NGF), thus demonstrating the role of TrkA as a receptor for NGF (Kaplan *et al*, 1991; Klein *et al.*, 1991a). This discovery paved the way for the identification of TrkB and TrkC as members of the same family of receptors. These receptors are capable of binding with high affinity to the following ligands: NGF for TrkA, brain derived neurotrophic factor (BDNF) or neurotrophin 4 (NT-4) for TrkB and neurotrophin 3 (NT-3) for TrkC. Of note, although NT-3 can bind with and activate all three Trk proteins, it has higher affinity for TrkC than for TrkA and TrkB (Cocco *et al.*, 2018; Thoenen, 1995).

1.1.2 Trk activation mechanism

Trk receptors are single-span transmembrane proteins and are generally activated by their receptor-specific ligands, the neurotrophins (Levi-Montalcini, 1987; Levi-Montalcini *et al*, 1954; Thoenen, 1995) (Figure 1). Neurotrophins are protein dimers of about 27 kDa and are high-affinity, soluble Trk ligands (Chao & Ip, 2010; Levi-Montalcini, 1987; Levi-Montalcini *et al.*, 1954). Binding of neurotrophins to the extracellular ligand-binding domain of Trk receptors induces receptor dimerization and a conformational change to enable the release of *cis*-auto-inhibition of the intracellular kinase activity and subsequent *trans*-auto-phosphorylation (Chao, 2003; Huang & Reichardt, 2003) . In TrkA, the transmembrane domain and the juxtamembrane regions carry specific molecular determinants for forming a specific dimer interface structure that is essential for neurotrophin-dependent Trk dimerization and kinase activation. Auto-phosphorylation of Trk recruits a wide variety of cancer-related signaling pathways (Chao, 2003). For instance, the Shc adaptor protein links kinase-active TrkB at a specific tyrosine phosphorylation site to the Pi3K/Akt pathway. This phosphorylation site, often called the Shc site, also activates the small GTPase Ras and the protein kinase MAPK (called ERK) (Huang & Reichardt, 2003). Downstream of ERK and Pi3K/Akt, the MAP kinase-interacting kinases (MNK) and mTOR-signaling regulate protein translation. Phosphorylation of a tyrosine residue at the carboxy-terminal end of TrkB is the adapter site for PLCγ, thereby linking kinase-active Trk to calcium signaling (Huang & Reichardt, 2001). Figure 1 here, highlights some of the important amino acid residues and downstream signaling pathways for TrkB.
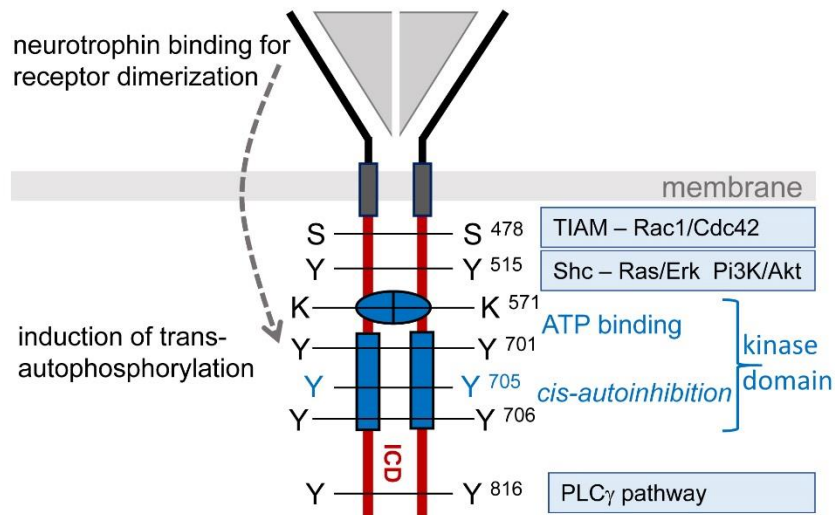
Figure 1. Model depicting TrkB-kinase signaling.

Neurotrophin (BDNF / NT-4) binding induces conformational changes and supports receptor dimerization. The kinase releases from cis-autoinhibition, ATP binds to the intracellular kinase domain and allows trans-autophosphorylation. Three tyrosine in the consensus motif YxxxYY residues, Y^{701}, Y^{705} and Y^{706} are phosphorylated in the activation loop of the receptor. ATP-binding and phosphorylation of the YxxxYY motif are upstream of further autophosphorylation and downstream signaling. In the intracellular domain (ICD), phosphorylation of the Y^{515} recruits Shc and activates the Ras/ERK and Pi3K-Akt pathways. Y^{816} forms the adaptor site for PLCγ. S^{478} signals to the TIAM-Rac1 pathway. Image source: article on bio archives - biorxiv (Gupta *et al*, 2020).

All receptor tyrosine kinases (RTKs) have a similar molecular architecture, with ligand binding domains in the extracellular region, a single transmembrane helix, and a cytoplasmic region that contains the protein tyrosine kinase (TK) domain plus additional carboxy (C-) terminal and juxtamembrane regulatory regions (Lemmon & Schlessinger, 2010). The overall topology of RTKs, their mechanism of activation, and key components of the intracellular signaling pathways that they trigger, are highly conserved in evolution from the nematode *Caenorhabditis elegans* to humans, which is also consistent with the key regulatory roles that they play (Lemmon & Schlessinger, 2010).

The Trk family receptors are initially synthesized as precursor proteins; the post-translational glycosylation of the extracellular domains of these precursors yields the mature protein products TrkA (140 kDa), TrkB (145 kDa) and TrkC (145 kDa) (Chao, 2003). All Trk proteins share similar structural domains in the extracellular region, including two immunoglobulin- like (Ig1 and Ig2) and three leucine- rich 24-residue motifs (LRR1–3). The LRR1–3 motifs, flanked by two cysteine clusters (C1 and C2), are specific to Trk proteins, and are not found in other

subfamilies of receptor tyrosine kinases (Lemmon & Schlessinger, 2010). Trk proteins interact with their cognate ligands predominantly via the Ig2 domain that is proximal to the transmembrane region, although other extracellular domains of Trk are known to be involved in neurotrophin binding (Lemmon & Schlessinger, 2010; Ultsch *et al*, 1999; Wehrman *et al*, 2007; Wiesmann *et al*, 1999).

A structure of the insulin receptor tyrosine kinase domain (TKD) was the first to illustrate RTK auto-inhibition (Hubbard, 2004; Hubbard *et al*, 1994) and this model was often used to explain how other homologous RTKs, such as Trk receptors, become active after ligand binding. A key tyrosine (Y^{1162}) in the activation loop of the insulin receptor TKD projects into the active site as if poised to be auto-phosphorylated by its own kinase domain (i.e., in *cis*) (Hubbard, 2004). This interaction stabilizes an activation loop configuration that occludes the active site, blocking access of both ATP and protein substrates. Thus, the insulin receptor TKD is auto-inhibited in *cis* by its own activation loop. When insulin activates the receptor, Y^{1162} in one TKD within the dimer, becomes phosphorylated by its partner (together with two additional tyrosines), and this *trans*-phosphorylation disrupts the *cis*-auto-inhibitory interactions. The phosphorylated activation loop of the insulin receptor TKD is then free to adopt the "active" configuration seen in all other activated TKDs (Lemmon & Schlessinger, 2010).

As previously stated, members of the RTK family have an extracellular ligand binding domain, a transmembrane domain, and an intracellular tyrosine kinase domain. The intracellular kinase domain is particularly well conserved in the RTK family (Hanks *et al*, 1988). TrkB autophosphorylation has been suggested to be a sequential cis/trans phosphorylation − a *cis* release from autoinhibition (the *cis* component is within the kinase domain) as an initial key step, followed by a *trans*-phosphorylation step which is dependent on the concentration of the intracellular TrkB kinase domain - TrkB-ICD (Iwasaki *et al*, 1997). In another study, the crystal structure of TrkA revealed a close resemblance to insulin receptor kinase (IRK) in its mode of autoinhibition (and presumably activation), relying only on occlusion of the substrate and ATP-binding sites by the activation loop (Artim *et al*, 2012; Su *et al*, 2017). Thus, since TrkB belongs to the same family of Trks, we can use similar deductions for its structure.

1.1.3 Trans-activation in absence of a ligand

Many studies have shown that TrkB can execute auto-phosphorylation activity and downstream signaling without stimulation by the ligand BDNF (Lee & Chao, 2001; Sasi *et al*, 2017). Activation of TrkB receptors in the absence of neurotrophins was shown to be mediated by

ligand activation of the G-protein-coupled adenosine 2A receptor (A2A-R) or the dopamine D1 receptor (Iwakura *et al*, 2008; Wiese *et al*, 2007) (Figure 2). G-protein-coupled receptors can trigger the trans-activation of TrkB in the range of tens of minutes to hours (Rajagopal *et al*, 2004). This effect is mediated by Src family of protein tyrosine kinases (SFKs) like Fyn (Rajagopal & Chao, 2006).

TrkB activation in the absence of neurotrophins can occur at intracellular sites, which includes calcium-dependent steps, and regulates the cell surface abundance of TrkB (Iwakura *et al.*, 2008; Puehringer *et al*, 2013). Puehringer *et al* in 2013 showed that during development of the cortex, intracellular TrkB and TrkC could be activated by a Src kinase-dependent pathway induced by EGF binding to the EGF receptor. This effect regulates the migration of newborn cortical neurons in the range of minutes. (Puehringer *et al.*, 2013). In hippocampal neurons, TrkB can be transactivated by zinc ions, which signal through C-terminal Src kinase (CSK) (Huang *et al*, 2008; Nagappan *et al*, 2008).
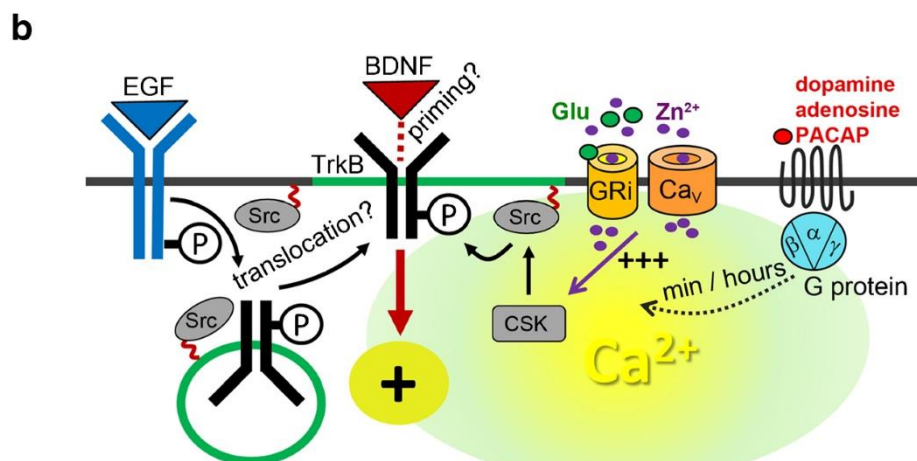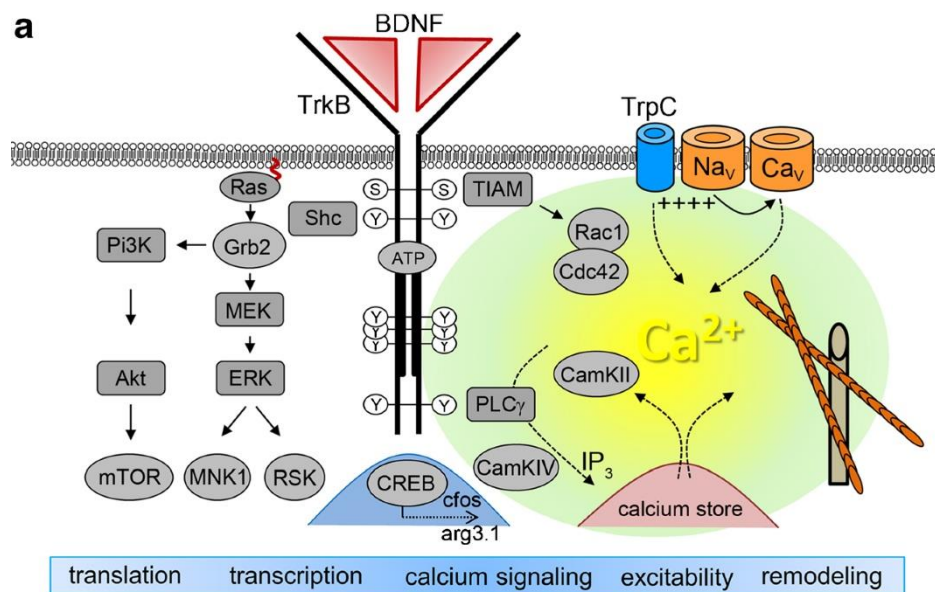
Figure 2. Model depicting the various known mechanisms that activate TrkB.

a Overview of BDNF/TrkB signaling in neuronal differentiation and synaptic plasticity.

b Activation of TrkB in the absence of neurotrophins. Details are given in the main text. Abbreviations: Akt (protein kinase B), arg3.1: activity-regulated gene 3.1 protein homolog (Arc), BDNF: brain-derived neurotrophic factor, CamK: Ca^{2+}/calmodulin-dependent protein kinase, Ca_V: voltage-gated calcium channel, Cdc42: GTPase cell division control protein 42, cfos: transcription factor cFos, CREB: transcription factor cAMP response element-binding protein, CSK: C-terminal Src kinase, ERK: extracellular signal regulated kinase, Grb2: growth factor receptor bound protein 2, GRi: ionotropic glutamate receptors, IP_3: inositol 1,4,5-trisphosphate, MEK: mitogen-activated protein kinase kinase, MNK: mitogen-activated protein kinase-interacting kinase, mTOR: mechanistic target of rapamycin, Na_V: voltage-gated sodium channel, PACAP: pituitary adenylate cyclase-activating peptide, Pi3K: phosphatidylinositol 3-kinase, PLC: phospholipase C, Rac GTPase: Ras-related C3 botulinum toxin substrate, Ras: GTPase rat sarcoma, RSK: ribosomal S6 kinase, Shc: Src homologous and collagen-like protein, Src: Src family of protein tyrosine kinases (SFKs, e.g., Fyn), TIAM: T cell lymphoma invasion and metastasis-inducing protein, TrkB: tropomyosin-receptor-kinase B, TrpC: canonical transient receptor potential channel, Zn^{2+}: zinc ions (Sasi *et al.*, 2017).

Before comprehending how other factors transactivate TrkB, more research is needed to understand better the structural basis of auto-transactivation between TrkB dimers (Sasi *et al.*, 2017). On a molecular level, additional structural data are needed to explain how TrkB undergoes intermolecular trans-activation and activation in the absence of a ligand. There is a wide gap in knowledge of how BDNF and TrkB are transported and localized within cells. Detailed studies are required on how TrkB cycles between the cell surface and intra-synaptic membranes to further understand the role of this receptor in the neurobiological context and eventually in the cancer paradigm.

1.2 Trk activation in cancer

Trk proteins can potentially be activated by a variety of mechanisms. Abnormal RTK activation in human cancers is mediated by four principal mechanisms: gain-of-function mutations, genomic amplification, chromosomal rearrangements, and / or autocrine activation (Du & Lovly, 2018). Somatic *NTRK* mutations have been identified in various tumor types, including colorectal cancer, lung cancers (large- cell neuroendocrine carcinoma and in NSCLC) as well as melanoma, and acute myeloid leukaemia (Cocco *et al.*, 2018). TrkA and TrkC overexpression is strongly predictive of favorable outcomes, while TrkB is mainly expressed in higher grade tumors that also harbor *MYCN* amplification (Nakagawara *et al*, 1994). One group showed that unfavorable neuroblastoma (NB) express full-length TrkB, but express little or no TrkA or TrkC, producing an autocrine loop of TrkB/BDNF, leading to cell survival,

proliferation and metastases (Yamashiro *et al*, 1997). The link between poor prognosis in neuroblastoma and TrkB signaling may reflect its more stringent autoinhibition and ability to signal transiently whereas TrkA signaling remains sustained – promoting differentiation and more favorable outcome (Artim *et al*, 2020). Additionally, *NTRK2* mutations affecting TrkB have been reported at two different kinase domain sites ($T^{695}I$ and $D^{751}N$) in patients with colorectal cancer (Geiger *et al*, 2011). *NTRK2* also showed significant increases in gene expression in squamous cell carcinoma (SCC). TrkB inhibition suppressed tumor growth, invasiveness and sensitized SCC cells to tyrosine kinase EGFR inhibition (Gomez *et al*, 2018).
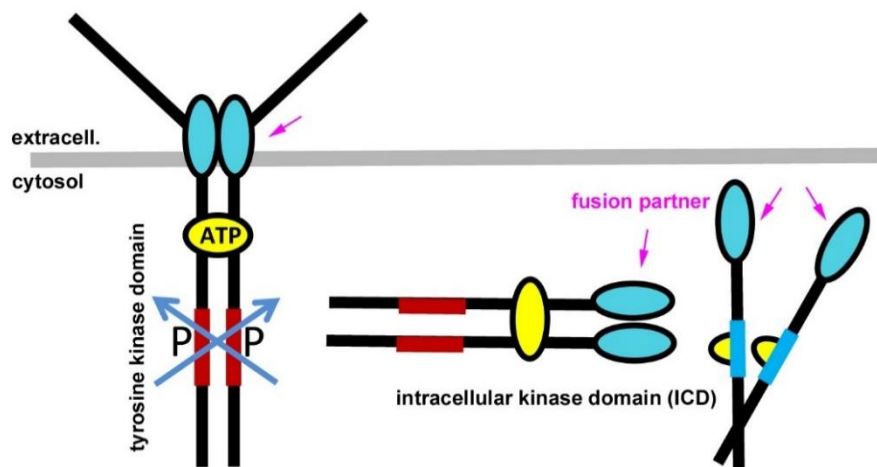
Figure 3. Model depicting oncogenic RTK fusion.

Chromosomal rearrangements result in the formation of a hybrid fusion oncoprotein consisting partly of the RTK and partly of the fusion partner, a distinct protein (shown in the figure by the cyan ovals and magenta arrows). These RTK fusion proteins can be membrane bound (left side of the figure) or cytoplasmic (right side of the figure) depending on the location of the genomic breakpoint. In either case, the result is an activated kinase domain. Figure inspiration is from (Du & Lovly, 2018)

In all reported Trk oncogenic gene fusions, the 3' region of the *NTRK* gene is joined with a 5' sequence of a fusion partner gene by an intra-chromosomal or inter-chromosomal rearrangement, and the oncogenic chimaera (Figure 3) is typically a constitutively activated or overexpressed kinase (Amatu *et al*, 2016). One study showed that, a change of proline 203 to alanine ($P^{203}A$), in the linker region between the leucine repeats and the first Ig-like domain, rendered TrkA capable of spontaneous dimerization and the receptor was found to be constitutively phosphorylated in the absence of NGF. Furthermore, expression of this TrkA-$P^{203}A$ receptor in fibroblasts induced DNA synthesis and transformation and generated tumors in nude mice (Arevalo *et al*, 2001). Intragenic partial duplication is a type of chromosomal

rearrangement that confers cancer cells the ability to acquire new protein isoforms. Kinase domain duplications (KDDs), constitute a type of intragenic partial duplication, resulting in a novel mechanism for RTK activation in tumor cells (Du & Lovly, 2018). RTK fusions (Figure 3) can regulate similar cell signaling pathways as the 'parental' RTK from which they are derived (including RAS/MAPK, PI-3K/AKT, and JAK2/STAT) and/or possibly even new pathways based on their altered cellular localization (Du & Lovly, 2018; Farago *et al*, 2015).

1.2.1 NTRK fusions as oncogenic drivers

Gene fusions of *NTRK1, 2* and *3* and their partner genes result in a constitutive activation or overexpression of Trk receptors, potentially leading to oncogenesis (Gatalica *et al*, 2019; Khotskaya *et al*, 2017). The *ETV6-NTRK3* fusion, seen in various cancers, leads to a constitutively active receptor and despite lacking the Shc binding site, activates the MAPK and P13K signaling pathways (Jin *et al*, 2007; Wai *et al*, 2000). This brings to light an important notion that although these fusions give rise to receptors that are structurally deficient in some regions, they can still function like their full-length counterparts in activating downstream signaling pathways. Another study showed that *BCAN-NTRK1* fusion caused by chromosomal rearrangement is a bona fide human glioma driver and highlights the importance of investigating such fusion causing chromosomal rearrangements that could promote tumorigenesis by interfering with gene regulatory elements such as enhancers or insulators, or affect gene expression by altering high-order chromatin structure (Cook *et al*, 2017)

The Trk kinase domain (TKD) is always included in the oncogenic fusion protein. By contrast, only some fusions harbor the transmembrane domain of the Trk protein, suggesting that this domain is not required for activation of the Trk kinase (Cocco *et al.*, 2018). Incorporation of the transmembrane domain might have an effect on cellular localization of the fusion protein, like targeting it to the plasma membrane (Cocco *et al.*, 2018). BCR-NTRK2 fusion was recently detected in low-grade gliomas with distinctive morphology and these tumors were shown to exhibit unexpected aggressive behavior (Jones *et al*, 2019). Some of the notable *NTRK2* fusion partners are – *TRIM24*, *PAN3*, *SQSTM1*, *TRAF2*, *STRN*, *QKI*, *ETV6*, *NACC2*, *BCR*, *TLE4*, *DAB2IP*, *VCL*, *AGBL4* and *AFAP1* (Cocco *et al.*, 2018)

Studies looking at the landscape of kinase fusions in cancer revealed *NTRK* gene fusion events in RNA-seq datasets that suggest protumorigenic, kinase-active fusion proteins lacking not only the extracellular-ligand-binding domain, but also the transmembrane and juxtamembrane domains (Cocco *et al.*, 2018; Stransky *et al*, 2014). Overexpression and genomic high-level

amplification of receptor tyrosine kinases has been observed in a variety of human cancers and correlate with poor outcomes for affected individuals. It is still not well understood how overexpressed Trk or corresponding *NTRK* kinase fusion proteins act in cells. That is to say, that the potential role of *NTRK* mutations in promoting tumorigenesis and cancer progression has not yet been fully established.

The product of these *NTRK* fusions are usually chimeric oncoproteins characterized by ligand-independent constitutive activation of the Trk kinase (Amatu *et al.*, 2016; Cocco *et al.*, 2018; Du & Lovly, 2018; Markl *et al*, 2019; Solomon *et al*, 2020; Vaishnavi *et al*, 2015). Newer advance methods of screening for *NTRK* fusions (like optimized immunohistochemistry-IHC, fluorescence in situ hybridization-FISH, reverse transcription polymerase chain reaction-RT-PCR, and DNA-based next-generation sequencing-NGS) are needed (Markl *et al.*, 2019; Solomon *et al*, 2019; Solomon & Hechtman, 2019; Solomon *et al.*, 2020). Moreover, finding evidence for these active fusions and their downstream signaling pathways is essential for finding better therapies.

1.3 Trk inhibition as therapy

NTRK fusions are found at high frequencies (up to or greater than 90%) in rare cancer types (secretory breast carcinoma, mammary analogue secretory carcinoma, cellular or mixed congenital mesoblastic nephroma and infantile fibrosarcoma) and at lower frequencies (commonly <1%) in a range of other tumor types (Cocco *et al.*, 2018). It has become evident that cancer cell resistance limits the effectiveness of target-based signal-transduction inhibitors as it has with conventional cytotoxic anticancer drugs. Therefore, developing mechanistically distinct inhibitors of the same targets or those targeting the receptors itself is essential.

1.3.1 Targeting the ERK pathway

Growth factors and mitogens use the Ras/Raf/MEK/ERK signaling cascade to transmit signals from their receptors to regulate gene expression and prevent apoptosis. Some components of these pathways are mutated or aberrantly expressed in human cancer. Gene fusion activating kinases represent an important class of oncogenes associated with both hematopoietic malignancies and solid tumors (Stransky *et al.*, 2014). They are produced by translocations or other chromosomal rearrangements, and their protein products often represent ideal targets for the development of cancer drugs. The Ras/Raf/MEK/ERK and Ras/PI3K/PTEN/Akt pathways interact with each other to regulate growth and in some cases tumorigenesis. Some of the

players in these pathways may interact with and affect those in another, for example, suppression of apoptotic factors in one pathway to promote cell survival in another (McCubrey *et al*, 2007).

Cancerous mutations in MAPK pathways are often mostly affecting Ras and B-Raf in the extracellular signal-regulated kinase pathway. Stress activated pathways, such as Jun N-terminal kinase and p38, largely seem to counteract malignant transformation. The balance and integration between these signals may widely vary in different tumors, but are important for the outcome and the sensitivity to drug therapy (Dhillon *et al*, 2007). The ERK pathway is the best studied of the mammalian MAPK pathways, and is deregulated in approximately, one-third of all human cancers. In the ERK MAPK module, ERK (ERK1 and ERK2) is activated upon phosphorylation by MEK (MEK1 and MEK2), which is itself activated when phosphorylated by Raf (Raf-1, B-Raf and A-Raf) (Roberts & Der, 2007). Most cancer-associated lesions that lead to constitutive activation of ERK signaling occur at these early steps of the pathway, namely, overexpression of receptor tyrosine kinases, activating mutations in receptor tyrosine kinases, sustained autocrine or paracrine production of activating ligands, Ras mutations and B-Raf mutations (Dhillon *et al.*, 2007).

Research efforts over the last couple of years have revealed a considerably greater complexity to the once simple linear Raf–MEK–ERK signaling cascade. These complexities suggest that targeting this pathway is no longer as straightforward as once imagined.

1.3.2 Trk receptors as a target in precision oncology

Existing cancer treatment uses a multimodal approach incorporating chemotherapy, surgery, radiation therapy, autologous stem cell transplantation, and immunotherapy. The current drawbacks being relapse, drug resistance or drug toxicity. The paradigm of cancer treatment is thus shifting toward individualized therapy. The main concept behind precision oncology is to give patients drugs that target specific mutations driving their cancer's growth. In other words, the same drug may work against many tumor types.

Mutations in RTKs and aberrant activation of their intracellular signaling pathways have been causally linked to cancers, diabetes, inflammation, severe bone disorders, arteriosclerosis, and angiogenesis. These connections have driven the development of a new generation of drugs that block or attenuate RTK activity (Lemmon & Schlessinger, 2010). RTK drugs belong to two main categories: small-molecule inhibitors that target the ATP-binding site of the intracellular

TKD (Shawver *et al*, 2002) and monoclonal antibodies that both interfere with RTK activation and target RTK-expressing cells (that display tumor surface antigens) for destruction by the immune system (Reichert & Valge-Archer, 2007).

Several tyrosine kinase inhibitors (TKIs) with varying degrees of activity against TrkA, TrkB and TrkC are available, which can broadly be grouped into multi-kinase inhibitors with varying degrees of selectivity. Promising recent clinical trial data and the subsequent accelerated FDA approval of the highly selective Trk inhibitor, Larotrectinib, for the treatment of solid tumors with an oncogenic *NTRK* fusion, has created an immediate need for *NTRK* fusion testing in the oncology community (Solomon *et al.*, 2020).

Larotrectinib (LOXO-101) is a small molecule, highly-selective, ATP-competitive Trk inhibitor that was developed by Loxo Oncology in collaboration with Bayer AG as a treatment for adult and pediatric patients whose cancers have a specific genetic biomarker, namely *NTRK* gene fusions (Drilon *et al.*, 2018). One major novelty of this therapy is – besides the target - its tumor-agnostic approach. This means that Larotrectinib can be applied in all cancers with proven *NTRK* fusion regardless of the tumor entity and the age of the patients (Drilon *et al.*, 2018; Hong *et al*, 2019; Laetsch *et al*, 2018; Markl *et al.*, 2019). On 26 November 2018, Larotrectinib received its first global approval (under accelerated approval) in the USA for the treatment of adult and pediatric patients with solid tumors that harbor an *NTRK* gene fusion without a known acquired resistance mutation, are metastatic or where surgical resection is likely to result in severe morbidity (Scott, 2019). This drug binds to and inhibits TrkA, TrkB and TrkC, thereby preventing Trk activation, resulting in both the induction of cellular apoptosis and the inhibition of cell growth in tumors that overexpress Trk (Vaishnavi *et al.*, 2015). An FDA-approved test for the detection of *NTRK* gene fusion is unavailable. In collaboration with 'Loxo Oncology', a Larotrectinib companion diagnostic is being developed by Illumina to identify patients with cancer who will best respond to treatment with Larotrectinib (Scott, 2019).

Entrectinib (RXDX-101) is another such potential TKI that binds to the three Trks. It is an ATP-competitive TKI. It has, along with Larotrectinib, received breakthrough designation status by the US-FDA for the treatment of cancers harboring *NTRK* fusions (Doebele *et al.*, 2020). Entrectinib is an orally available pan-TRK inhibitor with additional activity against ROS1 and ALK (Rudzinski *et al*, 2018). It is primarily being studied in preclinical models of neuroblastoma (NB) and has shown favorable results in Phase I clinical studies (Pacenta &

Macy, 2018). In phase 1-2 trials, Entrectinib showed durable and clinically relevant responses in patients with *NTRK* fusion-positive solid tumors (Doebele et al 2020).

In tumors with complex karyotypes, it may therefore be advisable specifically to investigate the fusion transcripts for functional impact before considering targeted treatment approaches using pan-*NTRK* TKIs. Next-generation Trk inhibitors, like LOXO-195, that overcome acquired resistance due to acquisition of *NTRK* kinase domain mutations to first- generation TKIs, are already being developed (Drilon *et al.*, 2018). The *NTRK* gene fusions and their oncogenic potential in tumors as oncogenes may have been underestimated, mostly because of the absence, until recently, of targeted therapies exploiting these gene abnormalities (Amatu *et al.*, 2016; Solomon *et al.*, 2020). Thus, a clear understanding of the role of *NTRK* fusions and constitutive Trk signaling in brain tumor and other cancers is urgently required for the development of novel, mechanism-based therapies in personalized cancer treatment. That is to say that, therapies that target these rather rare, constitutionally active *NTRK* fusions are crucial. One move in that direction is to understand the role of the Trk receptors and its components in physiological and pathological states. In this thesis, constitutive signaling of TrkB receptors, the most common Trk receptor in glioblastoma, and the signaling consequence of *NTRK2*-fusions was investigated, in order to build a new understanding of signaling functions of constitutively active Trk.

1.4 Research question- Aim of the thesis

Under physiological conditions, Trk receptors are activated by neurotrophins, (for example, TrkB by BDNF) but there are plenty of instances where these receptors are activated in absence of their ligands. Moreover, not much is known about the role of the kinase domain of TrkB in trans-activation or in constitutive activation. The aim of the thesis is to find out the molecular and cellular prerequisites of TrkB receptor in constitutive kinase activation (referred to as 'self-activation' in this study). We thus set out first to find out the role of Y^{705} residue, in the TrkB kinase domain, in self-activation. This is followed by elucidating the role of self-active TrkB in modifying the actin cytoskeleton of cells. *NTRK*-fusions are tumorigenic and to demonstrate the TrkB kinase ligand-independent signaling mediated via Y^{705}, we use a modified glioblastoma derived cell line expressing an *NTRK2*-fusion. We then ask if this TrkB signaling property is prevalent in human glioblastoma tissue, which is a highly aggressive and often fatal type of brain tumor.

2. Materials and Methods

2.1 Materials

2.1.1 Antibodies

ANTIBODY	SOURCE	IDENTIFIER
Primary antibodies		
Rabbit monoclonal anti-panTrk C-term region - A7H6R (1:500)	Cell Signaling Technology	92991
Rabbit monoclonal anti-pY490-TrkA (anti-pY516-TrkB) C35G9 – Shc site (1:500)	Cell Signaling Technology	4619
Rabbit monoclonal anti-pY674/675-TrkA (anti-pY706/707–TrkB) C50F3 - (kinase site) (1:500)	Cell Signaling Technology	4621
Rabbit monoclonal anti-pY785TrkA (anti-pY816-TrkB) C67C8 – PLCγ site (1:500)	Cell Signaling Technology	4168
Goat polyclonal anti-TrkB N-term region (1:1000)	R&D Systems	AF1494
Rabbit polyclonal anti-FAK (1:500)	Cell Signaling Technology	3285
Rabbit polyclonal anti- pY397-FAK (1:500)	Cell Signaling Technology	3283
Rabbit polyclonal anti-pY576/577-FAK (1:500)	Cell Signaling Technology	3281
Rabbit monoclonal anti-44/42-MAP Kinase 137F5 (1:1000)	Cell Signaling Technology	4695
Rabbit monoclonal anti-p44/42-MAP Kinase (D13.14.4E) (1:1000)	Cell Signaling Technology	4370
Mouse anti-HA.11 (16B12) (1:1000)	Covance	MMS-101P
Rabbit polyclonal anti-Cofilin (1:1000)	Cell Signaling Technology	3312
Rabbit monoclonal anti-pS3-Cofilin 77G2 (1:1000)	Cell Signaling Technology	3313
Mouse monoclonal anti-Nestin (human) 10C2 (1:1000)	Merck Millipore	5326
Mouse monoclonal anti-γ-Adaptin (1:1000)	BD Biosciences	610385
Rabbit polyclonal anti-p75 [NTR] (human) (1:1000)	Promega	G3231
Secondary antibodies		
Donkey anti goat IgG affiniPure (H+L)-Alexa488 (1:800)	Jackson	705-545-147
Donkey anti goat affiniPure-Alexa647	Jackson	705-605-003
Donkey anti goat HRP IgG (H+L) (1:5000)	Jackson	705-035-147
Donkey anti rabbit IgG affiniPure (H+L)-Cy3-550 (1:800)	Jackson	711-165-152
AffiniPure Goat Anti-Rabbit IgG (H+L) (1:5000)	Jackson	111-005-003
Goat anti mouse IgG affiniPure (H+L)-Alexa488 (1:800)	Invitrogen	A11029
Goat anti mouse IgG affiniPure (H+L) (1:5000)	Jackson	115-035-146

2.1.2 Chemicals, Peptides, Recombinant Proteins and Supplements

REAGENT or RESOURCE	SOURCE	IDENTIFIER
Acti-stain-670-Phalloidin	Cytoskeleton	PHDN1
Ampicillin	Roth	K029
Aquapolymount	Polyscienes Inc.	18606
Blotting Grade Blocker – non-fat dry milk	BioRad	1706404
β-mercaptoethanol	Sigma	M7154
BSA (Bovine Serum Albumin)	Sigma Aldrich	A7030
BDNF (brain-derived neurotrophic factor)	recombinant protein, in house	-
Bromophenol blue	Sigma	B-8026
CheLuminate-HRP PicoDetect	Applichem	A3417,1200
cOmplete Tablets mini EDTA-free	Roche	4693159001
DAPI - (4',6-diamidino-2-phenylindol)	Sigma-Aldrich	D9542
DMEM (1×) + GlutaMAX	Gibco	61965-026
Opti-MEM + GlutaMAX	Gibco	51985-034
DMSO (Dimethylsulfoxide)	Roth	4720
Doxycycline	Sigma-Aldrich	D9891-1G
ECL Prime	GE Healthcare	RPN2232
Entrectinib (RXDX-101)	Selleckchem	S7998
Fetal calf serum (FCS)	Linaris	-
Gene Ruler - 1 kb DNA ladder	Fermentas	SM0311
Gene Ruler - 100 bp DNA ladder	Thermo Scientific	SM0241
Hank's Balanced Salt Solution (HBSS)	Gibco	14170
HD Green Plus DNA stain	Intas	ISII-HDGreen Plus
HEPES	Sigma	H4034-25G
Immobilon Western HRP substrate	Merck Milipore	P90720
K252a	Abcam	ab120419
Larotrectinib (LOXO-101) sulfate	Selleckchem	S7960
Lipofectamine 2000	Invitrogen	11668-019
Luminaris HiGreen qPCR Master Mix	Thermo Fisher Scientific	K0992
Nonidet P40 Substitute	Sigma	74385
Paraformaldehyde	Merck	A113 13
Penicillin-Streptomycin (5,000 U/mL)	Gibco	15070-063
Puromycin	InvivoGen	ant-pr-1
Polyacrylamide 30 %	BioRad	1610158
Poly-D,L-ornithine hydrobromide (PORN)	Sigma	P8638
Poly-L Lysine hydrobromide (PLL)	Sigma	P2636
Prestained protein ladder	Thermo Scientific	26616
SDS (Sodiumdodecylsulfate)	Applichem	A2572,1000
Stripping buffer - Restore Plus Western	Thermo Scientific	46430
Superscript III RT	Invitrogen	18080
TEMED (N,N,N′,N′-Tetramethylethylenediamine)	Merck	UN2372
Tris base	Roth	4855.3

Tris HCl	Roth	6771.1
Triton X100	Sigma-Aldrich	9002-93-1
TrypLE-Express	Gibco	12605-010
Tween 20	Sigma	P1379

2.1.3 Critical commercial assays

KIT	SOURCE	IDENTIFIER
Pierce BCA Protein Assay Kit	Thermo Scientific	23225
NucleoBond Xtra Midi EF	Macherey Nagel	740420
Monarch-PCR & DNA Cleanup Kit	New England Biolabs	T1030S
Monarch-DNA Gel Extraction Kit	New England Biolabs	T1020S
RNeasy Mini Kit	Qiagen	74104
Quick Blunting Kit	New England Biolabs	E1201
Quick Change II XL - Site directed mutagenesis Kit	Agilent Technologies	200521

2.1.4 Buffers, solutions and media

SOLUTION	COMPOSITION
10% Ammoniumpersulfate (APS)	100 mg APS in 1 ml dH$_2$O
Blocking buffer for immunohistochemistry	1% BSA in 1×PBS
Blocking buffer for immunoblotting	5% Blocking grade milk powder in 1× TBST, boiled and filtered
0.5 M EDTA	380.2 g in 1 l dH$_2$O, pH 8.0
10× Electrophoresis buffer	30.5 g Tris Base, 144 g Glycine, 10 g SDS in 1 l of dH$_2$O
Elution buffer	10 mM Tris HCl pH 8.5, BSA (1 mg/ml);
6× Gel loading dye	40% Glycerol, 0.02% Bromophenol blue, 0.06% Xylene-cyanol, 1× TAE in dH$_2$O
1 M HEPES	23.8 g in 100 ml sterile dH20, pH 7.3, sterile filter.
4× Lämmli sample buffer	In 20 ml: 4 ml 1 M Tris HCl pH 6.8, 8 ml 20% SDS, 5 ml Glycerol, 1.6 ml β-Mercaptoethanol, 1.4 ml H$_2$O, 10 mg Bromophenol blue
Lysis buffer	50 mM HEPES pH 7.5, 150 mM NaCl, 10% Glycerol, ½ cOmplete mini-EDTA free tablet, 200 mM Na-ortho-vanadate, 100 mM Na-pyrophosphate, 100 mM NaF, 0.5 M EDTA pH 8.0, 10% NP40
Maintenance medium for secondary cultures / all cell lines	DMEM (1×) + GlutaMAX (500 ml) + 10% FCS + 1% Pen/Strep, incubate at 37°C, 5% CO$_2$
4% Paraformaldehyde	40 g Paraformaldehyde in 500 ml dH$_2$O with few drops of 5 M NaOH, stir for 20-30 min at 60°C until paraformaldehyde dissolves. Pass through a filter paper and add 410 ml of Buffer A (0.2M Na$_2$PO$_4$×2H$_2$O in dH$_2$O) and 90 ml Buffer B (0.2M NaH$_2$PO$_4$×2H$_2$O in dH$_2$O). pH 7.4
1 M Phosphate buffer	13.61 g KH$_2$PO$_4$, 17.42 g K$_2$HPO$_4$ in 100 ml dH$_2$O, pH 6.5
10× Phosphate buffered saline (PBS)	80 g NaCl, 2 g KCl, 2 g KH$_2$PO$_4$, 11.75 g Na$_2$HPO$_4$ × 2H$_2$O in 1 l dH$_2$O
10× RT	7 µl Tris HCl pH 8.00 (10 mM stock), 1 µl dNTPs (20 mM stock), 2 µl random primer N6 (5 mM stock)

10% SDS	5 g in 50 ml dH$_2$O
1 M Sodium chloride	58.44 g in 1 l of dH$_2$O
50× TAE buffer	242 g Tris Base, 292 g EDTA in 1 l dH$_2$O, pH 8.0
10× TBS	12.1 g Tris Base, 87.7 g NaCl, adjust to pH 8.0 in 1 l of dH$_2$O
TBST	100 ml TBS, 10 ml 20% Tween20, 890 ml dH$_2$O
Transfer buffer	100 ml 10×Electrophoresis buffer, 700 ml H$_2$O, 200 ml Methanol
100 mM Tris HCl	157.6g in 1 l dH$_2$O, pH 7.5
20% Tween 20	50 ml Tween 20 in 250 ml dH$_2$O.
Washing buffer for immunostaining	0.1% Triton × 100 (from 20% Triton × 100 stock), 0.1% Tween 20 (from 20% Tween 20 stock) in 1× PBS

2.1.5 Recombinant DNA vectors

pcDNA3 (# identifier)	LV FuGW	LV pCW
pcDNA3-TrkB wt (#715)	pFU-HA-TrkBwt (#717)	pCW-TrkB wt (#1029)
pcDNA3-TrkB Shc (#747)	pFU-HA-TrkB Shc (#780)	
pcDNA3-TrkB ATP (#749)	pFU-HA-TrkB ATP (#761)	
pcDNA3-TrkB YFF (#759)	pFU-HA-TrkB YFF (#788)	pCW-TrkB YFF (#1030)
pcDNA3-TrkB PLCγ (#752)	pFU-HA-TrkB PLCγ (#792)	
pcDNA3-TrkB YYF (#837)	pFU-HA-TrkB YYF (#847)	
pcDNA3-TrkB YFY (#838)	pFU-HA-TrkB YFY (#846)	
pcDNA3-TrkB YDY (#871)	pFU-HA-TrkB YDY (#917)	
pcDNA3-TrkB YEY (#872)		
pcDNA3-TrkB Shc/PLCγ (#873)	pFU-HA-TrkB Shc/PLCγ (#918)	
pcDNA3-TrkB ATP-YDY (#894)	pFU-HA-TrkB ATP-YDY (#919)	
pcDNA3-TrkB ATP-YEY (#895)		
pcDNA3-TrkB S478A (#974)		
	pFU-TrkB-ICD (#993)	pCW-TrkB ICD (#1032)
	pFU-TrkB-myrICD (#995)	pCW-TrkB MyrICD (#1033)
	pFU-SQSTM1-NTRK2 (#1020)	pCW- SQSTM1-NTRK2 (#1035)
	pFUGW (Lois *et al*, 2002)	

2.1.6 Primer sequences

PRIMER	Reference sequence	Amplicon (in reference)	SEQUENCE
Primer sequences for quantitative RT-PCR			
hBDNF	NM_170735	(position 1301 – 1398)	5´– TGAGGACCAGAAAGTTCGGC –3´ 3´– GAGGCTCCAAAGGCACTTGA –5´
hTrkB-kin 2	NM_006180	(position 2844 – 3082)	5´– ACCAGCTGTCAAACAATGAG –3´ 3´– ACGTTGGGAAGGATCGGT –5´
hTrkB-splice	NM_006180	(position 2271 – 2454)	5´– CTGTGGTGGTGATTGCGTCT –3´ 3´– GGGCTGGCAGAGTCATCATC –5´
RNA Pol II (POLR2A)	NM_000937	(position 4466 – 4732)	5´– GCACCACGTCCAATGACAT –3´ 3´– GTGCGGCTGCTTCCATAA –5´

TBP	NM_003194	(position 904 – 1035)	5´– TGCACAGGAGCCAAGAGTGAA –3´ 3´– CACATCACAGCTCCCCACCA –5´

2.1.7 Consumables

MATERIAL	SOURCE	IDENTIFIER
4-well Cellstar cell culture dishes	Greiner Bio-One	627 170
Easy Grip Tissue Culture dishes – 35 x 10 mm	Falcon	353001
Coverslips (Ø 10 mm)	Marienfeld	0111500
Coverslips (Ø 18 mm)	Marienfeld	0111580
Fuji Medical X-Ray film Super RX-N	Fujifilm	47410-19289
Ibidi dishes - µ-high 35 mm	Ibidi	81156
Ibidi 2-well inserts	Ibidi	81176
Immersion oil	Olympus	IMMOIL-F30CC
Neubauer chamber	Marienfeld	0640110
Nunclon Delta Surface 4 well plates	Thermo Scientific	176740
Objective slides – 76 x 26 mm	R. Langenbrick	8037/1
Pasteur pipette	Brand	747720
PVDF membrane	BioRad	1620177
T75 Cell culture flasks	Greiner Bio-One	658 170
T25 Cell culture flasks	Greiner Bio-One	690 160

2.1.8 Cell lines

CELL LINE	SOURCE	IDENTIFIER
HEK293	human primary embryonal kidney	ACC #305
U87MG	human malignant glioma	ATCC #HTB-14

2.1.9 Equipment

EQUIPMENT	SOURCE
Automatic film processor CP1000	Agfa
Bacterial Hood	Thermo Scientific
Cryostat – CM1950	Leica
Cell culture CO$_2$ Incubator	Binder
Cell culture Hood	Heraeus
Centrifuge – 5424R	Eppendorf
Centrifuge – 5810R	Eppendorf
Criterion™ Blotter with Wire Electrodes - 1704071	BioRad
Hypercassette – 18 × 24 cm	Amersham Biosciences
Leica SP5 confocal microscope	Leica
Mini-PROTEAN Tetra Vertical Electrophoresis Cell for Mini Precast Gels - 1658004	BioRad
Mini Trans-Blot® Electrophoretic Transfer Cell - 1703930	BioRad

Nanodrop Spectrophotometer – ND1000	PeqLab Biotechnologie
BioPhotometer plus	Eppendorf
Olympus confocal microscope – Fluoview FV 1000	Olympus
PowerPac™ Basic Power Supply	BioRad
LightCycler 96	Roche
PCR-Mastercycler 96-well	Eppendorf
Rocking platform -Duomax 1030	Heidolph
Thermomixer comfort	Eppendorf
Ultrasonic Processor – UP50H	Hielscher

2.1.10 Software and Algorithms

SOFTWARE	SOURCE	IDENTIFIER
ImageJ	https://imagej.nih.gov/ij/	RRID:SCR_003070
Adobe Photoshop CS5 Extended	http://www.adobe.com/	RRID:SCR_014199
OriginPro	https://www.originlab.com/	RRID:SCR_014212
GraphPad Prism	http://www.graphpad.com/	RRID:SCR_002798
Olympus Fluoview – FV10-ASW 3.0	http://www.olympus-lifescience.com/en/	RRID:SCR_014215
Leica LAS AF Image Acquisition Software	http://www.leica-microsystems.com/	RRID:SCR_013673
LightCycler Roche	http://www.roche-applied-science.com/	RRID:SCR_012155
Microsoft Office	https://www.office.com	

2.2 Methods

2.2.1 Cell culture and transfections

2.2.1.1 HEK293

HEK293 cells (ACC #305) – are established from a human primary embryonal kidney transformed by adenovirus type 5 (Ad 5), classified as risk category 1 according to the German Central Commission for Biological Safety (ZKBS). Cells were grown in DMEM, high glucose, GlutaMAX™ Supplement (Gibco #61965-026) with 10% FCS and 1% Penicillin-Streptomycin (Gibco #15070063). Cells were incubated at 37°C in 5% CO_2. For transfection of DNA plasmids, HEK293 cells were transfected using Lipofectamine 2000 (Invitrogen #1168019), media was replaced after 24 h and the expression was maintained for 30 h – 48 h before being processed for immunofluorescence microscopy or western blot analysis.

2.2.1.2 U87MG

U87MG (ATCC #HTB-14) is one of a number of cell lines derived from malignant gliomas by J. Ponten and associates from 1966 to 1969 (Ponten & Macintyre, 1968). Cells were grown in DMEM, high glucose, GlutaMAX™ Supplement (Gibco #61965-026) with 10% FCS and 1% Penicillin-Streptomycin (Gibco #15070063). Cells were incubated at 37°C in 5% CO2. Stable U87MG cell lines expressing TrkB mutants and SQSTM1-NTRK2 fusion was generated using suitable lentiviral vectors (see LV pCW in section *2.1.5*) and positively selected with Puromycin (1 µg/ml). TrkB expression was induced by treating cells with 1 µg/ml doxycycline for a minimum of 24 h.

2.2.2 Plasmids, transfection, and viral packaging

2.2.2.1 Plasmids and cloning

pcDNA3-, lentiviral FuGW- and lentiviral pCW-TrkB constructs were used in this study (see section *2.1.5*). Expression constructs containing an ATG start codon in pcDNA3 backbone (CMV promoter) for transient transfection or in FuGW backbone (UbiC promoter) for lentiviral expression were generated. The lentiviral variants were tagged with an affinity tag for hemagglutinin (HA tag). DNA sequence of *Ntrk2* (*trk*B full-length – *trk*B.FL) encoded by *Mus musculus* (reference: NM_001025074) was used in all the constructs. Constructs containing mutations of lysine 571 (K^{571}) to asparagine (N^{571}) or tyrosine 515 to phenylalanine (F^{515}), etc. were cloned using synthetic oligonucleotides and site-directed mutagenesis (Quick Change II

XL - Site directed mutagenesis Kit; Agilent Technologies #200521). Constructs containing intracellular fragments of TrkB were also cloned into FuGW lentiviral backbones. An additional *Ntrk2* fusion construct (SQSTM1 fused to TrkB kinase (Stransky *et al.*, 2014)) was generated by DNA synthesis (Eurofins) and cloned into pcDNA3 backbone.

2.2.2.2 Lentivirus production

Lentiviral particles were packaged in HEK293TN producer cells (SBI biosciences) with pCMV-VSVG and pCMVΔR8.91 (Zufferey *et al*, 1997) helper plasmids. Cells were transfected with Lipofectamine 2000 (Invitrogen) in OptiMEM medium with 10% FCS for 12–14 h. Viral supernatants were harvested 72 h after transfection by ultracentrifugation. Viral particles were suspended in (in mM) 50 Tris–HCl, pH 7.8, 130 NaCl, 10 KCl, 5 MgCl2 and stored at −80°C. The viral titer was tested in HEK293 cells. The number of infectious particles was determined using serial dilutions of the viral vectors on HEK293 cells.

2.2.3 Indirect Immunofluorescence labelling for confocal microscopy

For this purpose, 10mm coverslips (Marienfeld #0111500) were placed in 4-well tissue culture dishes (Cell Star #627170) and coated with poly-L-lysine (PLL, Sigma # P2636). HEK293 were grown on these coverslips − 150,000 cells per dish, transfected with DNA plasmids and Lipofectamine 2000. At 30 h, cells were fixed with 4% PFA for 15 min at 37°C. Cells were then washed twice with PBS, blocked (blocking solution − 1% BSA in PBS) and incubated with primary antibodies diluted in blocking solution for 1 h at RT. Coverslips were then washed 8 times (wash solution − 0.1% Tween 20 in PBS) and incubated with fluorochrome-conjugated secondary antibodies (Alexa-Fluor-488, Cy3-550 nm and Cy5-650 nm from Jackson Laboratories) for 1 h at RT. Cells were washed 8 times with wash solution and cell nuclei were then labelled with DAPI (2 mg/ml stock solution, freshly diluted 1:5000 in PBS) for 5 min at RT. For some experiments, cells were also further incubated for 30 min at RT with Alexa-670-phalloidin (Cytoskeleton #PHDN1) after secondary antibody treatment. Cells were then washed twice with PBS. The coverslips were finally dipped in water, air dried and mounted with Aquapolymount (Polyscienes Inc. #18606) onto an object slide for microscopic imaging.

2.2.4 Confocal Laser scanning microscopy and image processing

Images were acquired using an inverted IX81 microscope equipped with an Olympus FV1000 confocal laser scanning system, a FVD10 SPD spectral detector and diode lasers of 405, 473, 559 and 635 nm. All images shown were acquired with an Olympus UAPO 20× (air, numerical aperture 0.75) or UPLSAPO 60× (oil, numerical aperture:1.35) objective. For high-resolution

confocal scanning, a pinhole setting representing one Airy disc was used. For high-resolution confocal settings, an optimal resolution of at least 3 pixels per feature in x-y direction was set. In z-direction, 300 nm steps were used. 12-bit z-stack images were processed by maximum intensity projection and were adjusted in brightness using Image J software (Rasband, W.S., ImageJ, U.S. National Institutes of Health, Bethesda, Maryland, USA, https://imagej.nih.gov/ij/). Images are shown as RGB images (8-bit per color channel). Fluorescence images presented are representative of cells imaged in at least five independent experiments and were processed for final presentation using Adobe Photoshop CS5.

2.2.5 Live Cell Imaging

For live imaging experiments, μ-high 35 mm Ibidi dishes (Ibidi #81156) were utilized. These dishes were first coated with poly-L-ornithine (PORN). HEK293 cells were grown on the coated dishes – 100,000 cells per dish. Cells were co-transfected with TrkB mutants and GFP-actin. After 24 h, old media was replaced with prewarmed HEPES-buffered DMEM (containing 10% FCS, 1% Penicillin-Streptomycin and 1 mM Sodium pyruvate). Cells were imaged using Leica SP5 inverted confocal microscope equipped with Leica objectives (HC PL Apo 20×/0.7; HCX Apo 60×/1.4–0.6 oil). GFP actin was excited with a 488 nm laser line. Fluorescence was detected with a spectral detector (12-bit) at Airy disc 1 settings.

2.2.6 Western blot analysis

2.2.6.1 HEK293 and U87MG

Cells were grown on 35 mm easy grip tissue culture dishes (Falcon #353001) – 200,000 cells per dish and transfected with DNA plasmids using Lipofectamine 2000. Cells were lysed at 30 h, on ice, using a cell scraper and 150 μl cold lysis buffer (lysis Buffer – 10% NP40, 50 mM HEPES pH 7.5, 150 mM NaCl, 10% Glycerol, 100 mM Sodium fluoride, 100 mM Sodium pyrophosphate, 200 mM Sodium ortho-vanadate, 0.5 M EDTA pH 8.0, 1 EDTA-free protease inhibitor mini tablet (Roche #4693159001). Lysates were incubated on ice for 15 min, sonicated twice for 5 seconds with 80% Hielscher sonifier UP50 and a M1 sonotrode and placed back on ice for 10 min. To remove cell nuclei, preparations were centrifuged for 5 min at 4°C at 15,000 × g. For protein quantification, 5 μl cell supernatant was diluted in 45 μl 1x PBS and the protein concentration of the samples was determined by using the Pierce BCA protein assay kit (Thermo Scientific #23225). Rest of the supernatant was mixed with 40 μl of 4× Laemmli sample buffer and heated for 5 min at 95°C. 20 μg of protein was loaded onto SDS electrophoresis gels for SDS PAGE, followed by immunoblotting onto PVDF membranes

(BioRad #1620177). Western blotting was done overnight using Mini Trans-Blot Cell Assembly (BioRad #1703930) at 25 V, 0.3 A for 15 h. Membranes were then blocked (blocking solution - 5% Milk BioRad blotting grade in TBST) for 30 min at RT and incubated with primary antibody diluted in blocking solution for 3 h at RT (or overnight at 4°C). Blots were washed thrice (20 min each) with TBST and then incubated with secondary antibody for 2 h at RT and washes were repeated as before. Wash times were extended to 40 min (instead of 20 min) when probing with phospho-antibodies to reduce background signal. Blots were developed using ECL (Immobilon Western HRP Substrate, Merck Millipore #WBKLS0500) and X-ray films (Fujifilm Super RX).

2.2.6.2 Patient glioblastoma

Frozen samples were thawed and washed twice in 1× PBS. Small chunks were then distributed into microfuge tubes and lysed with cold lysis buffer as mentioned above (in *2.2.6.1*). Sonification and centrifugation steps were repeated as needed until a homogenous suspension was obtained. After BCA protein quantification, samples were loaded onto SDS-PAGE gels and then immunoblotted as described above in *2.2.6.1*.

2.2.7 RNA isolation and quantitative RT–PCR

Frozen patient glioblastoma samples were thawed and washed twice in 1× PBS. Very small chunks were then distributed into microfuge tubes and RNA isolation was performed using the RNeasy Mini Kit (Qiagen). To generate cDNA, Superscript III Reverse Transcriptase first strand synthesis kit (Invitrogen, #12371-019) was used with 500 ng RNA and 50 ng random hexamer primer. cDNA reaction was 5-times diluted in 10 mM Tris-HCl, pH8.5 containing 1 mg/ml BSA. Light cycler 96 Detection System (Roche) was used to perform RT-qPCR using the Luminaris HiGreen qPCR Master Mix Kit (Thermo Fischer) with a standard amplification protocol (denaturation: 95°C, 15 s; annealing: 60°C, 30 s; 72°C, 30 s) and an equivalent of 5 ng RNA as input. The following primers were tested: hBDNF, hTrkB-kin-2, hTrkB-splice, RNA Pol II and TBP (for primer sequences see section *2.1.6*). Signals were normalized either to RNA Pol II or to TBP by using the ΔΔCT method.

No.	Name of Primer pair	NCBI Ref Seq	Product Length (bp)	Tm (°C)
1.	TBP	NM_001172085	132	62
2.	RNA pol II	NM_000937	267	58
3.	Human-BDNF	NM_001709	98	57
4.	TrkB-Kinase-2	NC_000009.12	239	59
5.	TrkB-T1-splice-site	NM_006180	184	57

2.2.8 Cell migration assay

U87MG cells expressing the TrkB constructs were seeded at a density of 3000 cells per well into a 2-well silicone insert (Ibidi #81176), positioned in a 35 mm μ-dish (35mm, high, Ibidi, #81156). 1 µg/ml doxycycline was added to induce expression of the corresponding TrkB-related constructs (Dox on). For control, the solvent DMSO was added. 24 h after Dox-induction, the cell culture dishes were filled with growth medium and the silicone insert was removed. Cells were monitored using brightfield microscopy directly after removal of the insert and after 24 h, to analyze cell migration. Subsequently cells were fixed and labelled by immunofluorescence. The detection and quantification of cells in the acquired brightfield images was automatized with custom written code in ImageJ (Rasband, W.S., ImageJ, U.S. National Institutes of Health, Bethesda, Maryland, USA, https://imagej.nih.gov/ij/). Images were converted to 8-bit grayscale and smoothed by replacing each pixel with the mean of its neighborhood (5-pixel radius). Cells were defined as local maxima with a prominence greater than 7.5 in the smoothened images (representative images shown in Figure 26A). The area of the removed silicon insert was annotated manually in each image and the number of cells detected within this area was quantified.

2.2.9 Statistical analysis

Statistical analyses were performed with GraphPad Prism 6 and Origin Pro. Data are presented with standard error of the means (± SEM). Column statistics were run to check for Gaussian distribution to decide whether to use parametric or non-parametric tests. If one of the groups to be analyzed failed the normality test or if value number was too small to run the normality test, non-parametric tests were chosen for further analysis. Either normality was tested with the Shapiro-Wilk test and Equality of variances (Levene's test). Based on the results the 2-sample t-test or the Mann-Whitney-U-test was used. Results were considered statistically significant at $p < 0.05$.

3. Results

3.1 Role of Tyr^{705} in kinase domain of TrkB in self-activation

The bioinformatic tool NCBI-BLAST was used to identify the TrkB coding sequence of the constructs used in this study. Figure 4 depicts the amino acid sequence of mouse TrkB with important features highlighted such as the start methionine, signal peptide, transmembrane domain and the intracellular kinase domain. Particularly important for this study is the intracellular kinase domain with its Shc-, ATP-binding, tyrosine triplet- and the PLCγ-sites. In adult mice, TrkB is abundantly expressed in brain tissue, with significant levels also observed in lung, muscle and ovaries (Klein *et al.*, 1989). This murine TrkB was identified to be highly homologous to the human *trk* proto-oncogene (Middlemas *et al*, 1991).

Mouse TrkB (reference sequence NM_001025074; NP001020245)

```
  1 MSPWLKWHGP AMARLWGLCL LVLGFWRASL ACPTSCKCSS ARIWCTEPSP GIVAFPRLEP
          signal peptide                        +1
 61 NSVDPENITE ILIANQKRLE IINEDDVEAY VGLRNLTIVD SGLKFVAYKA FLKNSNLRHI

121 NFTRNKLTSL SRRHFRHLDL SDLILTGNPF TCSCDIMWLK TLQETKSSPD TQDLYCLNES

181 SKNMPLANLQ IPNCGLPSAR LAAPNLTVEE GKSVTLSCSV GGDPLPTLYW DVGNLVSKHM

241 NETSHTQGSL RITNISSDDS GKQISCVAEN LVGEDQDSVN LTVHFAPTIT FLESPTSDHH

301 WCIPFTVRGN PKPALQWFYN GAILNESKYI CTKIHVTNHT EYHGCLQLDN PTHMNNGDYT

361 LMAKNEYGKD ERQISAHFMG RPGVDYETNP NYPEVLYEDW TTPTDIGDTT NKSNEIPSTD

421 VADQSNREHL SVYAVVVIAS VVGFCLLVML LLLKLARHSK FGMKGPASVI SNDDDSASPL
              transmembrane domain                 start ICD (intracellular kinase domain)     +478
481 HHISNGSNTP SSSEGGPDAV IIGMTKIPVI ENPQYFGITN SQLKPDTFVQ HIKRHNIVLK
                                          +515 (Shc)
541 RELGEGAFGK VFLAECYNLC PEQDKILVAV KTLKDASDNA RKDFHREAEL LTNLQHEHIV
                                          +571 (ATP-binding)
601 KFYGVCVEGD PLIMVFEYMK HGDLNKFLRA HGPDAVLMAE GNPPTELTQS QMLHIAQQIA

661 AGMVYLASQH FVHRDLATRN CLVGENLLVK IGDFGMSRDV YSTDYYRVGG HTMLPIRWMP
                                                     YxxxYY (tyrosine triplett)
721 PESIMYRKFT TESDVWSLGV VLWEIFTYGK QPWYQLSNNE VIECITQGRV LQRPRTCPQE

781 VYELMLGCWQ REPHTRKNIK SIHTLLQNLA KASPVYLDIL G
                                          +816 (PLCγ)
```

Figure 4. Mouse TrkB (reference sequence NM_001025074; NP001020245).
Deduced amino acid sequence of Ntrk2 (trkB full-length – trkB.FL) encoded by *Mus musculus* (reference: NM_001025074; NP_001020245). In the depicted amino acid sequence, in bold underline and blue is the initiating methionine and signal peptide, in orange is the transmembrane domain, in purple the lysine residue of the ATP-binding site and in green are the important Serine or Tyrosine residues of the kinase domain. Highlighted in yellow and red are the 12 N-glycoslation sites (Gupta *et al.*, 2020).

In order to characterize the functional prerequisite of TrkB for self-activation, we used site-directed mutagenesis and PCR techniques to clone a set of mouse TrkB mutants (based on reference sequence: NP001020245, Figure 4.). The various TrkB mutants thus generated have been summarized in Table 1. The SQSTM1-NTRK2 fusion construct was synthetically designed based on reported studies showing the presence of these fusions in gliomas (Ferguson *et al*, 2018; Passiglia *et al*, 2016; Stransky *et al.*, 2014). This particular fusion product was chosen because it lacks the TrkB juxtamembrane domain and the Shc site, thereby making it primarily an intracellular protein with an intact kinase domain.

constructs	synonym	Features, signaling pathway regulation
TrkB - wt	wildtype	Wildtypic TrkB, BDNF / NT4/5 receptor
TrkB – $S^{478}A$	TrkB – $S^{478}A$	Interaction to TIAM1 / Rac1 pathway
TrkB - $Y^{515}F$	Shc mutant	Shc adaptor site, Ras / MAPK pathway, Pi3K / Akt pathway
TrkB – $K^{571}N$	ATP mutant	ATP-binding, kinase-dead mutant
TrkB – $Y^{705}F$	YFY mutant	Yxxx**Y**Y motif mutant, critical mutation in the in the activation loop
TrkB – $Y^{706}F$	YYF mutant	YxxxY**Y** motif mutant mutant, kinase-active
TrkB – $Y^{705,706}F$	YFF mutant	Yxxx**YY** motif double mutant
TrkB – $Y^{705}D$	YDY mutant	Phospho-mimicking mutation Yxxx**Y**Y motif
TrkB – $Y^{705}E$	YEY mutant	Phospho-mimicking mutation Yxxx**Y**Y motif
TrkB – $Y^{816}F$	PLCγ mutant	Adaptor site for PLCγ / IP_3 / calcium pathway
TrkB - $Y^{515}F$, $Y^{816}F$	Shc-PLCγ double mutant	Shc adaptor site and PLCγ site are mutated
TrkB – $K^{571}N$, $Y^{705}D$	YD-ATP double mutant	Double mutant: phospho-mimicking mutation in Yxxx**Y**Y motif, and kinase-dead mutation at K^{571}
TrkB – $K^{571}N$, $Y^{705}E$	YD-ATP double mutant	Double mutant: phospho-mimicking mutation in Yxxx**Y**Y motif, and kinase-dead mutation at K^{571}
TrkB-Myr ICD	Myr-ICD	Intracellular domain: K^{454} – STOP, membrane anchored by N-terminal myristoylation motif
TrkB-ICD	ICD	cytosolic, intracellular domain K^{454} – STOP
TrkB-12×$N^{mut}A$	TrkB^{12gly}	Mutation of 12 predicted N-glycosylation sites
SQSTM1-*NTRK2*	SQSTM1-NTRK2	SQSTM1-NTRK2 kinase fusion construct

Table 1. TrkB mutants used in this study.

All mutants are based on reference sequence NP001020245. In the kinase-dead TrkB-ATP mutant, corresponding tyrosine residues are not mutated, but autophosphorylation is inhibited due to a missense mutation ($K^{571}N$). The SQSTM1-NTRK2 fusion construct was synthetically designed according to a human *NTRK2*-fusion sequence.

3.1.1. Antibody specificity of Trk receptors

The specificity and properties of the antibodies were verified with the help of these TrkB mutants by employing immunofluorescence and western blotting techniques and the results are summarized in Table 2.

antibody	TrkB wt (western)	TrkB wt (ICC)	TrkB-ATP mut. (western)	TrkB-ATP mut. (ICC)	human tissue	comment
panTrk (C-term) – A7H6R	+	+	+	+	+	detects TrkA, TrkB, TrkC
anti-TrkB (receptor domain)	+	+	+	+	+	detects TrkB-T1 and TrkB kinase at 130kDa (glycosylated) and 90 kDa
anti-pY674/675-TrkA (anti-pY706/707–TrkB) C50F3	+	+	-	-	+	Detects YYF mutant, does not detect YFY, YDY, YEY mutants
pY785-TrkA (anti-pY516-TrkB) C35G9 – Shc site	+	+	-	-	n.d.	detects Shc mutant $Y^{515}F$ in ICC
pY490-TrkA (anti-pY816-TrkB) C67C8 – PLCγ site	+	+	-	-	+	detects PLCγ mutant $Y^{816}F$ in ICC

Table 2. Table describing properties of anti-Trk antibodies used for TrkB detection.

Antibody specificity for the different TrkB antibodies used in this study are summarized in this table. Immunocytochemistry (ICC) and western botting techniques were used as read outs. + indicates positive signal; - indicates no signal seen; n.d.-not determined.

Immunofluorescence labelling of the various TrkB mutants against the antibodies summarized in Table 2 are depicted below (in Figures 5, 6, 7 and 8). As a means of confirming transfection, the cells were co-transfected with GFP. Post labelling, these samples were imaged at 20× magnification. In Figure 5, cells were labelled for total Trk (red, anti-panTrk (C-term) – A7H6R). There was a homogeneous mixture of cells expressing GFP and Trk. The C-terminal antibody bound successfully to all the conditions, irrespective of the type of Trk mutation, indicating a structurally intact protein. The pTrk-kin antibody (Figure 6) on the other hand was found to bind the tyrosine residues 705/706 with high specificity and thus a mutation at either of these sites (YYF, YFY, YDY and YEY) made the antibody incapable of binding to these proteins. When the ATP site (K^{571}) is mutated, the receptor can no longer recruit ATP at the YxxxYY motif, which in turn means that the gamma phosphate in ATP can no longer be transferred to the tyrosine residues, thereby rendering the receptor inactive and unphosphorylated at the kinase sites. Consequently, mutation of K^{571} creates a kinase-dead

TrkB mutant (ATP and YD-ATP). These kinase-dead mutants additionally prove that, the here used anti-pTrk antibodies, are phospho-specific to TrkB.

The pTrk-PLCγ and pTrk-Shc antibodies also behaved in a similar way (Figures 7 and 8). These antibodies showed no signal for the kinase-dead mutants (ATP and YD-ATP). They showed some level of activity for the kinase domain mutants (YYF, YFY, YDY and YEY), perhaps suggesting an ongoing independent phosphorylation at the PLCγ and Shc sites. A directed missense mutation at the PLCγ ($Y^{816}F$) or Shc-site ($Y^{515}F$) unfortunately creates a phospho-independent, immunoreactive site after paraformaldehyde fixation (Shc, PLCγ and Shc-PLCγ double mutant) and hence these antibodies were additionally verified, in later experiments, by western blotting.
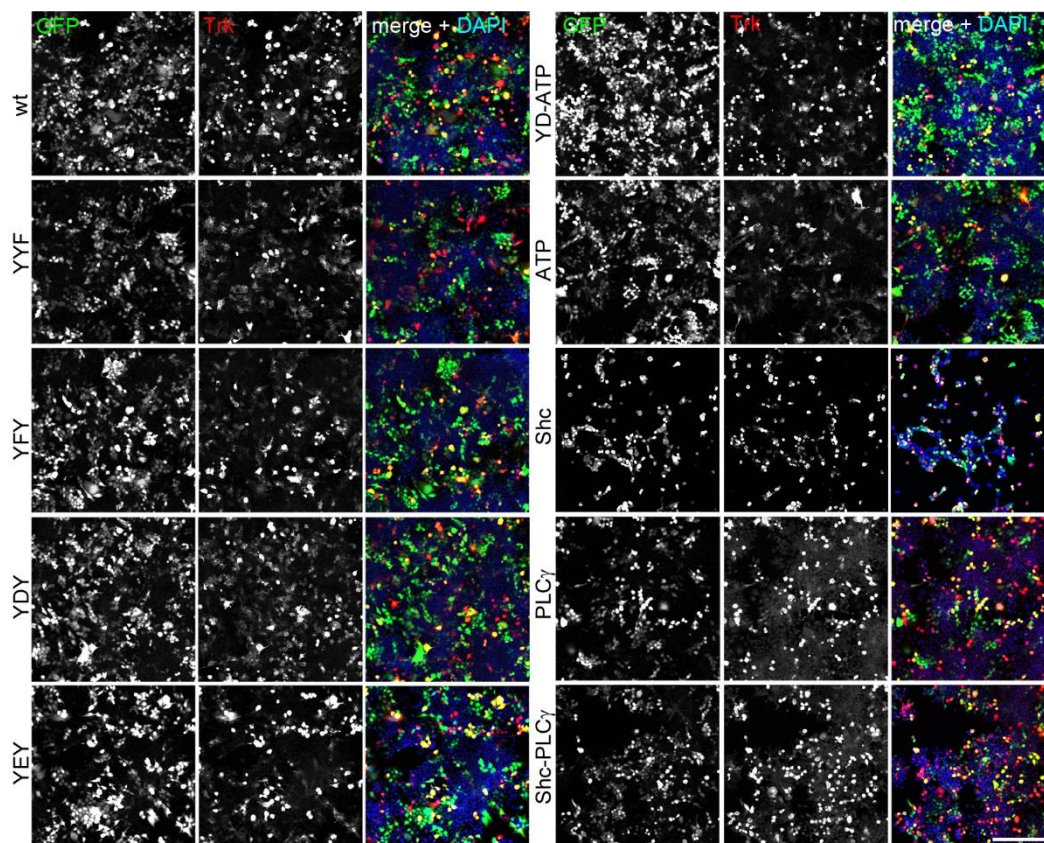
Figure 5. Confirmation of anti-Trk immunoreactivity of TrkB mutants.

Immunostaining of HEK293 cells expressing either TrkB wildtype or indicated TrkB mutants. Cells were co-transfected with GFP. Immunofluorescence of GFP (green) and panTrk (red, anti-panTrk (C-term) − A7H6R), together with DAPI as nuclear counterstain (blue). Cells were immunostained after an expression time of 48 h. panTrk binds to the C-terminus of the receptor and shows thereby the integrity of the open reading frame of all mutants. Note: HEK293 themselves do not express TrkB. Confocal images; scale bar: 100 μm.
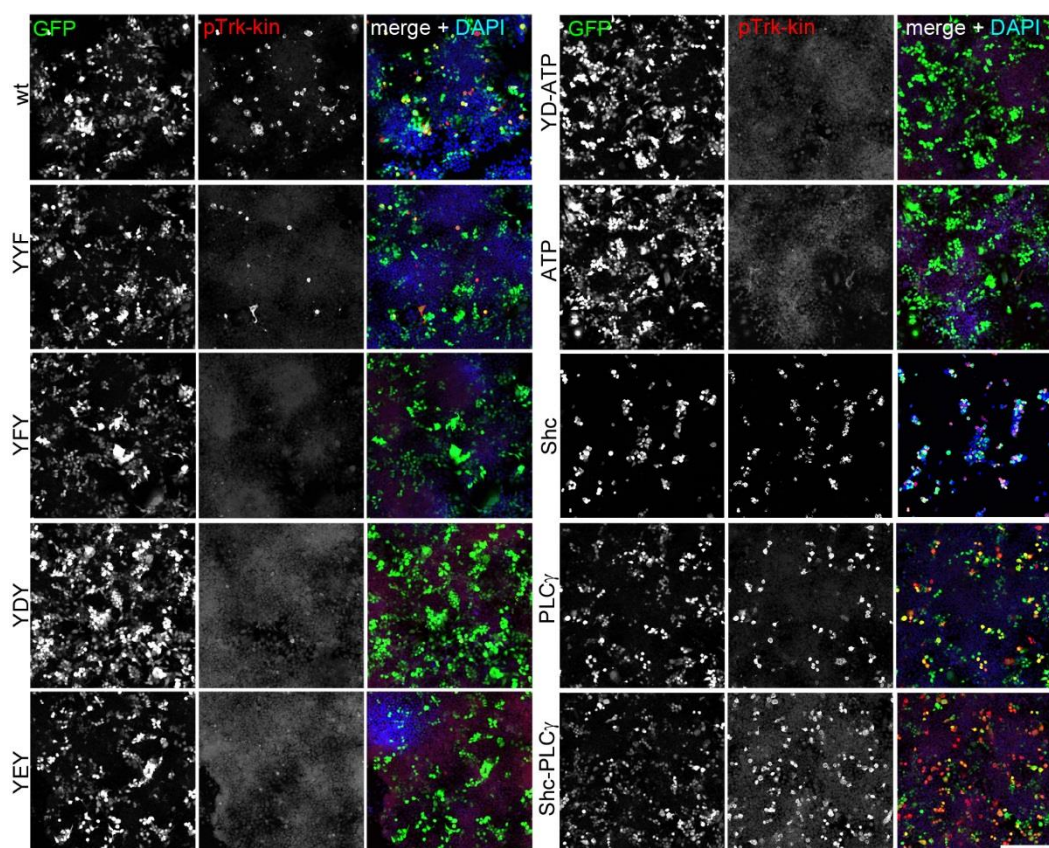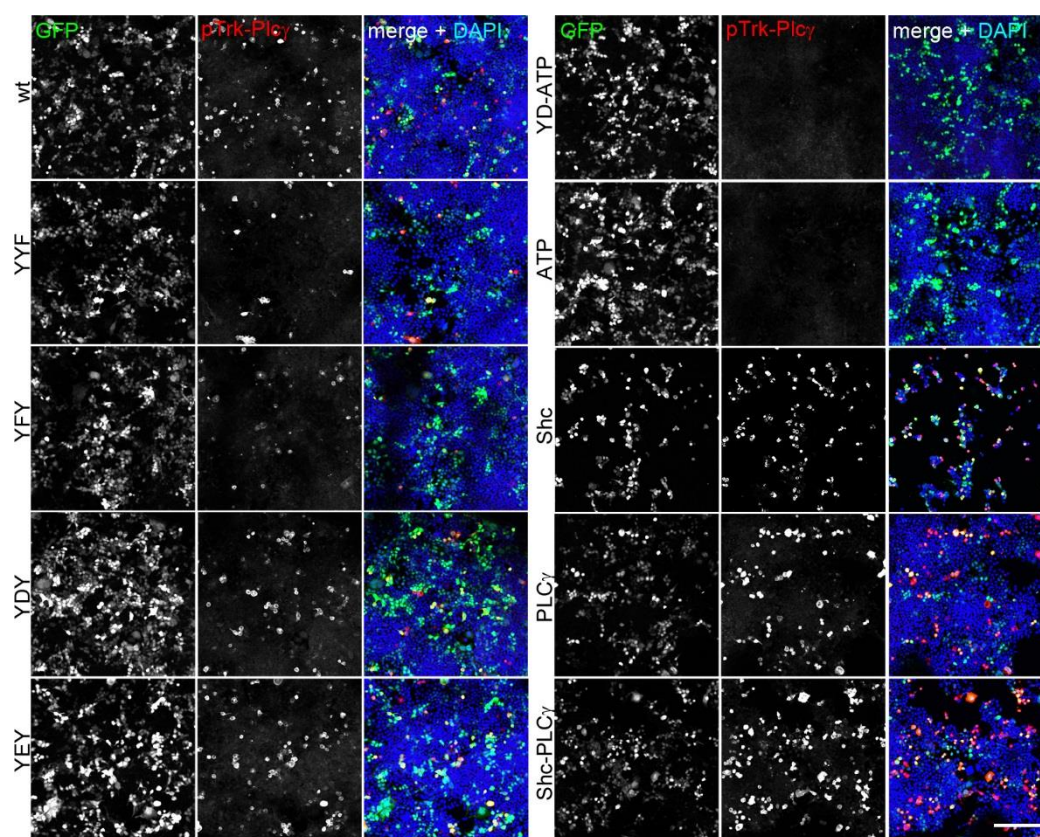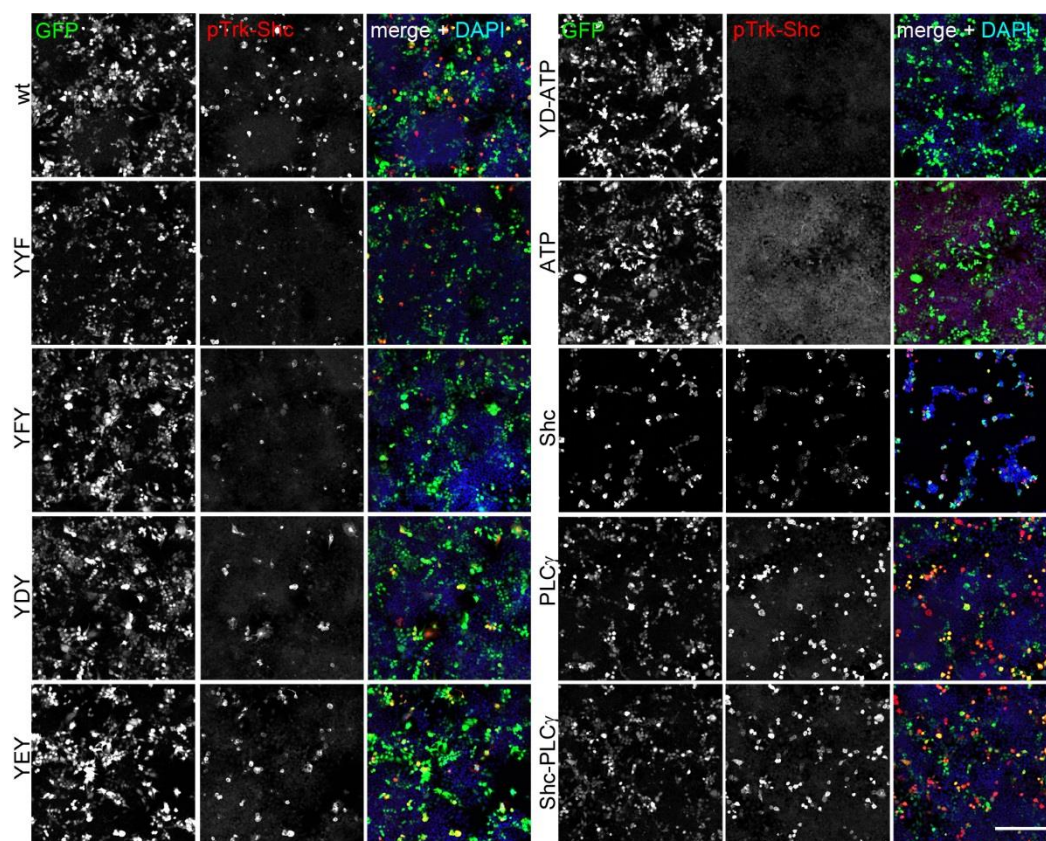
Figure 6. Constitutive activation of TrkB by overexpression and immunoreactivity profile of anti-pTrk-kin.
Immunostaining of HEK293 cells expressing either TrkB wildtype or indicated TrkB mutants. Cells were co-transfected with GFP. Immunofluorescence of GFP (green) and pTrk-kin (red, anti-pY674/675-TrkA (anti-pY706/707–TrkB) C50F3), together with DAPI (blue). Cells were immunostained 48 h after transfection. pTrk-kin antibody binds to the phosphorylated 2nd and 3rd Y residues in the YxxxYY motif of the Trk kinase domain. When these sites are mutated ($Y^{705,706}F$), there is no fluorescence seen as the antibody no longer recognizes them (YYF, YFY, YEY). When the ATP site is mutated ($K^{571}N$), lack of ATP prevents TrkB autophosphorylation and the Y residues in the kinase domain remain unphosphorylated (ATP, YD-ATP). All missense mutations in Y^{705} for D,E,or F, interrupted the anti-pTrk-kin immunoreactivity TrkB. Mutations in the Shc ($Y^{515}F$) and PLCγ ($Y^{816}F$) sites did not affect the phosphorylation of the YxxxYY residues and cells remain positive for pTrk-kin (Shc, PLCγ, Shc- PLCγ). Confocal images; scale bar: 100 μm.

Figure 7. Constitutive activation of TrkB by overexpression and immunoreactivity profile of anti-pTrk-PLCγ.
Immunostaining of HEK293 cells expressing either TrkB wildtype or indicated TrkB mutants. Cells were co-transfected with GFP. Immunofluorescence of GFP (green) and pTrk-PLCγ (red, anti-pY785-TrkA (anti-pY816-TrkB) C67C8), and a DAPI counterstain (blue). Cells were immunostained 48 h after transfection. Confocal images; scale bar: 100 µm. In kinase-dead TrkB mutants (ATP, YD-ATP) TrkB remains unphosphorylated. This shows that the antibody is phospho-specific in TrkB. Constitutive phosphorylation is seen in all other mutants, albeit at different intensities. A directed missense mutation at the PLCγ-site ($Y^{816}F$) creates a phospho-independent, immunoreactive site after paraformaldehyde fixation.

Figure 8. Constitutive activation of TrkB by overexpression and immunoreactivity profile of anti-pTrk-Shc.
Immunostaining of HEK293 cells expressing either TrkB wildtype or indicated TrkB mutants. Cells were co-transfected with GFP. Immunofluorescence of GFP (green) and pTrk-Shc (red, anti-pY490-TrkA (anti-pY516-TrkB) C35G9), and a DAPI counterstain (blue). Cells were immunostained 48 h after transfection. Confocal images; scale bar: 100 μm. In kinase-dead TrkB mutants (ATP, YD-ATP) TrkB remains unphosphorylated. This shows that the antibody is phospho-specific in TrkB. Constitutive phosphorylation is seen in all other mutants, albeit at different intensities. A directed missense mutation at the Shc-site ($Y^{515}F$) creates a phospho-independent, immunoreactive site after paraformaldehyde fixation (see Shc and Shc-PLCγ double mutant).

3.1.2. Effect of serum depletion on TrkB activation

Once the antibodies were verified, it was vital to check for TrkB functionality by stimulating the receptor with brain-derived neurotrophic factor (BDNF), the natural ligand for TrkB. On transient transfection of HEK293 with wildtype mouse TrkB (TrkB-wt), it was seen that TrkB was highly expressed and phospho-active in these cells (as depicted in the Trk western blot-lanes 1 to 6 in Figure 9A) as expected (Dewitt et al, 2014; Watson et al, 1999).
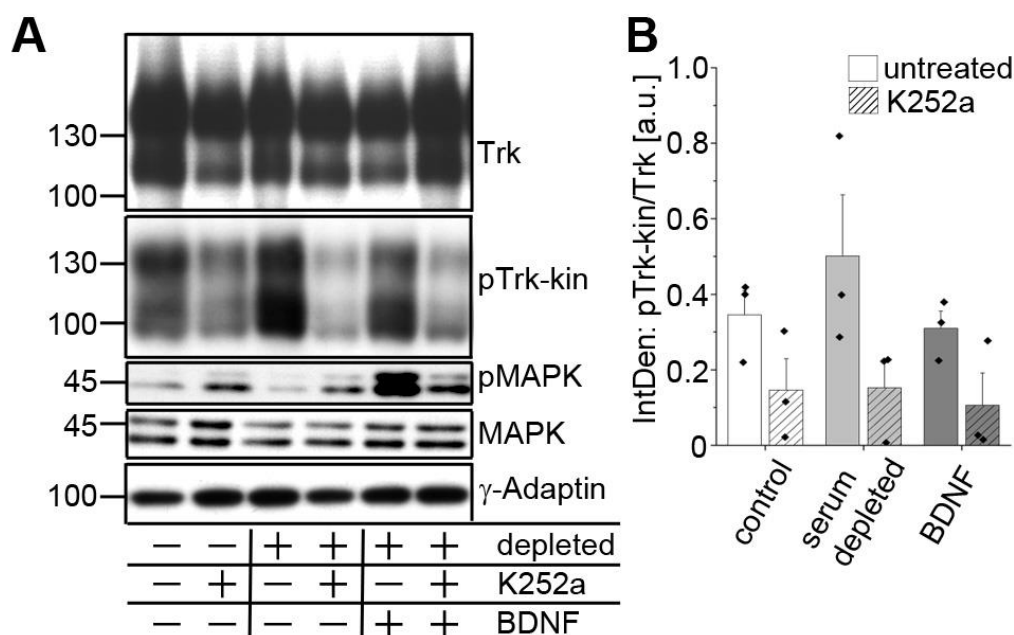
Figure 9. Self-activation of TrkB in absence of a ligand.

A. TrkB phosphorylation in absence of BDNF is unaffected by serum depletion. Western blotting of whole-cell lysates generated from HEK293 cells expressing TrkB. Control cultures were kept in serum before total lysates were produced. Cell cultures were treated as indicated. Serum-depletion was performed for 3h. To inhibit TrkB kinase activity, cultures were preincubated with 150 nM K252a, a Trk kinase inhibitor, for 30 min. DMSO served as solvent control. When indicated, cells were also treated with 10 nM BDNF for 15 min and were compared with BDNF stimulated cells under K252a treatment.

B. Quantification of western blots for pTrkB-kin normalized to total TrkB levels with densitometry. Relative integrated densities are shown. K252a treatment for 30 min caused a reduction in TrkB phosphorylation levels under control, serum-depleted and BDNF-stimulation conditions. Bar graph: mean ± SEM, overlaid with single data points; n = 3.

Immunoblotting of pTrk was performed with α–pTrk-kin, an antibody detecting phosphorylation at Y^{705} and Y^{706} in TrkB. Total and pTrk appeared at 130 kDa, representing the glycosylated TrkB kinase, and 90 kDa, typically representing the immature TrkB (Watson

et al., 1999). Some samples were also treated with BDNF. Interestingly TrkB was phosphorylated even in the absence of BDNF (lanes 1 to 4 in Figure9A). To further eliminate the possible role of serum components in the activation of TrkB, the cells were serum depleted for 3 h prior to lysis. As shown here in Figure 9A, in all cases (serum depleted, serum undepleted, BDNF stimulated and BDNF unstimulated), TrkB was phosphorylated. Treatment of HEK293-TrkB cells with 150 nM K252a for 30 min could acutely reduce TrkB phosphorylation (lanes 2, 4 and 6). The small-molecule K252a is a prototypical and potent Trk inhibitor (Tapley *et al*, 1992). Stimulation with 20 ng/ml BDNF could not further increase the pTrkB-kin levels (lane 5) as compared to undepleted and depleted conditions (lanes 1 and 3). Quantification of these blots indicate a reduction in TrkB phosphorylation on K252a treatment (shown in 9B). This shows that during TrkB overexpression, K252a interrupts an ongoing kinase activity in the absence of neurotrophins. Serum depletion was not sufficient to stop the constitutive activity of overexpressed TrkB, but MAPK phosphorylation downstream of TrkB was reduced (Figure 9A).

3.1.3. Role of Tyr^{705} in TrkB self-activation

Soluble Insulin/IGF-1 receptor kinases were shown to be primed to rapid auto-phosphorylation by an increase in the local concentration of both phosphoryl donor and phosphoryl acceptor sites (Baer *et al*, 2001). This is achieved by a conformational change of the activation loop after dimerization, which leads to an efficient transphosphorylation of the regulatory tyrosine residues in the absence of the ligands.

For a better understanding of what was happening to these highly phospho-active TrkB cells, immunolabelling techniques were employed and cells were imaged at a higher magnification (60×). After an expression time between 30–48 h, in the absence of neurotrophins, the cells were triple-labelled for TrkB, phospho-TrkB-PLCγ and filamentous actin (F-actin). F-actin was stained with a phalloidin-Cy5 conjugate and was used to evaluate the gross morphology of the cell. Cells expressing TrkB-wt showed not only a pronounced phosphorylation signal, but also a round cell body (Figure 10, for higher resolution see Figure 11). In contrast, cells expressing the Y^{705}-TrkB mutant (TrkB-YFY) did not show the phosphorylation at the PLCγ-site (pPLCγ), indicating a reduction of autophosphorylation in this mutant.

Another surprising observation was the changes in cell morphology on TrkB-wt expression (Figure 10, 11). Here, the TrkB-wt cells appeared roundish and were lacking the characteristic filopodia or filamentous appearance of HEK293 cells as seen in the YFY mutant cells. This was further confirmed by phalloidin staining. Phalloidin-Cy5 conjugate binds to F-actin and it could be seen that the phospho-active TrkB-wt cells also appeared roundish with this stain.
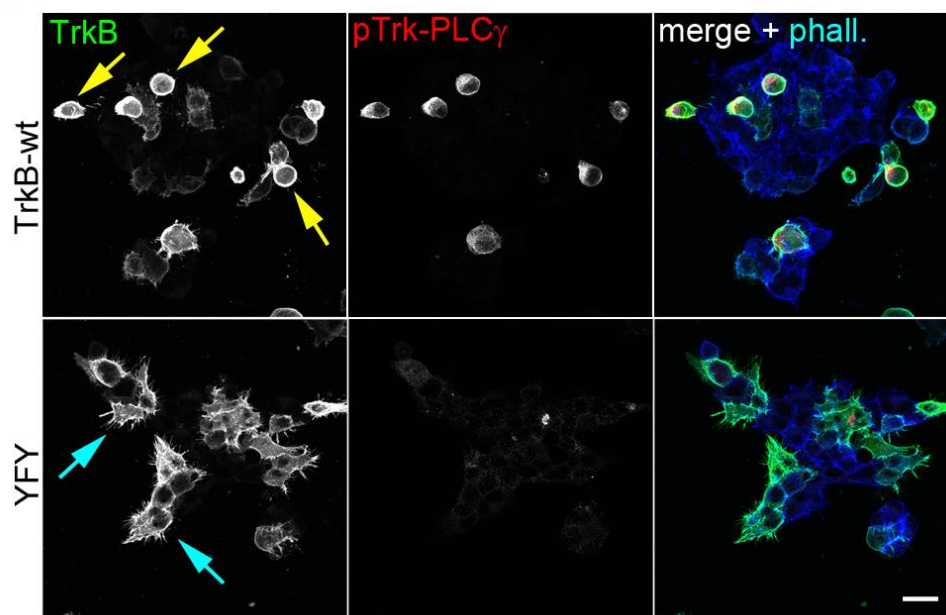

Figure 10. Self-activation of TrkB causes changes in cell morphology.
In the absence of neurotrophins, TrkB overexpression induces TrkB phosphorylation and changes in cell morphology. Immunofluorescence of TrkB receptor (green) and pTrk-PLCγ (red). F-actin was labelled with Acti-stain-670 phalloidin (blue). HEK293 cells were transfected with either TrkB-wildtype or TrkB-YFY kinase mutant. Cells were immunostained after 30h. Yellow arrows point to roundish, pTrk-positive cells. Cyan arrows point to filamentous, pTrk-negative cells. Confocal images; scale bar: 25 μm.
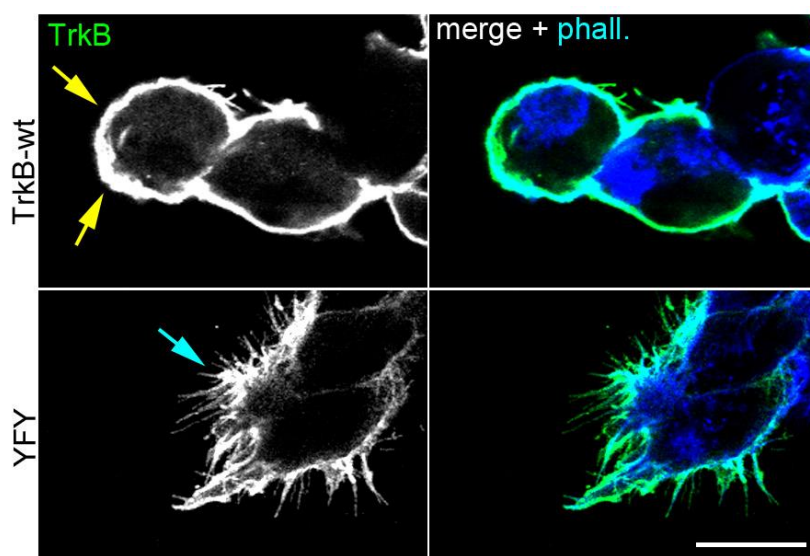
Figure 11. High resolution image. Self-activation of TrkB causes changes in cell morphology.
Filopodia phenotype of TrkB expressing cells (high-resolution confocal stack image of Figure 10). Confocal images; scale bar: 25 μm.

3.1.4. Self-active TrkB alters cell morphology

To further confirm the fact that phospho-positive TrkB cells change the cellular morphology as compared to the phospho-inactive ones, the various TrkB mutants were triple labelled for TrkB, phospho-Trk and filamentous actin (F-actin) and imaged at high resolution (Figure 12). Typically, the cells that were phospho-Trk positive (red) appeared to be roundish, while the kinase dead (ATP) and the kinase domain mutants (YFY and YFF) were filamentous. Surprisingly, the YYF mutant was active and roundish, perhaps indicating a role of the Y^{705} and not the Y^{706} in this particular cellular phenomenon. The constitutive active (YDY) behaved much like the wildtype and both seemed to lose this round morphology after undergoing 30 min K252a treatment. This means that this cellular spectacle is reversible and is due to the receptor's inherent kinase activity. Moreover, mutation in the Shc, PLCγ or TIAM/Rac1/CDC42 interaction (S^{478}A mutant) sites showed a roundish cell shape. S^{478} phosphorylation of TrkB regulates its interaction with the Rac1-specific guanine nucleotide exchange factor TIAM1, leading to activation of Rac1 and phosphorylation of S6 ribosomal protein, for instance during activity-dependent dendritic spine remodeling (Lai *et al*, 2012). Even the double mutant TrkB-Shc-PLCγ destroyed the filopodia-like phenotype, altogether signifying that the classical Shc/PLCγ signaling and TIAM pathways of TrkB (Chao, 2003; Huang & Reichardt, 2003) did not cause this change in cell morphology.
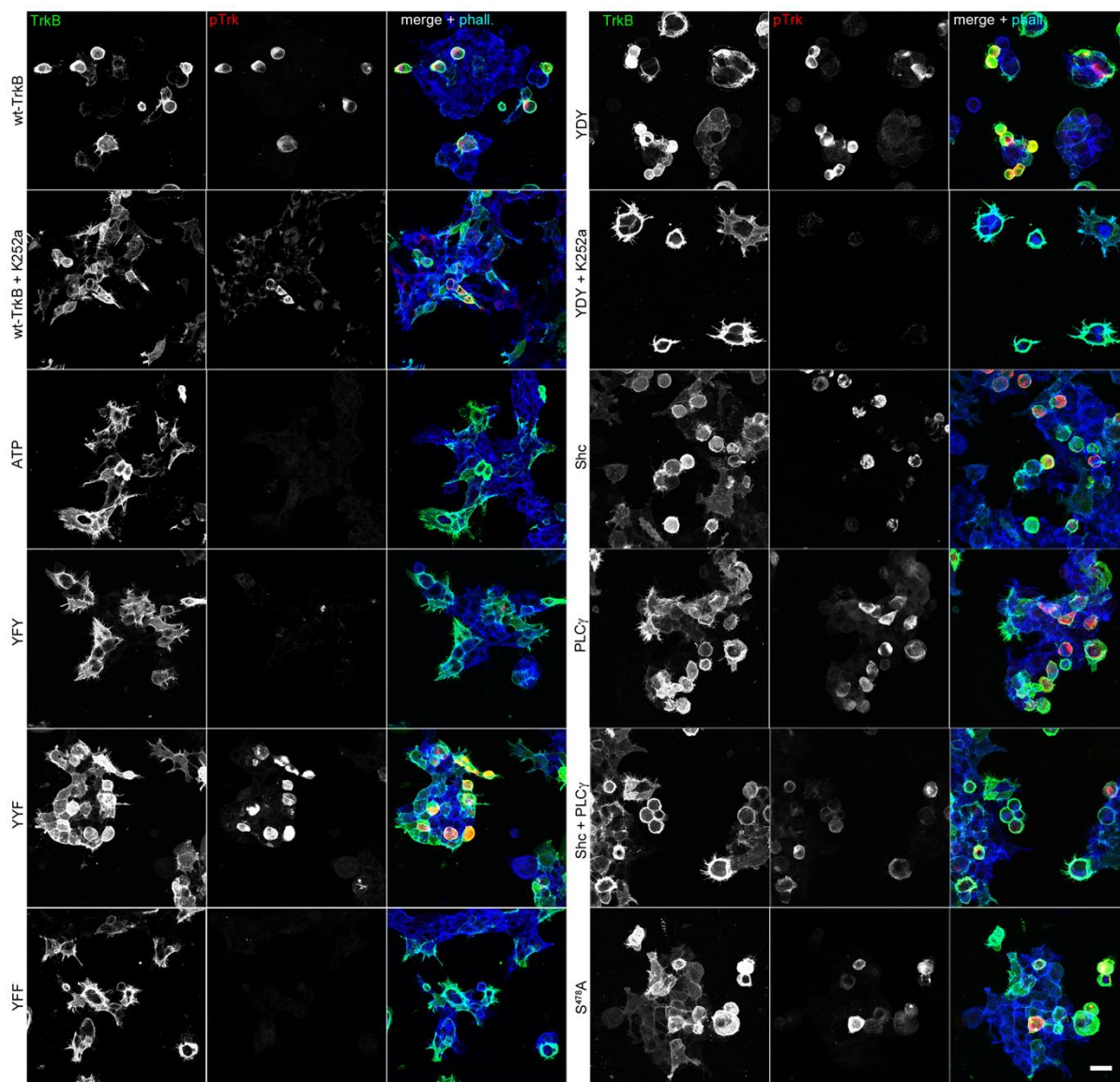
**Figure 12. Abundance-dependent self-activation of TrkB kinase induces changes in actin morphology.**
Round-shaped cells express kinase-active TrkB mutants. Immunostaining of HEK293 cells expressing either TrkB wildtype or indicated TrkB mutants. Immunofluorescence of TrkB receptor (green) and pTrk-PLCγ (red). PLCγ (Y^{816}F) mutants (TrkB-PLCγ, TrkB-Shc-PLCγ) were stained with pTrk-kin (red). F-actin was labelled with Acti-stain-670 phalloidin (blue). Typically, filamentous cells express the kinase-dead ATP mutant of TrkB or the YxxxYY mutants (YFY and YFF). Treatment with 150 nM K252a for 30 min reverses the round shape of cells expressing TrkB wt or TrkB-YDY. Confocal images; scale bar: 25 µm.

A quantification (Figure 13) of these conditions was done by counting 10 fields of view of immunofluorescence staining (as shown in Figure 12) for each mutant. This shows that interfering with the receptor's kinase activity within the kinase domain, reverses the cell morphological changes caused by phospho-active TrkB. This is further visualized in Figure 14, which focuses on total TrkB labels alone (from Figure 12).
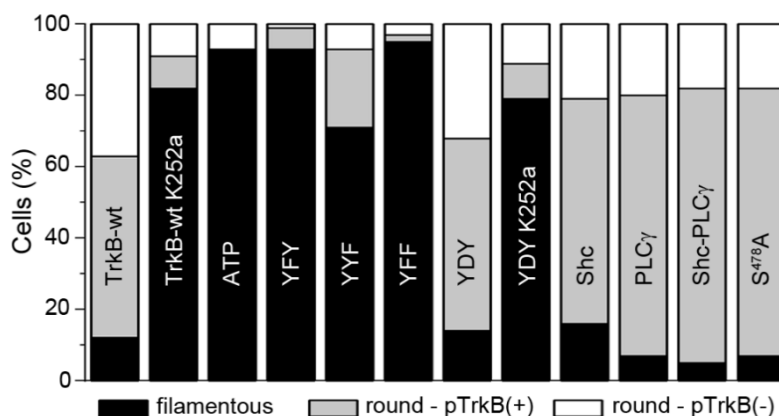
Figure 13. Quantification of the percentage of cells showing either a round shape or typical filopodia.
Round cells were further subdivided into those that were either positive (+) or not (-) for pTrk. Stainings with anti-pTrk and Acti-stain-670 phalloidin in corresponding TrkB mutants are given in Figure 12. Data acquired from 10 fields of view in 3 independent experiments. Scale bar: 25 μm.
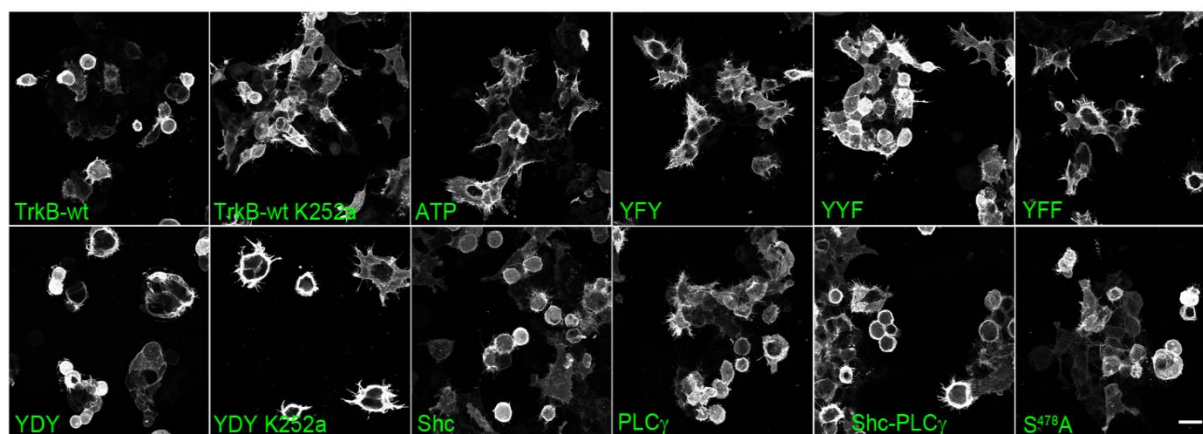
Figure 14. Round-shaped cells express kinase-active TrkB mutants.
Immunostaining of HEK293 cells expressing either TrkB-wt or indicated TrkB mutants. Cells expressing TrkB-wt or the constitutive active mutant TrkB-YDY were also subjected to K252a treatment. Typically, filamentous cells express the kinase-dead ATP mutant of TrkB or the YxxxYY mutants (YFY and YFF). Treatment with 150 nM K252a for 30 min reverses the round shape of cells expressing TrkB-wt or TrkB-YDY. Confocal images; scale bar: 25 μm.

3.1.5. An abundance of TrkB causes auto-phosphorylation

It is known that overexpression of Trk or other receptor tyrosine kinases can lead to auto-activation (Lemmon & Schlessinger, 2010). Baer et al., have shown that an increase in the local concentration of kinase molecules can lead to an increased rate of trans-phosphorylation, resulting in a more efficient activation of the kinase (Baer *et al.*, 2001). To test for abundance effects, TrkB was overexpressed in HEK293 cells and labelled with either TrkB or pTrkB-kin. The integrated density of corresponding immunolabels was determined on the single cellular level in confocal microscope images using ImageJ. The data confirmed a linear, statistically significant correlation between the abundance of TrkB and pTrkB-kin intensity, despite a rather large variation in single data points (Figure 15).
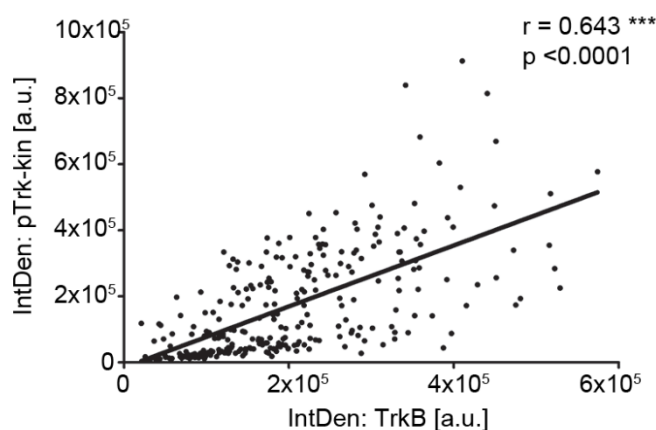
Figure 15. TrkB phosphorylation correlates with TrkB abundance.
Linear, positive correlation of the integrated density of α–TrkB and α–pTrkB-kin immunoreactivity in TrkB-expressing HEK293 cells. Immunolabels per cells were measured as integrated density per cell from maximum intensity projection images of confocal z-stacks. Shown are single cell data, n = 280 cells; data collected from 20 confocal image fields and 4 cell cultures.

3.1.6. Self-active TrkB modifies actin cytoskeleton

It is clear from the data so far that, when overexpressed in HEK293, TrkB undergoes activation in absence of a ligand. It does so when the receptor is in abundance. Additionally, it seemed that this self-activation changed the morphology of these cells. Thus, in order to further understand the probable actin-cytoskeletal changes associated with these changes in cell morphology, confocal live cell imaging was performed (Figure 16).
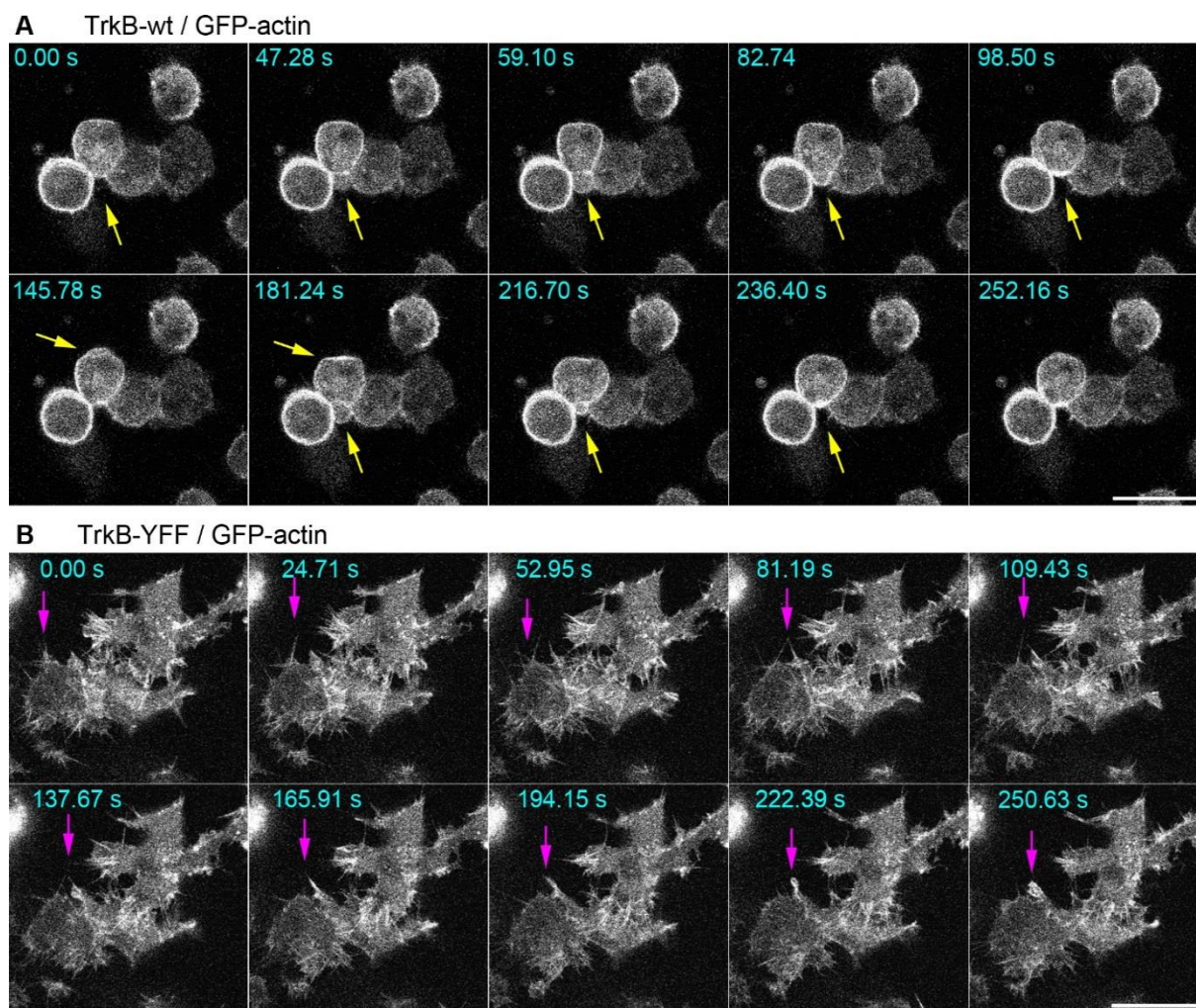
Figure 16. Mutating of the YxxxYY-motif in TrkB restores actin filopodia dynamics.

A, B Overexpression of TrkB kinase induces a round-shaped cell morphology and loss of actin filopodia dynamics. HEK293 cells co-expressing GFP-actin and TrkB-wt (in A) or the TrkB-YFF mutant (in B). Time-lapse images (in seconds) are shown. Living cells were imaged using a confocal laser-scanning microscope. GFP-actin was excited with a 488 nm laser line and fluorescence was detected with a spectral detector (510 – 570 nm). (In A) Arrows point to a roundish cell that forms typical blebs. (in B) Arrow points to typical dynamic filopodia, labelled by GFP-actin. Scale bar: 25 µm.

Cells were co-transfected with TrkB and TrkB mutants (here representatively shown is the mutant TrkB-YFF) and GFP-actin. In TrkB-wt cells, two phenotypes were characteristically observed: (1.) round cells displaying very less GFP-actin dynamics, or (2.) some single cells forming bleb-like structures (Figure 16A). Bleb formation is a type of cell motility that is observed when the cytoskeleton is decoupled from the plasma membrane (Charras *et al*, 2006; Parsons *et al*, 2010). In contrast, cells expressing TrkB-YFF showed typical actin filopodia dynamics (Figure 16B). Thus, it could be concluded that, actin filopodia formation is disturbed in TrkB overexpressing cells.

TrkB protein is expressed either as the TrkB full-length receptor kinase or as the kinase-deficient TrkB splice isoform TrkB-T1 (Klein *et al*, 1991b; Middlemas *et al.*, 1991). TrkB-T1 has the complete extracellular region and transmembrane domain of its full-length counterpart, but carries only a short cytoplasmic tail of 23 amino acids. Overexpression of TrkB-T1 (Rose *et al*, 2003) did not round-up the cells and did not destroy filopodia formation (Figure 17B). Overexpression of TrkA and TrkC, the TrkB isoforms, also formed a roundish cell shape (Figure17C,D). This further strengthened the idea that, the destruction of actin filopodia dynamics in HEK293 cells, depends on Trk kinase activity and is not caused by the ligand-binding domain or the transmembrane domains of the receptor.
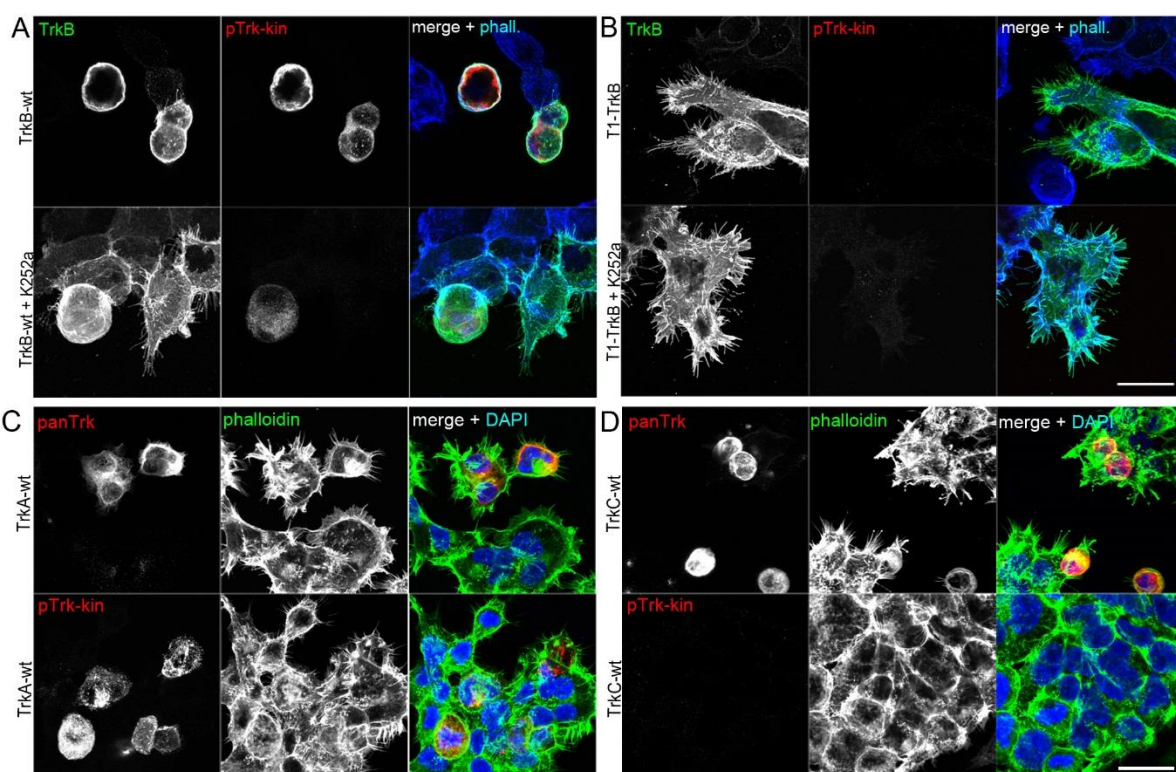
Figure 17. Filopodia formation is preserved in the kinase deficient TrkB-T1 expressing cells, but not in Trk kinase expressing cells.

A, B TrkB overexpression causes changes in actin morphology of HEK293 cells. This effect can acutely be reversed by the Trk inhibitor K252a. HEK293 cells expressing the kinase-deficient, truncated slice variant TrkB-T1 remain phospho-inactive and filamentous for control and K252a-treated conditions. Immunofluorescence of TrkB receptor (green) and pTrk-kin (red). F-actin was labelled with Acti-stain-670 phalloidin (blue). Confocal images; scale bar: 25 µm.

C, D TrkA and TrkC kinase overexpression leads to roundish cells. Immunofluorescence of panTrk receptor or pTrk-kin (red). Note that TrkC autophosphorylation is not detected by anti-pTrk-kin. F-actin was labelled with Acti-stain-670 phalloidin (blue). Confocal images; scale bar: 25 µm.

3.1.7. Accumulation of pTrkB at intracellular sites

Confocal imaging of the TrkB phosphorylation signal suggested that most of the phospho-Trk-wt signal derived from intracellular sites (Figure 11). For this reason, a series of experiments were performed to test whether TrkB self-activation indeed occurs at intracellular sites. First, TrkB-wt and the kinase-dead TrkB-ATP was expressed in HEK293 cells. Western blotting confirmed TrkB-wt at 90 and 130 kDa. However, the TrkB-ATP mutant appeared exclusively at 130 kDa (Figure 18A). The 90 kDa band of TrkB-wt can be probed with antibodies against the amino- and carboxyterminal end of the receptor suggesting that the 90 kDa band showed a lower level of glycosylation and was not a degradation product, but rather the well-described immature isoform of TrkB (Klein *et al.*, 1991b). To further test how glycosylation affects the relative molecular weight and autophosphorylation, first four (TrkB^{4gly}), then seven (TrkB^{7gly}) and finally 12 (TrkB^{12gly}) predicted N-glycosylation sites were mutated. Mutation of the N-glycosylation sites led to a reduced relative molecular weight, while preserving the self-activation by overexpression phenomenon. (Figure 18B).
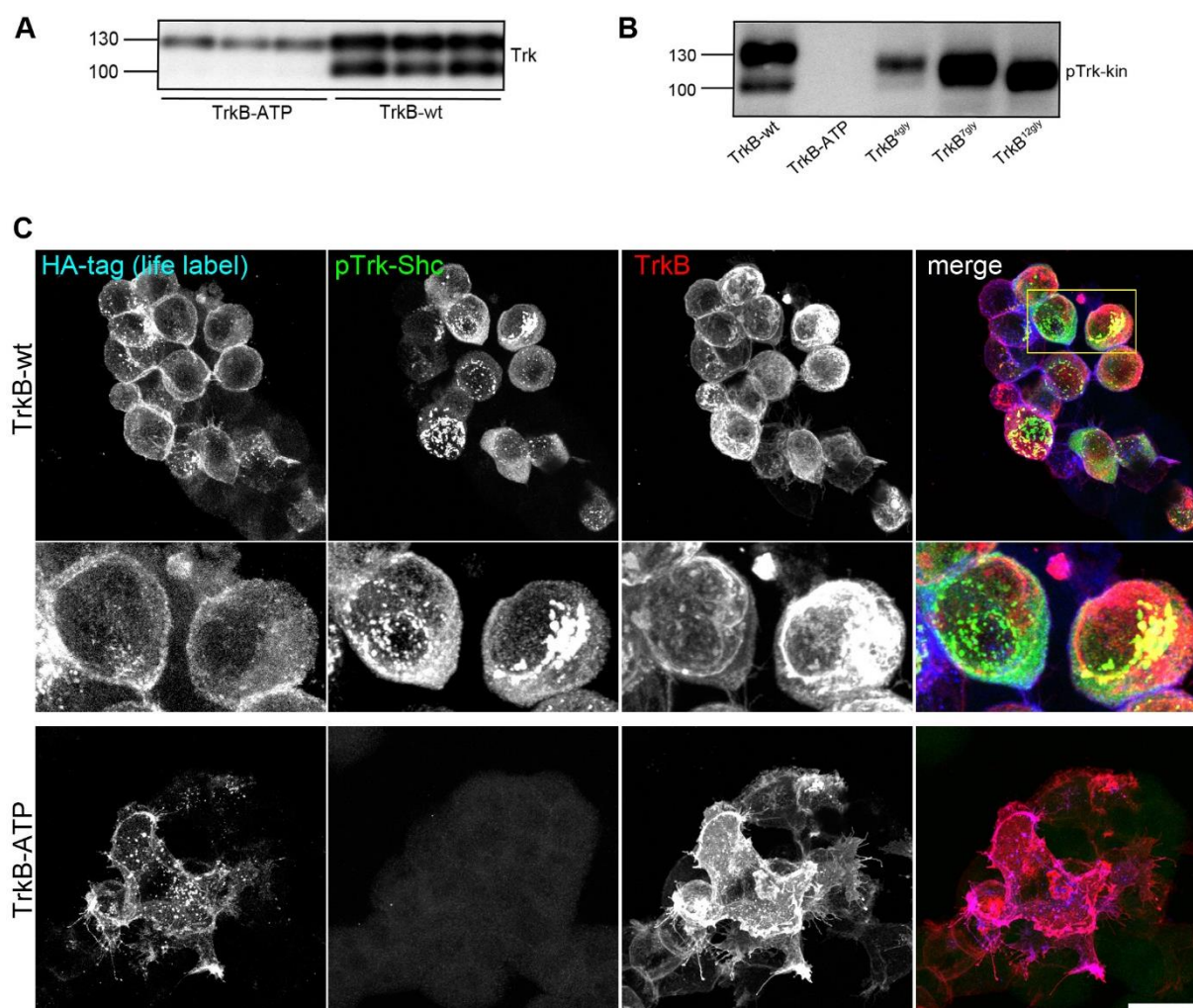
Figure 18. Intracellular localization and delayed glycosylation of constitutive active TrkB.

A Western blotting of whole-cell lysates generated from HEK293 cells expressing TrkB-wt or the kinase dead mutant TrkB-ATP. After transient transfection, TrkB was expressed for 30 h. Lysates were probed with anti-panTrk, an antibody that detects TrkB at the intracellular C-terminus. TrkB-ATP shows a Mr of about 130 kDa, while TrkB-wt also runs at 90 kDa, a western blotting band typical for immature TrkB.

B Western blotting of whole-cell lysates generated from HEK293 cells expressing TrkB-wt, the kinase dead mutant TrkB-ATP or the TrkB-glycosylation mutants. After transient transfection, TrkB was expressed for 30 h. Lysates were probed with anti-pTrk-kin. All mutants are self-activated except for the kinase dead ATP mutant. The glycosylation mutants appear at different heights depending on the number of mutated sites (higher the number of mutations, shorter is the fragment).

C Life labelling of TrkB-wt and TrkB-ATP. Cells expressing TrkB were life-labelled via an extracellular HA-tag for 15 min. Then cells were fixed and postlabeled with pTrk and anti-TrkB. Note accumulation of pTrk at intracellular, perinuclear sites and in vesicular clusters (cyan arrows).

For cell surface live labelling of TrkB, a hemagglutinin-affinity (HA) tag was cloned between the signal peptide and the amino-terminal end of TrkB. It is known that putting an HA-tag at this side of the TrkB receptor does not disrupt its functionality (Nikoletopoulou *et al*, 2010). Living HEK293 cells expressing either HA-TrkB-wt or the mutant HA-TrkB-ATP were incubated with an HA-antibody for 15 min at 37°C. Cells were washed to remove residual α-HA, fixed, permeabilized with Triton X100 and labelled against total TrkB and pTrk-Shc. Secondary antibodies against all three labels were added after permeabilization. High-resolution confocal microscopy showed that cell surface labels against the HA-tag barely overlap with pTrk, thus verifying that most of the pTrk signal was labelled at intracellular sites (Figure 18C). In cells expressing HA-TrkB-ATP, the cell surface label was also present in filopodia (Figure 18C) and in vesicle-like structures that are typical after cellular uptake of cell-surface bound antibody/receptor complexes at 37°C (Blum & Lepier, 2008).Vesicle-like pTrk signals were not co-labelled by anti-TrkB (strongly labelled vesicles in the color-merged image), indicating that these pTrk signals do not carry the epitope for the receptor domain or were not accessible for the label.

3.2 Self-active TrkB signals to Focal Adhesion Kinase (FAK)

The blebs observed in actin live cell imaging (Figure 16) raises the question of whether self-active TrkB kinase induces the phosphorylation of proteins involved in actin dynamics (Blanchoin *et al*, 2014; Parsons *et al.*, 2010). To this effect, diverse TrkB mutants were again overexpressed in HEK293cells and probed for total cellular protein with α−Trk and α−pTrk-PLCγ. Furthermore, these lysates were tested for phosphorylated cofilin, a protein involved in reorganization of F-actin (Shah & Rossie, 2018), and focal adhesion kinase (FAK), a cytosolic tyrosine kinase regulating focal adhesion site assembly, membrane protrusion formation and cell motility (Parsons *et al.*, 2010).

3.2.1. Intact TrkB kinase domain phosphorylates FAK
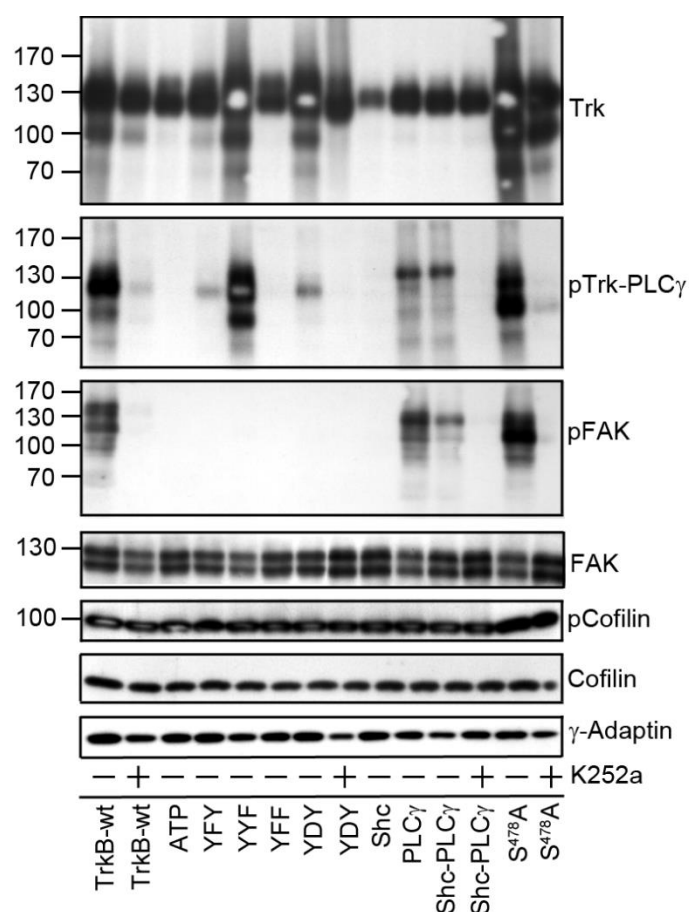
Figure 19. Self-active TrkB is upstream of focal adhesion kinase (FAK) phosphorylation.

Self-active TrkB with an intact kinase domain induces phosphorylation of focal adhesion kinase (FAK), a key player of actin dynamics, but not of Cofilin. Western blotting of whole-cell lysates generated from HEK293 cells expressing indicated TrkB mutants. To inhibit TrkB kinase activity, cultures were preincubated with 150 nM κ252a for 30 min. DMSO served as solvent control. Antibodies against total FAK, Cofilin and γ-Adaptin served as loading control.

Cofilin phosphorylation inhibits cofilin binding to F-actin, leading to F-actin stabilization. Cofilin dephosphorylation stimulates F-actin depolymerization and severing which then promotes actin-nucleation (via Arp 2/3), initiating additional actin assembly, and directional motility (Huang *et al*, 2006). Anti-phospho-Cofilin immunoblotting was inconspicuous, but a strong phosphorylation of FAK at Y576/577 was seen in TrkB-wt expressing cells (Figure 19). Cells expressing the kinase-dead TrkB-ATP mutant or cells expressing TrkB with a site-directed missense mutation in Y^{705} or Y^{706} did not show phosphorylation of FAK.
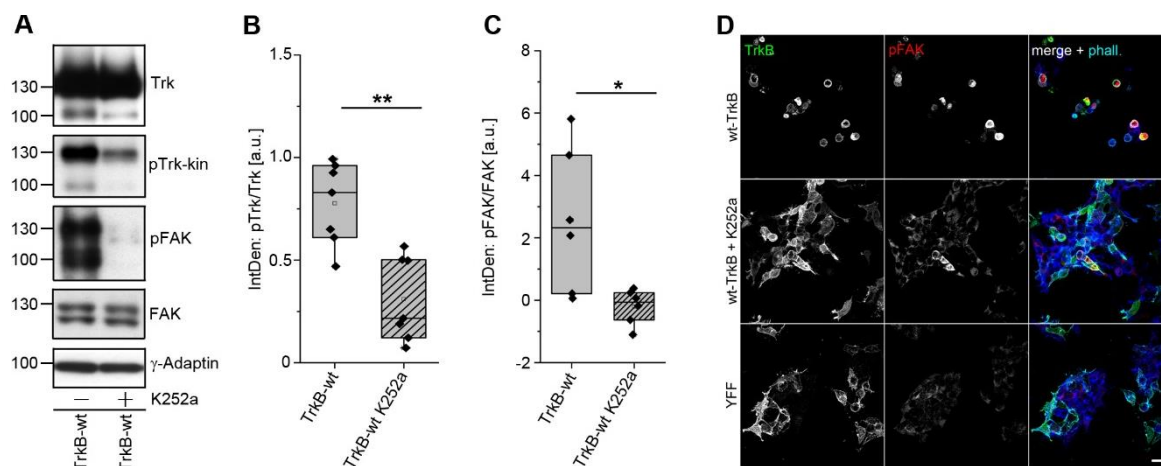
Figure 20. Self-active TrkB induced phosphorylation of FAK can be acutely blocked with K252a.

A Self-active TrkB induced phosphorylation of FAK can acutely be blocked with the Trk kinase inhibitor K252a. Western blotting of whole-cell lysates generated from HEK293 cells expressing TrkB-wt. To inhibit TrkB kinase activity, cultures were preincubated with 150 nM K252a for 30 min. DMSO served as solvent control.

B Quantification of western blots for pTrkB-kin normalized to total TrkB levels with densitometry. Relative integrated densities are shown. K252a treatment causes a reduction in TrkB phosphorylation levels. Bar graph: mean ± SEM, overlaid with single data points; n = 7; p = 0.00104.

C Quantification of western blots for pFAK normalized to total FAK levels with densitometry. Relative integrated densities are shown. K252a treatment causes a reduction in FAK phosphorylation levels. Bar graph: mean ± SEM, overlaid with single data points; n = 6; p = 0.03186.

D Immunofluorescence of TrkB receptor (green) and pFAK (red). F-actin was labelled with Acti-stain-670 phalloidin (blue). HEK293 cells were transfected with either TrkB-wildtype or TrkB-YFY kinase mutant. TrkB-wildtype cells were also treated with K252a for 30 min. Cells were immunostained after 30h; scale bar: 25 µm.

FAK activation is involved in signal-mediated effects on actin polymerization, the assembly, or disassembly of focal contacts and the regulation of protease activation or secretion (Mitra *et al*, 2005). As kinase-deficient TrkB mutants or YFY mutants did not show pFAK activation, it was not surprising that FAK phosphorylation could be acutely inhibited by the Trk inhibitor K252a (Figure 20A), indicating that the event is downstream of active TrkB. Western blotting showed reduced intensity of phospho-proteins levels on 30 min K252a treatment of TrkB

expressing cells. Total Trk, FAK and γ-Adaptin levels remained constant. This was further confirmed by quantitative analysis of the western blot results (Figure 20B-C). These are data from seven independent experiments and indicate that K252a inhibition significantly reduces the phosphorylation of the TrkB kinase receptor and consequently of downstream FAK phosphorylation. Studies have found that FAK could be activated by either ECM or growth factors, and that tyrosine phosphorylation of FAK was a rapid event that was associated with the formation of focal contacts (Parsons, 2003). Immunofluorescence labelling of pFAK confirmed the round phenotype of pFAK-positive cells expressing TrkB-wt (Figure 20D). Treatment with K252a turned off the pFAK and cells appear more filamentous, just as in the YFF mutant (Figure 20D) further corroborating the western results.

3.2.2. Intracellular domain (ICD) of TrkB induces FAK phosphorylation

Most of the self-active pTrkB was found at intracellular sites (Figure 18). As FAK is a cytosolic protein kinase, it became apparent to test whether cytosolic expression of the intracellular domain of TrkB would be sufficient to induce FAK phosphorylation. For this purpose, two prototypical intracellular kinase domain constructs were cloned and expressed in HEK293 cells. One, TrkB-ICD, carried the complete intracellular domain of TrkB (K^{454} to C-terminal end). The other, Myr-ICD, consisted of the TrkB ICD coupled to an aminoterminal myristoylation (Myr) / S-acylation targeting motif, combined with a GGSGG-linker sequence. This motif was used to target Myr-ICD to the plasma membrane (Kabouridis *et al*, 1997; Lemmon & Schlessinger, 2010; Rathod *et al*, 2012) (Figure 21A).
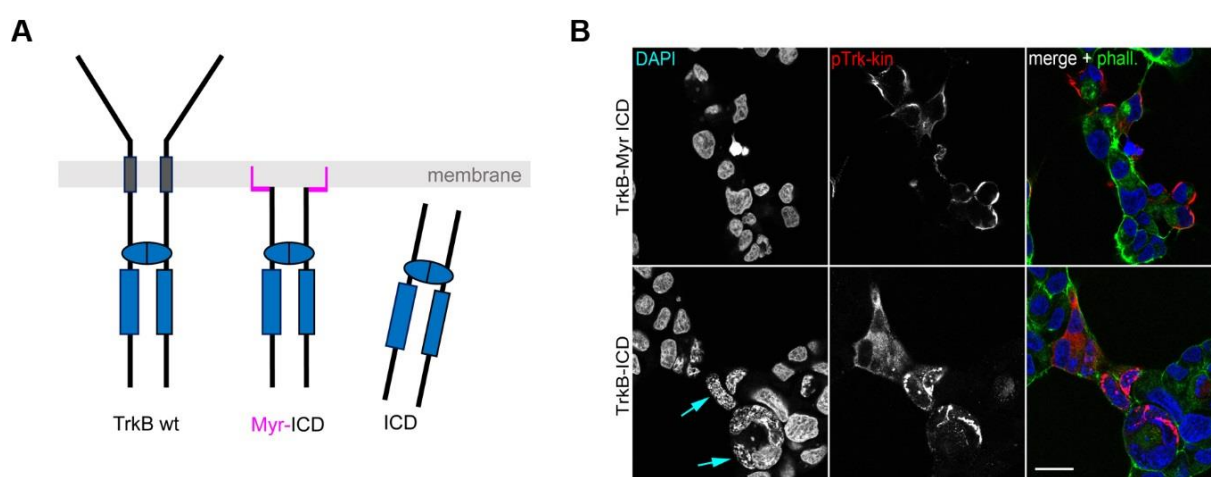
Figure 21. The intracellular domain (ICD) of TrkB undergoes self-activation.

A Intracellular, kinase-active domain constructs of TrkB. In Myr-ICD, an N-terminal myristoylation consensus motif with a glycine-serine (GGSGG)-linker was used to target the ICD to the plasma membrane. In contrast to TrkB-wt, the ICD (intracellular domain) construct lacks the ligand-binding and transmembrane domain.

B TrkB-ICD and TrkB-Myr-ICD undergo self-activation but differ in their cellular localization pattern. Immunofluorescence of pTrk-kin (red) and DAPI (blue). F-actin was labelled with Acti-stain-670 phalloidin (phall, green). HEK293 cells were immunostained 30 h after transfection. TrkB-ICD is preferentially seen at intracellular sites. The Myr-ICD construct shows typical plasma membrane targeting. Note morphology changes in Dapi of ICD-expressing cells, indicating changes in chromatin compaction (cyan arrows). Confocal images; scale bar: 20 μm.

Both, the ICD and the Myr-ICD, constructs were expressed in HEK293 cells and subsequent immunolocalization experiments were performed (Figure 21B). Immunolabelling confirmed that both, TrkB-ICD and Myr-ICD were phosphoactive at Y^{705}/Y^{706}, albeit the cellular localization profile was different. It has been previously shown that the autophosphorylation rate depends on the ICD concentration and the mechanism is a sequential *cis/trans* phosphorylation (Iwasaki *et al.*, 1997). As is seen in Figure 21B, TrkB-ICD appeared at intracellular sites throughout the cytosol, while phospho-active Myr-ICD outlines the cell surface, indicating its efficient targeting to the plasma membrane from the intracellular site.

Furthermore, ICD and Myr-ICD total protein lysates were probed with diverse antibodies (Figure 22A). TrkB-wt and TrkB-YFF mutant was also probed along with them. Western analysis confirmed that ICD-protein and Myr-ICD were phospho-active and migrated at the predicted relative molecular weight of 40-45 kDa. Surprisingly, the ICD domain was sufficient to cause a dramatic induction of p-FAK phosphorylation at Y^{397} in the range of $100 - 130$ kDa, while MAPK phosphorylation was not induced. In striking contrast, Myr-ICD caused almost no pFAK signal but led to the typical brief activation of MAPK. Again, TrkB-wt was able to induce both, pFAK and pMAPK, and K252a could reduce pTrk and pFAK signals (Figure 22B-C). The kinase mutant TrkB-YFF did not show pFAK activation, but supported MAPK phosphorylation (Figure 22D).

It can thus be assumed that Myr-ICD TrkB protein, when targeted to the plasma membrane, can provide a platform for adapter proteins and thereby support ubiquitous Ras/MAPK signaling cascades, even in the absence of neurotrophins.
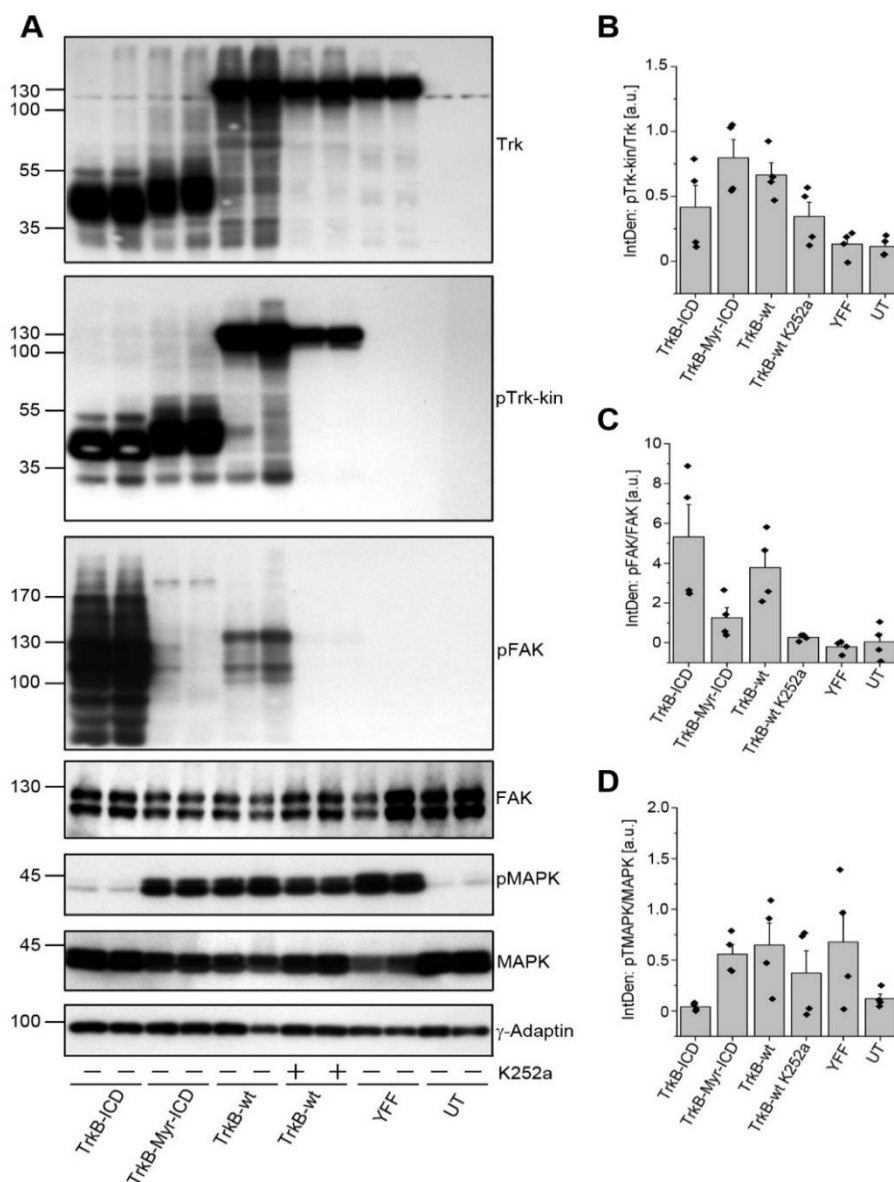
Figure 22. TrkB-ICD, but not TrkB-Myr-ICD induces FAK phosphorylation.

A TrkB-ICD, but not TrkB-Myr-ICD induces FAK phosphorylation. Western blotting of whole-cell lysates generated from HEK293 cells expressing TrkB-ICD, TrkB-Myr-ICD, TrkB-wt and TrkB-YFF. K252a was used to inhibit Trk kinase activity. TrkB-wt expression increases MAPK and FAK phosphorylation. ICD signals to FAK, but not MAPK. In striking contrast, Myr-ICD induces MAPK phosphorylation, but fails to activate FAK.

B-D Quantification of western blots for pTrkB-kin normalized to total TrkB levels (in B), pFAK to total FAK (in C) and pMAPK to total MAPK (in D). Relative integrated densities are shown. Bar graph: mean ± SEM, overlaid with single data points; n = 4.

3.3 Trk inhibitors acutely block Trk and cytosolic *NTRK2*-fusion signaling

The clinically approved Trk inhibitors LOXO-101 (Larotrectinib) and Entrectinib are used to suppress classical and oncogenic Trk activity (Doebele *et al.*, 2020; Drilon *et al.*, 2018) and thus it was essential to check whether they would also block downstream signaling of intracellular active TrkB. Here, all small molecule Trk inhibitors (K252a, LOXO-101 and Entrectinib) efficiently blocked constitutive TrkB activation and pFAK phosphorylation within 60 min (Figure 23A,B). Constitutive pMAPK activation by TrkB was efficiently blocked by LOXO-101 and Entrectinib (Figure 23B). The same was also seen in the case of SQSTM1-NTRK2, a cytosolic *NTRK2*-fucion (Figure 23C,D) when expressed in HEK293 cells.
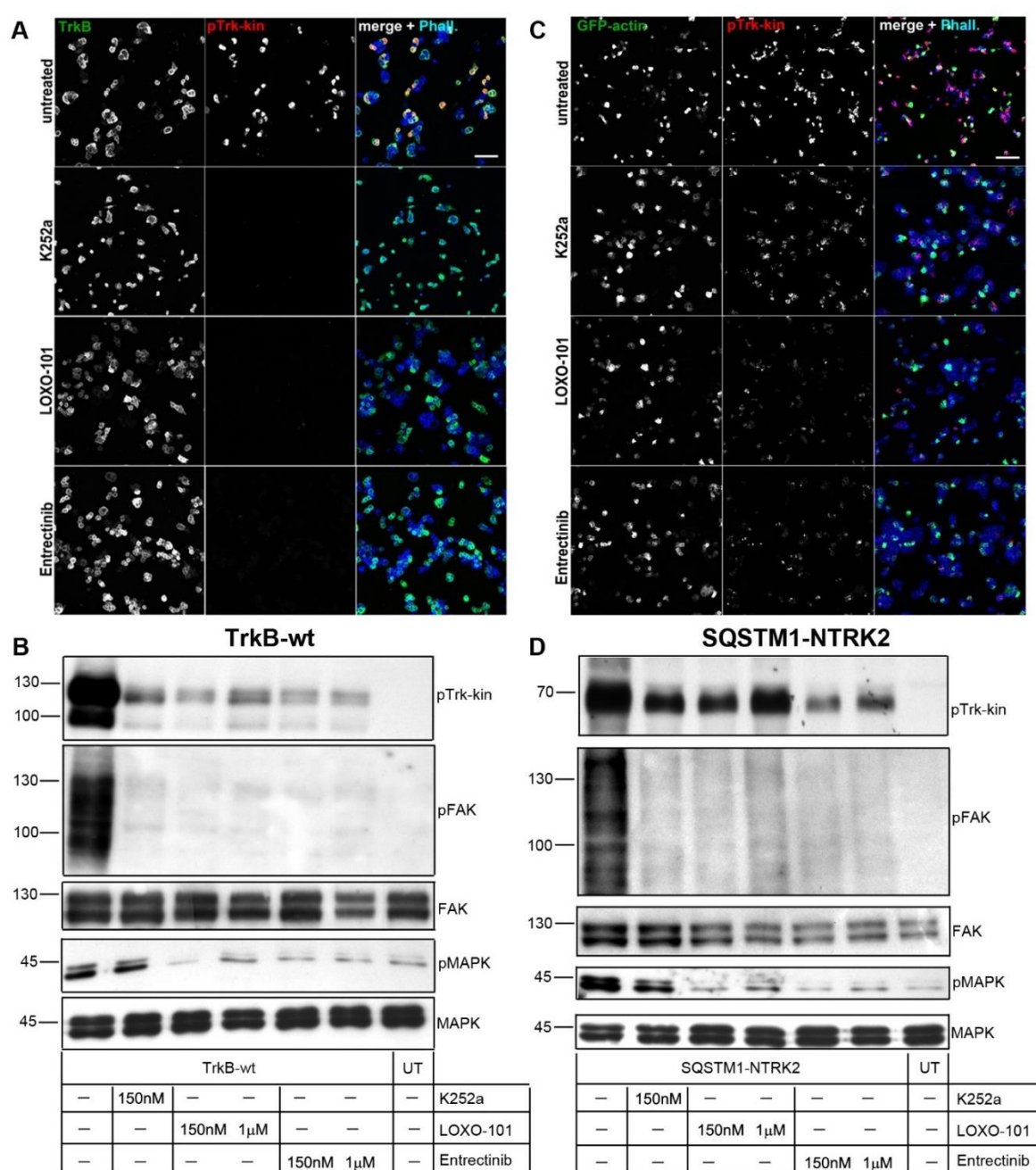
Figure 23. Treatment of TrkB-wt and SQSTM1-NTRK2, a TrkB fusion product, with small molecule Trk inhibitors reduces or hinders downstream Trk activated pathways.

A Immunostaining of HEK293 cells expressing TrkB-wt. Immunofluorescence of TrkB (green), pTrk-kin (red) and Acti-stain-670 phalloidin (phall, blue). Cells were treated with small molecule Trk inhibitors like K252a, LOXO-101 and Entrectinib. TrkB self-activity is reduced upon inhibitor treatment. Confocal images; scale bar: 100 μm.

B Western blotting of whole-cell lysates generated from HEK293 cells expressing TrkB-wt. After transient transfection, TrkB was expressed for 30 h and then treated with small molecule Trk inhibitors like K252a, LOXO-101 and Entrectinib (concentrations are as depicted). Lysates were probed with the indicated antibodies. Trk, FAK and MAPK activity is reduced upon inhibitor treatment.

C Immunostaining of HEK293 cells expressing a synthetically designed TrkB fusion construct – SQSTM1-NTRK2. This particular fusion product was chosen because it lacks the TrkB juxtamembrane domain and the Shc site, thereby making it primarily an intracellular protein with an intact kinase domain. Cells were co-transfected with GFP-actin. Immunofluorescence of GFP-actin (green), pTrk-kin (red) and Acti-stain-670 phalloidin (phall, blue). Cells were treated with small molecule Trk inhibitors like K252a, LOXO-101 and Entrectinib. TrkB fusion self-activity is reduced upon inhibitor treatment. Confocal images; scale bar: 100 μm.

D Western blotting of whole-cell lysates generated from HEK293 cells expressing TrkB fusion construct – SQSTM1-NTRK2. After transient transfection, TrkB fusion was expressed for 30 h and then treated with small molecule Trk inhibitors like K252a, LOXO-101 and Entrectinib (concentrations are as depicted). Lysates were probed with the indicated antibodies. While Trk activity is not hampered, downstream activity of FAK and MAPK is reduced upon inhibitor treatment.

Some cancer-related *NTRK* fusion proteins lack the aminoterminal receptor domain and are fused to cytosolic proteins (Martin-Zanca *et al.*, 1986; Stransky *et al.*, 2014). Structural features suggest that, these proteins are localized at intracellular sites and become oncogenic drivers due to kinase activation by a yet elusive mechanism (Cocco *et al.*, 2018). SQSTM1-NTRK2 was found in a lower grade glioma, in RNA-seq data. In this fusion protein, exons 1 – 5 of sequestosome 1 (SQSTM1), a multifunctional signaling adapter involved in autophagy, are fused to exons 16 - 20 of *NTRK2* (Cocco *et al.*, 2018; Gatalica *et al.*, 2019; Stransky *et al.*, 2014). This creates an open reading frame and links the aminoterminal part of SQSTM1 with the kinase domain of human TrkB. The TrkB domain includes the complete kinase region and an intact C-terminus but lacks the Shc adapter site and the juxtamembrane region. In this study, SQSTM1-NTRK2 showed constitutive phosphorylation, caused a roundish cell phenotype, was able to induce phosphorylation of FAK$^{Y576/577}$ and, in contrast to the Trk-ICD, also MAPK (Figure 23C,D).

3.4 Self-active TrkB inhibits migration of U87MG cells

Thus far, the data indicate intracellular signaling of constitutively active TrkB to actin filopodia dynamics and FAK, which are both involved in cell migration. Naturally, the next step was to check for TrkB activation effects on cell migration. Therefore, a migratory-active glioblastoma-like cell line was employed, to investigate this. Human U87MG glioblastoma-like cells are commonly used in brain cancer research but have an unknown patient origin. The clone U87MG (ATCC #HTB-14) is of CNS origin and carries bona fide glioblastoma-like characteristics (Allen *et al*, 2016). The cells are migratory and are suited to better understand how candidate proteins interfere with non-directed cell migration (Diao *et al*, 2019).

To better control protein abundance in this cell model, the TrkB-wt, TrkB-YFY, and the NTRK gene fusion construct SQSTM1-NTRK2 were expressed in a doxycycline-inducible lentiviral expression system (Wang *et al*, 2014). A second resistance gene cassette was used to select Trk-positive cells with 1μg/ml puromycin after lentiviral transduction.

U87MG cells expressing the different constructs were seeded into 2-well silicon inserts with a defined cell-free gap for testing random migration (Figure 24A). 1 mg/ml doxycycline was added during cell seeding to induce the expression of the three constructs. DMSO was added as solvent control. After 24 h, the silicon inserts were removed and cells were observed to see whether TrkB induction sped up or slowed down random cell migration. The experiment showed that expression induction significantly reduced the cell migration of TrkB-wt expressing cells compared to TrkB-YFF expressing cells (Figure 24A,C). Morphological alterations and cell migration effects of SQSTM1-NTRK2 expressing cells were extreme (Figure 24A,C). These cells appeared roundish and cell migration was rather weak, and instead cell clone formation was observed. Surprisingly, in absence of neurotrophins, the pure abundance and expression of the construct was responsible for the dramatic changes of the cellular properties with respect to random migration and cell clone formation. Another interesting observation was that the SQSTM1-NTRK2 protein, with a predicted molecular weight of 61 kDa, appeared at about 60 and at 120 kDa under standard SDS-PAGE Western blotting conditions (Figure 24B). This indicates that the protein tends to aggregate and form a stable, SDS-resistant dimer. In absence of doxycycline, expression of all proteins was below detection limits (Figure 24B).
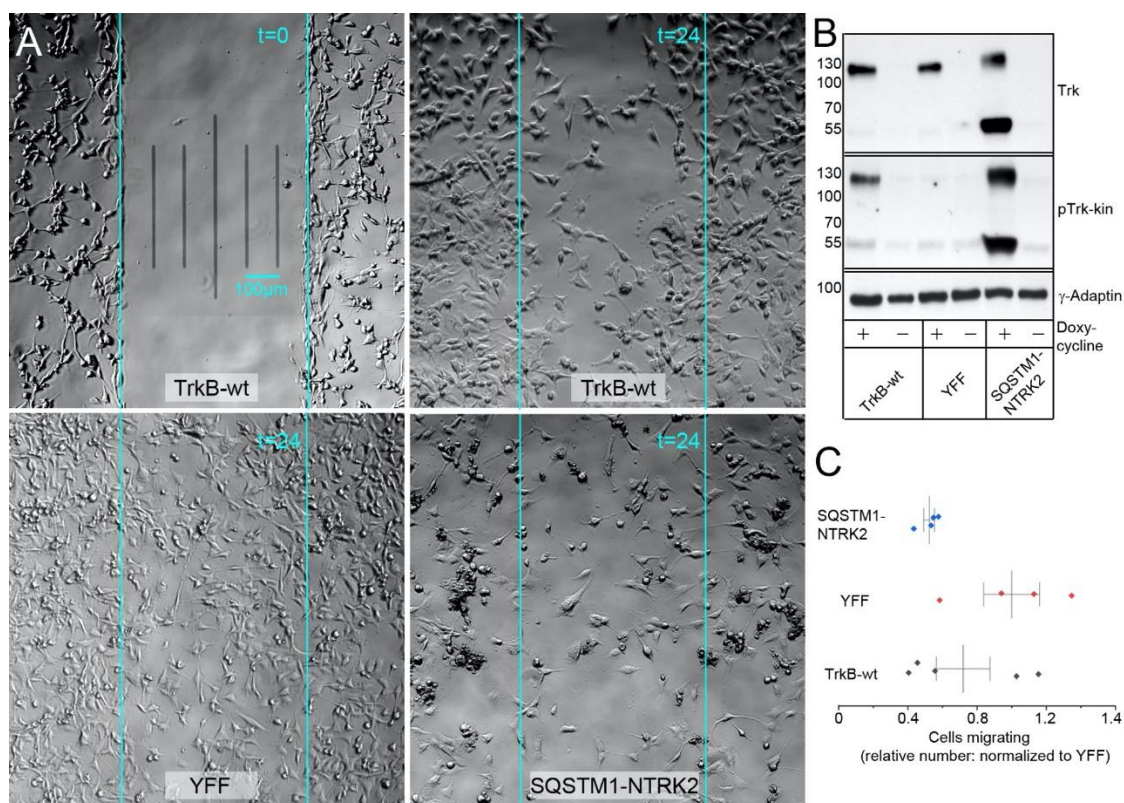
Figure 24. Self-active TrkB kinase reduces the migratory activity of glioblastoma-like cells.

A Representative phase contrast microscopy images of migration assay. Shown are U87MG cells expressing either TrkB-wt, TrkB-YFF or the fusion protein SQSTM1-NTRK2. The image in the upper left corner shows the cells in culture after removing the silicon insert (t=0). The other images representatively show the situation 24 h later. Note the cell morphology changes in TrkB-wt and SQSTM1-NTRK2 expressing cells versus TrkB-YFF.

B Western blotting of whole-cell lysates generated from U87MG cells expressing indicated TrkB kinase construct. Cells transduced with indicated lentiviral constructs were maintained as a polyclonal cell line and puromycin was used to select transduced cells. In absence of Doxycycline, cells did not express the corresponding proteins. Doxycycline was added to induce Trk-construct expression for 48h. Constitutive activation of Trk was verified with pTrk-kin. γ–Adaptin = loading control.

C Migratory activity of U87MG cells, expressing indicated Trk-kinase constructs. Shown are relative numbers of cells to the initially cell-free gap. Cell count was normalized to the mean of TrkB-YFF expressing cells. Migratory activity is shown relative to TrkB-YFF, which expresses the same structural protein domains as TrkB-wt, but is mutated at Y^{705} and Y^{706} (for a representation of how the cells were counted see Figure 26A).

Induction of expression with 1µg / ml doxycycline for 48 h led to TrkB expression and constitutive activation of TrkB (Figure 25). In this cell system, TrkB was strongly enriched close to F-actin-rich protrusions (Figure 25, yellow arrows in phalloidin staining). The distribution pattern of TrkB and F-actin was reminiscent of typical cell morphology in non-migrating cells (Etienne-Manneville, 2008). The intracellular protein SQSTM1-NTRK2 also became constitutively active (Figure 25, lowermost panel).
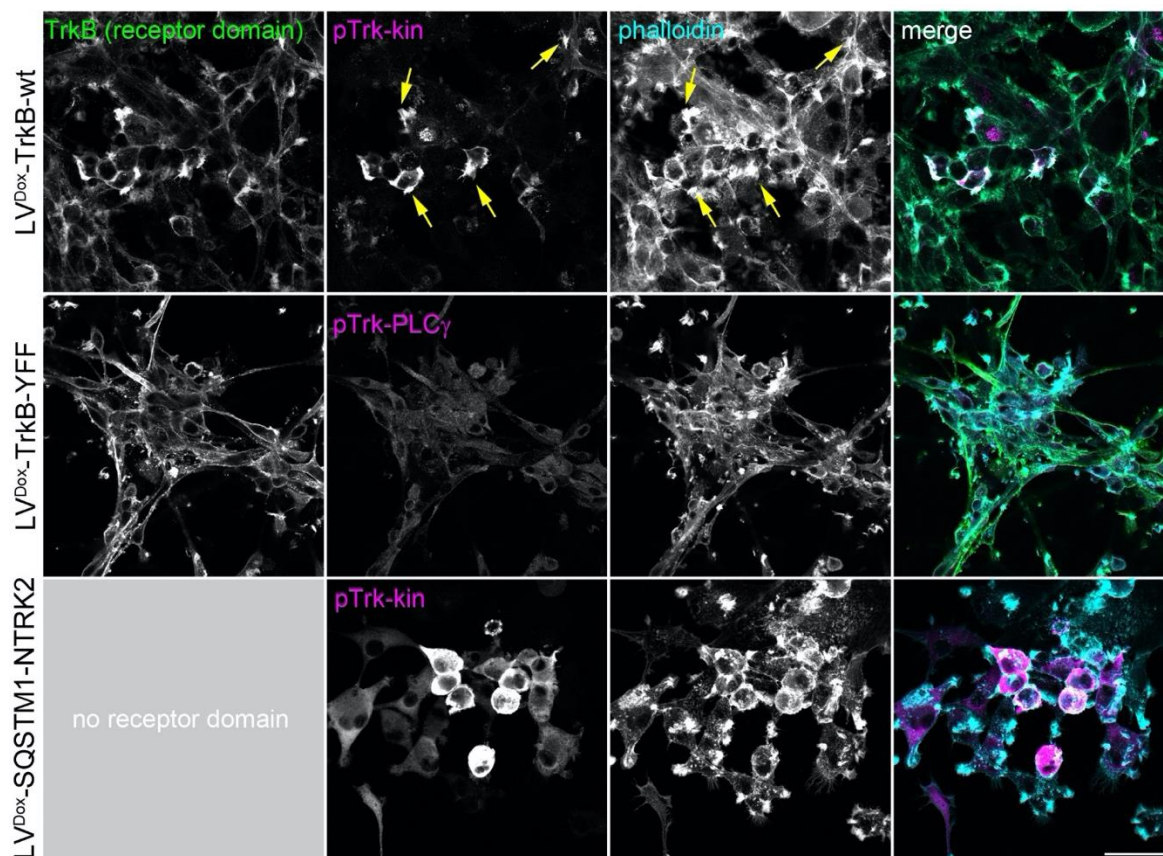

Figure 25. U87MG cells expressing active Trk-kinase undergo self-activation and modify actin cytoskeleton. Immunostaining of U87MG cells expressing inducible TrkB-wt, TrkB-YFF and the NTRK fusion construct SQSTM1-NTRK2. Immunofluorescence of TrkB receptor domain (green), pTrk-kin (red) and Acti-stain-670 phalloidin (phall, blue). Yellow arrows point to constitutive pTrk close to F-actin. TrkB-YFF-expressing cells were labelled with anti-pTrk-PLCγ because the antibody binding site of anti-pTrk-kin is mutated in this construct. SQSTM1-NTRK2 does not have a receptor domain, as indicated. Confocal z-stack images; scale bar: 50 µm.

The drastic changes in cellular morphology seen in these cells on TrkB induction (Figure 24, 25) made it necessary to test for unnatural cell death or apoptosis over a period of 96 h. Interestingly, after expression induction, U87MG cells expressing TrkB-wt, TrkB-YFF or SQSTM1-NTRK2 retained their ability to grow (Figure 26B).
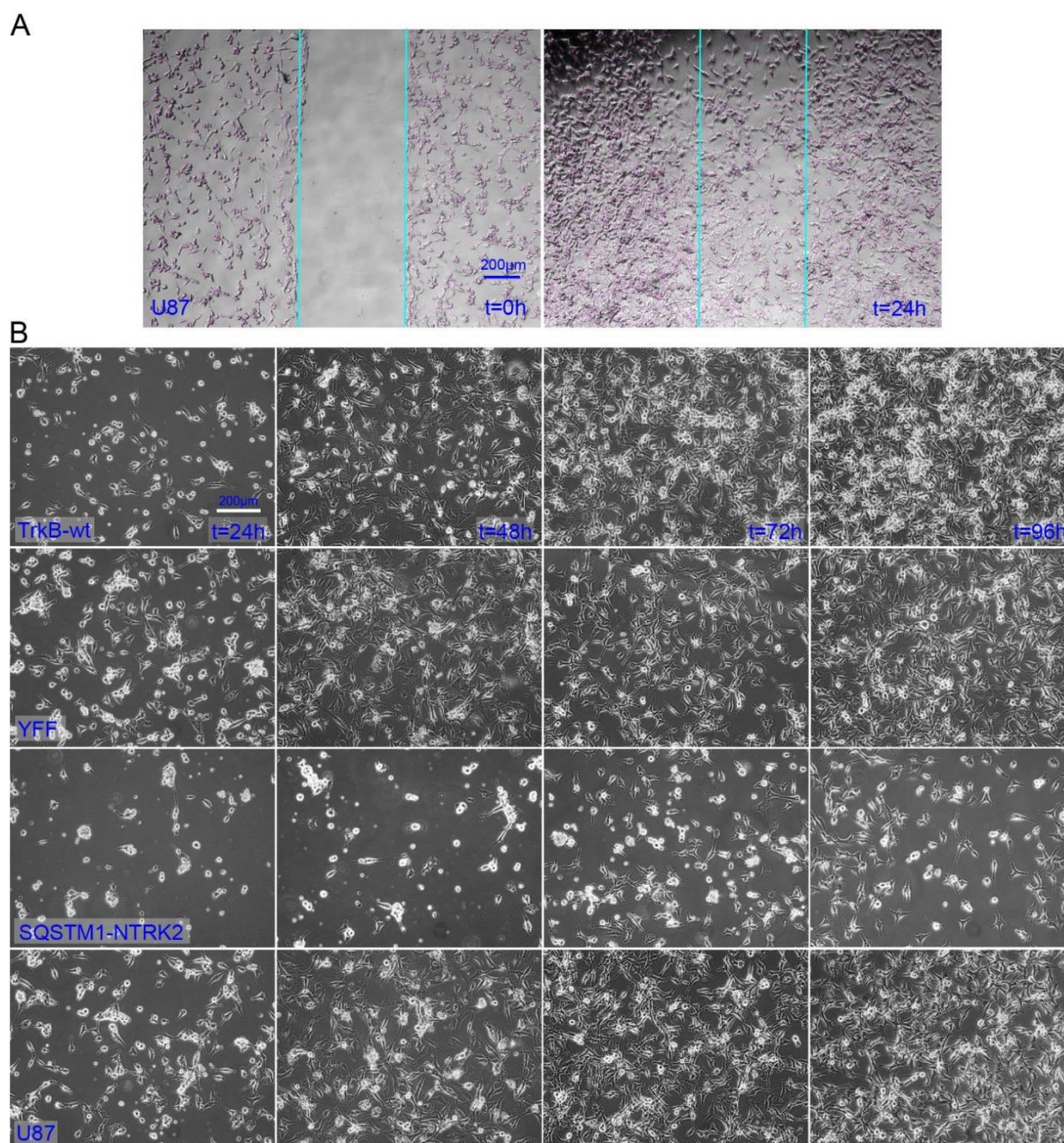

Figure 26. U87MG cells expressing active Trk-kinase constructs do not cause cell death.

A Migration of U87MG cells. Representative phase contrast microscopy images. Indicated in magenta are cells that were automatically counted by unbiased cell counting with ImageJ.

B U87MG cells expressing TrkB-wt or SQSTM1-NTRK2 were not dying within the indicated time span of 96 hours, albeit the cells express a rather high amount of intracellular Trk kinase activity (Figure 24, 25). Representative phase contrast microscopy images; scale bar: 200 µm.

3.5 TrkB activation in human glioblastoma samples

Up to here, the experiments revealed an unusual, novel signaling property of the intracellular Trk kinase domain via Y^{705}. However, Trk effects were observed in a rather artificial situation, namely constitutive Trk signaling after recombinant expression of TrkB or TrkB mutants in HEK293 or U87MG cells. Consequently, human glioblastoma (grade IV) tissue samples were examined, to find evidence for intracellular, constitutively active TrkB under pathological, yet physiological conditions.

The TrkB-encoding gene *NTRK2* is abundantly expressed in neural cells during neural development and in the adult brain. Besides that, the receptor is also highly abundant in diverse types of glioblastoma, the most common tumors of the brain (Wadhwa *et al*, 2003). Constitutive Trk receptor signaling is pro-tumorigenic in glioblastoma (Lawn *et al*, 2015; Wang *et al*, 2018) and fusions of *NTRK1*, *NTRK2*, and *NTRK3* genes belong to the genomic landscape of diverse types of gliomas (Cook *et al.*, 2017; Lawn *et al.*, 2015; Wu *et al*, 2014).

Glioblastoma tissue was harvested during brain surgery of patients suffering from glioblastoma (first diagnosis or recurrence, male and female, age 33 – 80 years old). For this study, tissues categorized by histological examination as grade IV glioma were selected. Frontal brain tissue (post-mortem, male and female, 33 – 72 years old) was used as control. To localize pTrk in glioblastoma tissue, frozen sections were taken and immunofluorescence labelling with anti-Nestin and pTrk was performed (by Gisela Wohlleben, Department of Radiation Oncology, University Hospital Würzburg). High Nestin expression can be used to distinguish glioma cells from unaffected brain tissue with high probability (Ma *et al*, 2008; Zhang *et al*, 2008). High-resolution z-stack confocal microscopy of pTrk-positive cells was performed (by PD Dr. Robert Blum, Institute of Clinical Neurobiology, University Hospital Würzburg) (Figure 27A). Single Nestin+ cells carried intracellular pTrk-positive clusters and even pTrk-positive bleb-like formations.

To ensure that the tissue expresses the TrkB kinase splice variant, RNA from cryosections was harvested, isolated and reverse-transcriptase qPCR was performed (Figure 27B). The upper primer was positioned to an exon encoding for the receptor domain and the lower primer was bound to an exon encoding for the TrkB kinase domain (see M&M sections *2.1.6* and *2.2.7*). By this strategy, transcripts for truncated TrkB-T1 are not detected. Relative expression was compared to RNA-Polymerase II transcripts and revealed a rather high expression level of the TrkB kinase transcript in the control samples of frontal brain tissue (about 50% of the

housekeeping gene RNA polymerase II). In glioblastoma cryosections a rather high, but variable expression of TrkB kinase was found (Figure 27B).
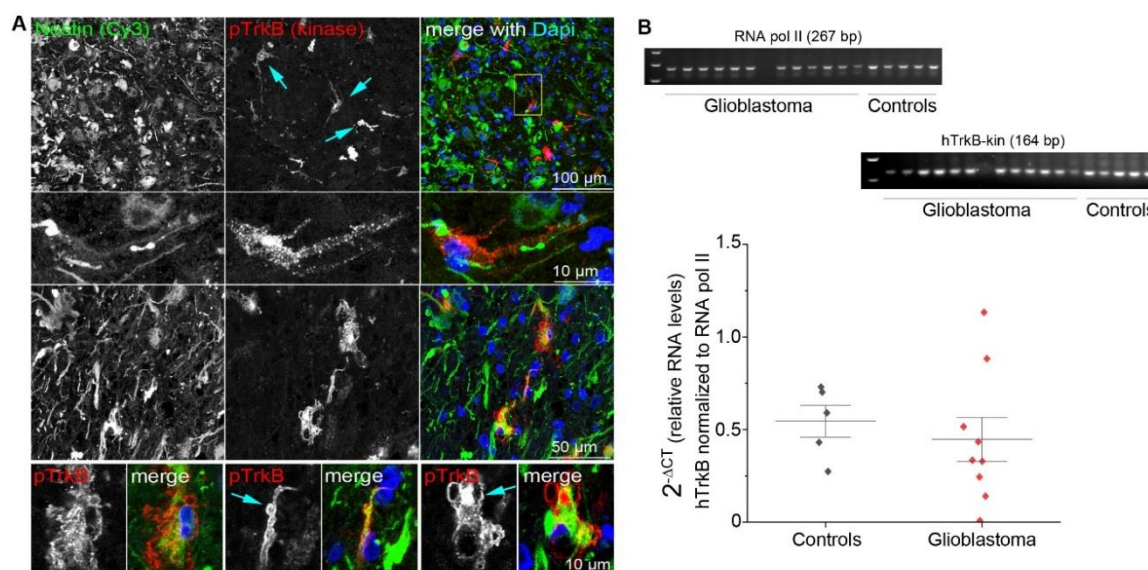

Figure 27. Localization and expression of TrkB and pTrk-kin in grade IV glioblastoma.

A Immunofluorescence analysis of a representative glioblastoma tissue cryosection. Confocal images are shown. Sections were labelled for anti-Nestin, for identification of the glioblastoma and pTrk. Single Nestin+ cells show a high abundance of pTrk (upper panel, cyan arrows). Second and third panel: High-resolution confocal image stack showing pTrk in intracellular, immunoreactive clusters. Lower panel. Membrane bleb-like structures in single cells with strong intracellular pTrk label.

B RT-qPCR reveals the abundant expression of the TrkB kinase transcript in grade IV glioblastoma. TrkB kinase expression levels are given in relation to RNA polymerase II. Single data points, the mean and the standard deviation are indicated. The size of the amplicons was verified by agarose gel electrophoreses, as indicated.

Next, frozen tissue samples (approximately 1cm^3) were thawed, dissected into smaller pieces and used to prepare total cell lysates. Figure 28A shows representative Western blots for two samples, a sample from a first diagnosis (N1249/16) and a recurrence sample from another patient (N50/18). Due to the neural origin of glioblastoma, probing samples with anti-TrkB gave a pronounced signal around 90 – 100 kDa, indicating the rather strong expression of the truncated TrkB-T1 isoform. Due to the strong immunoblotting signal at 90 kDa, the mature TrkB-kinase at 130 kDa could not be clearly resolved. Probing with anti-Trk, an antibody detecting all Trk isoforms, verified the expression of Trk-kinase (Figure 28A). Furthermore, probing with pTrk (PLCγ-site)-antibodies confirmed strong phosphorylation signal at 90 kDa, suggesting phosphorylation of the non-glycosylated immature Trk isoform (Figure 28A). One of the six tissue pieces showed a much higher abundance of Trk kinase (Figure 28A, lane 2). In the second tissue sample (N50/18), neither the Trk kinase, nor the pTrk could be detected.
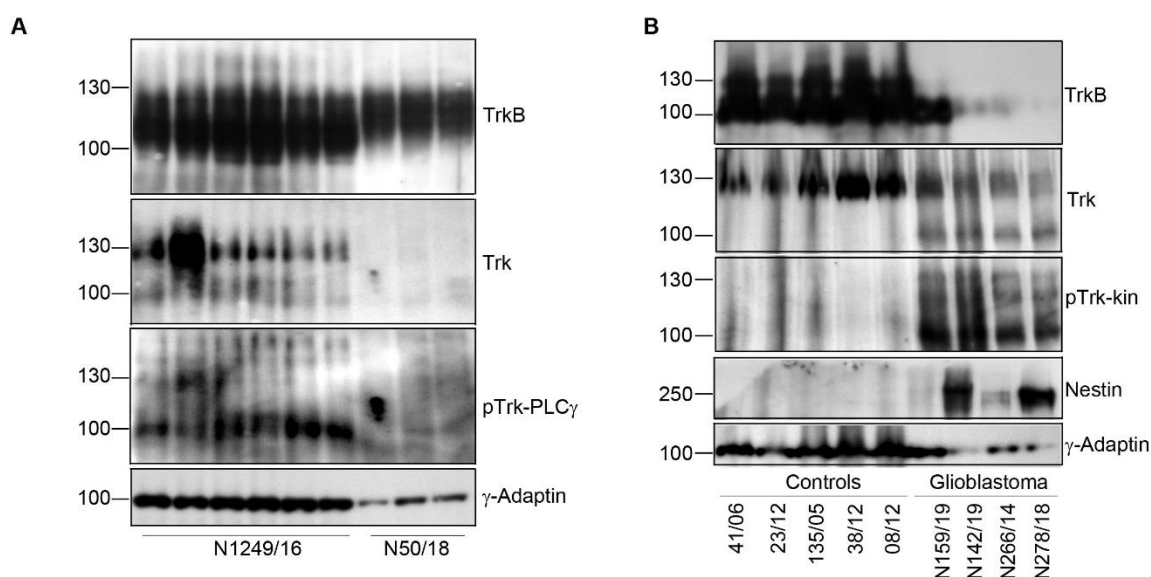
Figure 28. Expression of TrkB, Trk and pTrk in grade IV glioblastoma.

A TrkB and phospho-active Trk kinase in glioblastoma. Western blotting of whole-cell lysates generated from frozen, post-mortem glioblastoma samples with indicated antibodies. Lane 1–6 shows lysates generated from different tissue pieces of the same glioblastoma sample. Note high abundance of Trk kinase and pTrk in one tissue piece (lane 2). Lane 7-9 shows a representative TrkB-positve, Trk kinase negative, pTrk-negative glioblastoma sample. γ-Adaptin, loading control.

B TrkB and phospho-active Trk kinase in glioblastoma. Western blotting of whole-cell lysates generated from human brain samples or glioblastoma samples. Lane 1–5 shows lysates generated from control brain samples (frontal brain). Trk kinase immunoreactivity is seen at 130 kDa, indicating mature Trk. Lane 6 – 9 represent total lysates from different grade IV glioblastoma. Note high abundance of Trk kinase and pTrk at about 90 kDa, indicating immature, phosphorylated Trk.

As a final step, protein lysates from human frontal brain were compared with protein lysates from different grade IV glioblastoma samples (recurrence samples) (Figure 28B). Again, pronounced TrkB and Trk-kinase signals were seen in Western blots. However, the 90 kDa Trk kinase signal was exclusively observed in glioblastoma samples. Trk kinase in frontal brain controls showed only the typical 130 kDa mature Trk band (Figure 28B). pTrk signals were abundant in glioblastoma and not visible in control brain tissue (Figure 28B). This experiment points to immature, phospho-positive Trk kinase in glioblastoma and more importantly shows that indeed this is a common phenomenon.

4 Discussion

Like all tyrosine kinase receptors, the TrkB receptor is activated by dimerization and subsequent autophosphorylation of intracellular tyrosine residues (Jura *et al*, 2011; Lemmon & Schlessinger, 2010). Release of cis-autoinhibition, following ligand-induced receptor dimerization, is the key event that has been proposed to trigger receptor tyrosine kinase activation (Artim *et al.*, 2012; Bertrand *et al*, 2012; Hubbard *et al.*, 1994; Lemmon & Schlessinger, 2010). However, classical concepts for ligand-dependent TrkB kinase activation fail to fully explain signaling mechanisms of intracellular TrkB (Watson *et al.*, 1999), or cancer-related, cytosolic *NTRK* fusion proteins (Cocco *et al.*, 2018). This study here gives one possible explanation for these events by introducing a new signaling outcome of the ligand-independent constitutive active Y^{705} residue of TrkB.

4.1 Trk activation and release from cis-autoinhibition

Our data (Gupta *et al.*, 2020), show that Y^{705} in TrkB plays an important role in abundance-dependent activation and downstream signaling of TrkB. Structural models for the activation mechanism of TrkB are mainly based on generalized models of receptor tyrosine kinase activation (Artim *et al.*, 2012; Hubbard *et al.*, 1994). These models suggest that in the absence of a ligand, receptor tyrosine kinases are autoinhibited in *cis* and that autoinhibition is released following ligand-induced receptor dimerization. In other words, they propose that the kinase is disengaged from the active site by *cis* phosphorylation and the active site becomes free and is able to *trans* phosphorylate other molecules. While the role of the Y^{515} and Y^{816} are known for being crucial adaptor sites for Shc and PLCγ respectively (Chao, 2003; Huang & Reichardt, 2003), the role of the three tyrosine residues within the TrkB kinase domain remain largely unknown. The Y^{1162} in the insulin receptor corresponds to the Y^{705} of the TrkB and since the Y^{1162} was reported to be involved in autoinhibition of kinase activity by binding to the active site (Hubbard, 2004; Hubbard *et al.*, 1994), it was proposed by (Iwasaki *et al.*, 1997) that Y^{705} in TrkB is a possible site that regulates the kinase activity through its phosphorylation.

On comparing the TrkB-Y^{705} and TrkB-YFY (based on pdb code 4at4) to the kinase domain of the insulin receptor (1gag) using GROMACS, it was observed that, there were large structural rearrangements between the TrkB model for molecular dynamics (MD) and the activated insulin receptor (modeling by Dr. Jochen Kuper, Rudolf Virchow Center for Experimental Biomedicine, Institute for Structural Biology, University of Würzburg) (Figure 29). Interestingly, the inactive form of the insulin receptor closely matched the conformation of the

TrkB model, indicating a similar autoinhibited state (Figure 29A). The phosphorylation at Y^{705} changes the autoinhibition loop position, which is indicated by the significant shift of the YxxxYY motif (3.7 Å at Gly^{712} located at the tip of the loop, Figure 29B). A similar change can be observed with the $Y^{705}F$ variant. This transition could be indicative for the concept that the release from cis-autoinhibition initiates Y^{705}-mediated signaling. Why phosphorylation Y^{705} and a variant ($Y^{705}F$) that cannot be phosphorylated, have a similar outcome remains, however, elusive. These small but significant differences indicate structural transitions in the receptor structure that may underlie TrkB activation by a ligand-independent release from cis-autoinhibition upon overexpression.
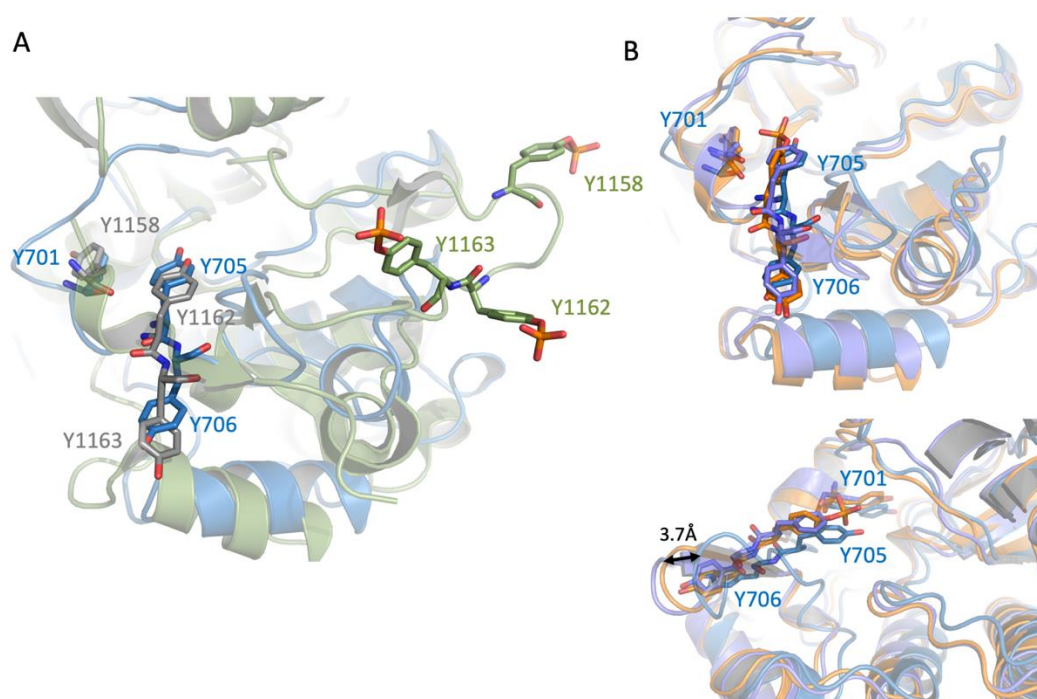

Figure 29. Modeling of TrkB.

A Superposition of TrkB MD model (blue) with the activated form of the insulin receptor (1gag, green). The YxxxYY motif is depicted in ball and stick mode. The YxxxYY motif of the autoinhibited insulin receptor is shown in grey and ball and stick mode. The backbone has been omitted for clarity.

B The upper panel shows a superposition of three MD models for TrkB. Wild type is shown in blue. Phospho Y^{705} in orange and $Y^{705}F$ in purple. The YxxxYY motif is shown in ball and stick mode and the movement is indicated by an arrow (Gupta *et al.*, 2020). Modeling performed by Dr. Jochen Kuper, Rudolf Virchow Center for Experimental Biomedicine, Institute for Structural Biology, University of Würzburg.

4.2 Self-activation of TrkB-ICD

In the Myr-ICD or ICD constructs (Figures 21 and 22), typical dimerization domains such as the juxtamembrane region or the single span transmembrane domain (Franco *et al*, 2020) are

missing. We can assume that the release of cis-autoinhibition happens in ICD monomers and subsequently a high abundance of ICD domains is needed to enable transactivation between ICDs. In this concept, cis-autoinhibition is not a stable conformation. Sequential *cis/trans*-activation and subsequent downstream signaling might be a contributing factor for ligand-independent TrkB functions.

From these data, it can be assumed that Myr-ICD, when targeted to the plasma membrane, can provide a platform for adapter proteins and thereby support a certain level of constitutive Ras/MAPK signaling, even in the absence of neurotrophins. The fact that the ICD alone does not promote MAPK activation is in line with earlier data by the group of R.S. Segal showing that unglycosylated, constitutively active TrkA, in tunicamycin-treated PC12 cells, does not activate MAPK (or ERK) (Watson *et al.*, 1999).

The ICD signaling shown here is different from typical BDNF-dependent (Klein *et al.*, 1991b) or neurotrophin-independent TrkB activation by adenosine, EGF or dopamine (Iwakura *et al.*, 2008; Lee & Chao, 2001; Puehringer *et al.*, 2013; Rajagopal & Chao, 2006; Rajagopal *et al.*, 2004; Wiese *et al.*, 2007). Intracellular ICD-mediated, constitutive activation is an independent category of signaling options of the TrkB kinase domain via Y^{705}. We thus suggest referring to this phenomenon as '**TrkB kinase self-activation**' (Gupta *et al.*, 2020).

4.3 TrkB signaling to FAK

Cell migration affects all morphogenetic processes and contributes to numerous diseases, including cancer and cardiovascular disease. The morphological features of migrating cells can vary considerably. On one hand, these cells can be round, highly protrusive and display blebbing (for example, lymphocytes and cancer cells in some environments) and migrate using weak adhesions. On the other hand, they can be cells that spread highly (for example, fibroblasts and endothelial cells) that have many large adhesions; their migration is often referred to as being mesenchymal (Parsons *et al.*, 2010).

Focal adhesion kinase (FAK) is an important receptor-proximal regulator of cell shape, adhesion, and motility. FAK is involved in many aspects of the metastatic process including adhesion, migration and invasion (Deramaudt *et al*, 2014). FAK was independently identified in 1992 by Steve Hanks, Jun-Lin Guan and Michael Schaller as a substrate of the viral Src oncogene and, in normal cells, as a highly tyrosine-phosphorylated protein that localized to integrin-enriched cell adhesion sites known as focal contacts (Guan & Shalloway, 1992; Hanks

et al, 1992; Kornberg *et al*, 1992; Mitra *et al.*, 2005). Focal contacts are formed at ECM–integrin junctions that bring together cytoskeletal and signaling proteins during the processes of cell adhesion, spreading and migration (Webb *et al*, 2004). Early studies found that FAK could be activated by either ECM or growth factors, and that tyrosine phosphorylation of FAK was a rapid event that was associated with the formation of focal contacts (Parsons, 2003).

In this study, we saw that constitutive activation of TrkB interrupts actin filopodia formation. Cells became round and showed membrane blebbing (Figures 10, 11 and 16). This led us to investigate whether FAK (Westhoff *et al*, 2004) is downstream of Y^{705} signals. However, we saw that Y^{705} signaling to FAK and to cell migration are independent/mutually exclusive events. Constitutive active TrkB-wt, but also YxxxYY-mutants such as YYF, YDY, or YEY, all interrupted actin filopodia formation, but could not activate FAK phosphorylation (Figures 19 and 22). Under controlled expression, TrkB also underwent self-activation and interrupted cell migration. This finding is important and should not be overlooked because it might be part of a yet undefined *NTRK*-fusion signaling pathway or ligand-independent TrkB signaling in cancer. The specificity of Y^{705} signaling is remarkable because it is blocked in the so-called 'constitutive active YDY' mutants, or YYF mutants. In future studies, it will be interesting to find out whether a high on-off dynamic of the pathway contributes to the turnover rate of focal adhesion sites in TrkB expressing cells in absence of ligands, before transactivating ligands or BDNF promote actin filopodia dynamics and chemotactic migration events.

4.4 Constitutive TrkB kinase self-activation in grade IV glioblastoma?

Glioblastoma multiforme (GBM) is the most aggressive of the gliomas, a collection of tumors arising from glia or their precursors within the central nervous system. Clinically, gliomas are divided into four grades; unfortunately, the most aggressive of these, grade IV or glioblastoma multiforme (GBM), is also the most common in humans. Because most patients with GBMs die of the disease in less than a year and essentially none show long-term survival, these tumors have drawn significant attention; however, they have evaded increasingly clever and intricate attempts at therapy over the last half-century (Amatu *et al.*, 2016; Drilon *et al.*, 2018; Drilon *et al*, 2017; Holland, 2000; Holland *et al*, 2000).

One of the reasons for the resistance of GBM to therapeutic intervention is the complex character of the tumor itself. As the name implies, glioblastoma is multiforme. It is multiforme grossly, showing regions of necrosis and hemorrhage. It is multiforme microscopically, with regions of pseudopalisading necrosis, pleomorphic nuclei and cells, and microvascular

proliferation. And it is multiforme genetically, with various deletions, amplifications, and point mutations (James & Olson, 1996). These tumors also show intratumor genetic heterogeneity with subclones existing within the tumor cell population (Ishii *et al*, 1999).

The Trk onocogene was one of the first transforming genes identified in human cancers (Barbacid, 1994). Fusion of ETV6 to TrkC with constitutive activation of the tyrosine kinase activity has also been reported in many cancers (Nakagawara, 2001). In fusion biology, upstream gene partners often contain oligomerization domains, such as coiled-coil domains, zinc finger domains or WD repeats. In some cases, these domains are required for full activation of the downstream kinase (Cocco *et al.*, 2018). In instances where fusion partners lack known dimerization domains, the contribution of the upstream partner in promoting activation of the downstream TRK kinase is unclear. One possibility is that the sequences derived from the gene partner simply replace the autoinhibitory domains present in the extracellular domain of the Trk proteins. Alternatively, the partner can be actively involved in the transformation process and might determine the subcellular localization of the fusion products (Cocco *et al.*, 2018).

In human grade IV glioblastoma tissue, we found marked differences in the TrkB profile, when compared with frontal brain control tissue. In GBM, Trk kinase phosphorylation was strong in the 90 kDa TrkB band, typical for non-glycosylated, immature TrkB (Figure 28). Immunolocalization and high-resolution microscopy confirmed intracellular pTrk-positive clusters, at least in some Nestin+ cells (Figure 27). These results do not exclude the possibility that the natural TrkB ligand BDNF from neurons, microglia, serum (Naegelin *et al*, 2018) or platelets (Fujimura *et al*, 2002) stimulates Trk phosphorylation. However, it has been shown that recombinant expression of a TrkB construct lacking the immunoglobulin-like domains of TrkB, meaning the BDNF-binding domain, is sufficient to confer an aggressive carcinogenic phenotype to a neural crest-derived cell line (Dewitt *et al.*, 2014). In patients with both primary tumor and peritoneal metastatic nodules, human colorectal cancer (CRC) cells at the peritoneal metastatic nodules expressed both BDNF and TrkB (Tanaka *et al*, 2014). In that study, they confirmed that anti TrkB antibody (R&D Systems, Foster City, CA, USA) detected both TrkB.FL and TrkB.T1 based on the results of Western blotting analysis using human CRC cell lines, however they did not look for phospho-Trk. Consequently, the bands at 95kDa (when probed for p-Trk-kin), could very well represent BDNF independent self-active immature TrkB and not just truncated TrkB.T1.

Therefore, in the context of the overall literature and the results here, there might be, among other signaling pathways, also abundance-dependent self-activation of endogenous, unmutated

intracellular TrkB, which is upstream of cytoskeletal functions and is pro-tumorigenic. Because of this idea, it will be valuable to test multiple tissue pieces of GBM biopsies (first diagnosed and recurrence samples) for pTrk-Y^{705} abundance. In clinical studies, it should be tested whether anti-Trk treatment can contribute to a better outcome for glioblastoma patients with a pronounced pTrk signal.

Furthermore, in this study we suggest that a pharmacologic, small molecule block of the release from cis-autoinhibition at Y^{705} or the stabilization of the YFY-like confirmation (Figure 29) would be interesting strategic options to block constitutively active *NTRK* in cancer, for instance in case of acquired resistance to prior Trk kinase inhibition (Drilon *et al.*, 2017; Okamura *et al*, 2018). In the near future, it is crucial for both further advances in our understanding of the autoregulatory mechanisms in RTKs and, hopefully, the emergence of new therapeutics that selectively modulate kinase activity to combat human diseases.

4.5 Conclusion

In this study, we had set out to elucidate the role of Y^{705} residue, in the TrkB kinase domain, in TrkB constitutive activation (referred to as 'self-activation' here). This study confirmed that the TrkB-ICD alone was sufficient for intracellular TrkB kinase dependent self-activation. This was possible when a high abundance of the kinase domain is available at intracellular sites. In this signaling process, Y^{705} of TrkB, previously known to be involved in kinase activity, in the course of this study was shown to be directly involved in downstream signaling to cytoskeletal features (Figure30). In short, this work showed that – (1.) persistent activity of intracellular Y^{705} of TrkB is upstream of a very specific signaling event that interrupts actin filopodia dynamics; (2.) it can inhibit random cell migration and (3.) induce focal adhesion kinase (FAK) phosphorylation. (4.) It persists in the absence of neurotrophins or serum components and (5.) can be stopped acutely with Trk inhibitors. This study thus highlights a never before shown TrkB signaling outcome of the ligand-independent constitutive active Y^{705} residue of TrkB. Moreover, we used a modified glioblastoma derived cell line-U87MG expressing an *NTRK2*-fusion and could successfully demonstrate this TrkB kinase ligand-independent ('self-active') signaling via Y^{705}. We were also able to show the occurrence of active phospho-TrkB in human grade IV glioblastoma. To conclude, this TrkB signaling property could be most relevant in case of constitutive activation of TrkB in glioblastoma or *NTRK*-fusion activity in other types of cancer and should be targeted for better therapies.
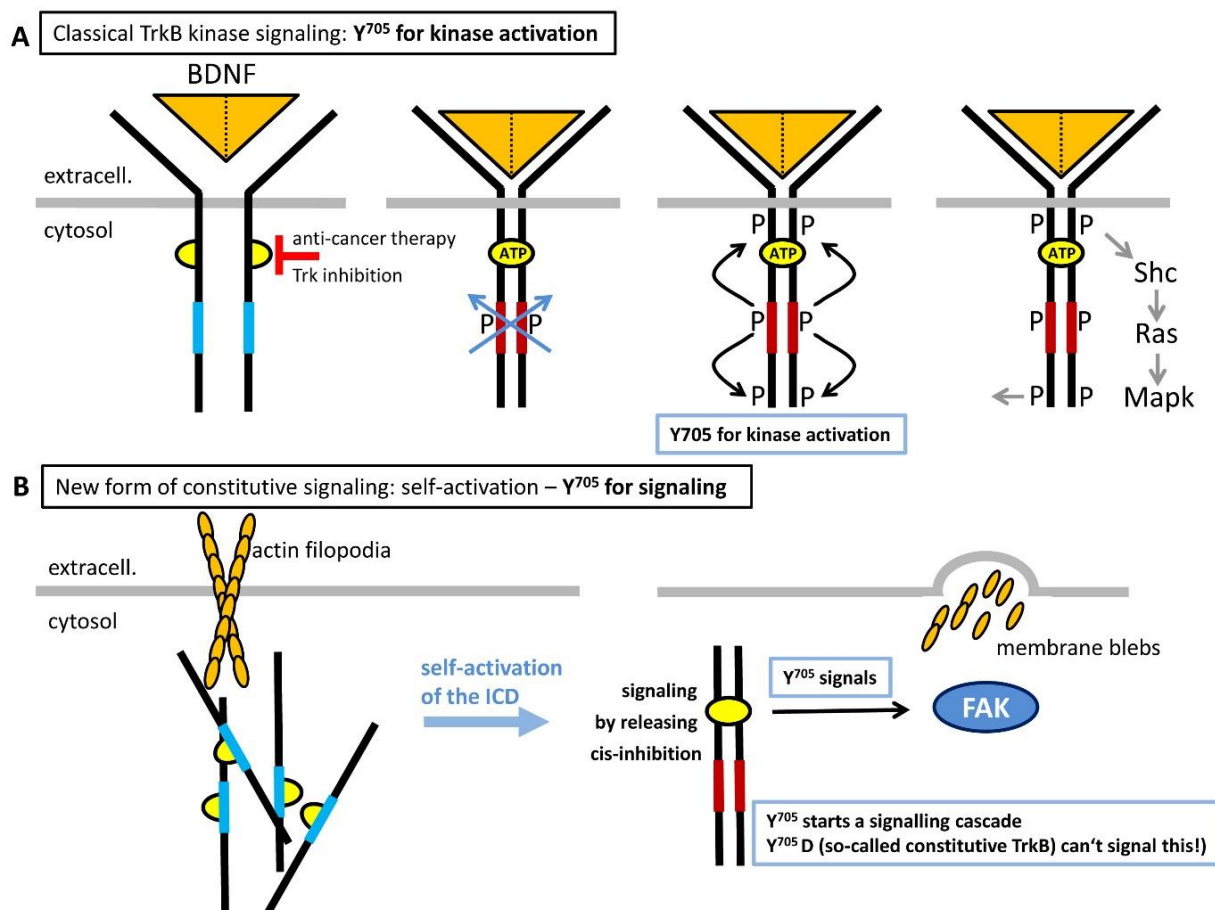
Figure 30. Graphical representation of this study.

A Classical TrkB kinase signaling - The ligand (here the neurotrophin BDNF) induces Trk dimerization and subsequent transphosphorylation. This causes subsequent autophosphorylation of tyrosine residues in the kinase domain and activation of downstream signaling pathways by recruitment of Shc and PLCγ at the adaptor sites.

B Self-activation of TrkB via Y^{705} - Abundance of intracellular domains of TrkB is sufficient to destabilize cis-autoinhibition, thus inducing autoactivation of the receptor. The intracellular ICD of TrkB alone can undergo self-activation. TrkB via Y^{705} on self-activation, disrupts the actin cytoskeleton of cells and activates focal adhesion kinase (FAK). Self-active TrkB is a possible explanation for the intracellular active *NTRK2*-fusions in cancers.

5 References

Allen M, Bjerke M, Edlund H, Nelander S, Westermark B (2016) Origin of the U87MG glioma cell line: Good news and bad news. *Sci Transl Med* 8: 354re353

Amatu A, Sartore-Bianchi A, Siena S (2016) NTRK gene fusions as novel targets of cancer therapy across multiple tumour types. *ESMO Open* 1: e000023

Arevalo JC, Conde B, Hempstead BI, Chao MV, Martin-Zanca D, Perez P (2001) A novel mutation within the extracellular domain of TrkA causes constitutive receptor activation. *Oncogene* 20: 1229-1234

Artim SC, Kiyatkin A, Lemmon MA (2020) Comparison of tyrosine kinase domain properties for the neurotrophin receptors TrkA and TrkB. *The Biochemical journal*

Artim SC, Mendrola JM, Lemmon MA (2012) Assessing the range of kinase autoinhibition mechanisms in the insulin receptor family. *The Biochemical journal* 448: 213-220

Baer K, Al-Hasani H, Parvaresch S, Corona T, Rufer A, Nolle V, Bergschneider E, Klein HW (2001) Dimerization-induced activation of soluble insulin/IGF-1 receptor kinases: an alternative mechanism of activation. *Biochemistry* 40: 14268-14278

Barbacid M (1994) The Trk family of neurotrophin receptors. *Journal of neurobiology* 25: 1386-1403

Bertrand T, Kothe M, Liu J, Dupuy A, Rak A, Berne PF, Davis S, Gladysheva T, Valtre C, Crenne JY *et al* (2012) The crystal structures of TrkA and TrkB suggest key regions for achieving selective inhibition. *J Mol Biol* 423: 439-453

Blanchoin L, Boujemaa-Paterski R, Sykes C, Plastino J (2014) Actin dynamics, architecture, and mechanics in cell motility. *Physiol Rev* 94: 235-263

Blum R, Lepier A (2008) The luminal domain of p23 (Tmp21) plays a critical role in p23 cell surface trafficking. *Traffic* 9: 1530-1550

Chao MV (2003) Neurotrophins and their receptors: a convergence point for many signalling pathways. *Nat Rev Neurosci* 4: 299-309

Chao MV, Ip NY (2010) Trophic factors: 50 years of growth. *Developmental neurobiology* 70: 269-270

Charras GT, Hu CK, Coughlin M, Mitchison TJ (2006) Reassembly of contractile actin cortex in cell blebs. *J Cell Biol* 175: 477-490

Cocco E, Scaltriti M, Drilon A (2018) NTRK fusion-positive cancers and TRK inhibitor therapy. *Nature reviews Clinical oncology* 15: 731-747

Cook PJ, Thomas R, Kannan R, de Leon ES, Drilon A, Rosenblum MK, Scaltriti M, Benezra R, Ventura A (2017) Somatic chromosomal engineering identifies BCAN-NTRK1 as a potent glioma driver and therapeutic target. *Nat Commun* 8: 15987

Deramaudt TB, Dujardin D, Noulet F, Martin S, Vauchelles R, Takeda K, Ronde P (2014) Altering FAK-paxillin interactions reduces adhesion, migration and invasion processes. *Plos One* 9: e92059

Dewitt J, Ochoa V, Urschitz J, Elston M, Moisyadi S, Nishi R (2014) Constitutively active TrkB confers an aggressive transformed phenotype to a neural crest-derived cell line. *Oncogene* 33: 977-985

Dhillon AS, Hagan S, Rath O, Kolch W (2007) MAP kinase signalling pathways in cancer. *Oncogene* 26: 3279-3290

Diao W, Tong X, Yang C, Zhang F, Bao C, Chen H, Liu L, Li M, Ye F, Fan Q *et al* (2019) Behaviors of Glioblastoma Cells in in Vitro Microenvironments. *Sci Rep* 9: 85

Doebele RC, Drilon A, Paz-Ares L, Siena S, Shaw AT, Farago AF, Blakely CM, Seto T, Cho BC, Tosi D *et al* (2020) Entrectinib in patients with advanced or metastatic NTRK fusion-positive solid tumours: integrated analysis of three phase 1-2 trials. *Lancet Oncol* 21: 271-282

Drilon A, Laetsch TW, Kummar S, DuBois SG, Lassen UN, Demetri GD, Nathenson M, Doebele RC, Farago AF, Pappo AS *et al* (2018) Efficacy of Larotrectinib in TRK Fusion-Positive Cancers in Adults and Children. *N Engl J Med* 378: 731-739

Drilon A, Nagasubramanian R, Blake JF, Ku N, Tuch BB, Ebata K, Smith S, Lauriault V, Kolakowski GR, Brandhuber BJ *et al* (2017) A Next-Generation TRK Kinase Inhibitor Overcomes Acquired Resistance to Prior TRK Kinase Inhibition in Patients with TRK Fusion-Positive Solid Tumors. *Cancer Discov* 7: 963-972

Du Z, Lovly CM (2018) Mechanisms of receptor tyrosine kinase activation in cancer. *Mol Cancer* 17: 58

Etienne-Manneville S (2008) Polarity proteins in migration and invasion. *Oncogene* 27: 6970-6980

Farago AF, Le LP, Zheng Z, Muzikansky A, Drilon A, Patel M, Bauer TM, Liu SV, Ou SH, Jackman D *et al* (2015) Durable Clinical Response to Entrectinib in NTRK1-Rearranged Non-Small Cell Lung Cancer. *J Thorac Oncol* 10: 1670-1674

Ferguson SD, Zhou S, Huse JT, de Groot JF, Xiu J, Subramaniam DS, Mehta S, Gatalica Z, Swensen J, Sanai N *et al* (2018) Targetable Gene Fusions Associate With the IDH Wild-Type Astrocytic Lineage in Adult Gliomas. *J Neuropathol Exp Neurol* 77: 437-442

Franco ML, Nadezhdin KD, Goncharuk SA, Mineev KS, Arseniev AS, Vilar M (2020) Structural basis of the transmembrane domain dimerization and rotation in the activation mechanism of the TRKA receptor by nerve growth factor. *J Biol Chem* 295: 275-286

Fujimura H, Altar CA, Chen R, Nakamura T, Nakahashi T, Kambayashi J, Sun B, Tandon NN (2002) Brain-derived neurotrophic factor is stored in human platelets and released by agonist stimulation. *Thromb Haemost* 87: 728-734

Gatalica Z, Xiu J, Swensen J, Vranic S (2019) Molecular characterization of cancers with NTRK gene fusions. *Mod Pathol* 32: 147-153

Geiger TR, Song JY, Rosado A, Peeper DS (2011) Functional characterization of human cancer-derived TRKB mutations. *Plos One* 6: e16871

Gomez DR, Byers LA, Nilsson M, Diao L, Wang J, Li L, Tong P, Hofstad M, Saigal B, Wistuba I *et al* (2018) Integrative proteomic and transcriptomic analysis provides evidence for TrkB (NTRK2) as a therapeutic target in combination with tyrosine kinase inhibitors for non-small cell lung cancer. *Oncotarget* 9: 14268-14284

Guan JL, Shalloway D (1992) Regulation of focal adhesion-associated protein tyrosine kinase by both cellular adhesion and oncogenic transformation. *Nature* 358: 690-692

Gupta R, Bauer M, Wohlleben G, Luzak V, Wegat V, Segebarth D, Bady E, Langlhofer G, Wachter B, Havlicek S *et al* (2020)

Hanks SK, Calalb MB, Harper MC, Patel SK (1992) Focal adhesion protein-tyrosine kinase phosphorylated in response to cell attachment to fibronectin. *Proceedings of the National Academy of Sciences of the United States of America* 89: 8487-8491

Hanks SK, Quinn AM, Hunter T (1988) The protein kinase family: conserved features and deduced phylogeny of the catalytic domains. *Science* 241: 42-52

Holland EC (2000) Glioblastoma multiforme: the terminator. *Proceedings of the National Academy of Sciences of the United States of America* 97: 6242-6244

Holland EC, Celestino J, Dai C, Schaefer L, Sawaya RE, Fuller GN (2000) Combined activation of Ras and Akt in neural progenitors induces glioblastoma formation in mice. *Nat Genet* 25: 55-57

Hong DS, Bauer TM, Lee JJ, Dowlati A, Brose MS, Farago AF, Taylor M, Shaw AT, Montez S, Meric-Bernstam F *et al* (2019) Larotrectinib in adult patients with solid tumours: a multi-centre, open-label, phase I dose-escalation study. *Ann Oncol* 30: 325-331

Huang EJ, Reichardt LF (2001) Neurotrophins: roles in neuronal development and function. *Annu Rev Neurosci* 24: 677-736

Huang EJ, Reichardt LF (2003) Trk receptors: roles in neuronal signal transduction. *Annual review of biochemistry* 72: 609-642

Huang TY, DerMardirossian C, Bokoch GM (2006) Cofilin phosphatases and regulation of actin dynamics. *Curr Opin Cell Biol* 18: 26-31

Huang YZ, Pan E, Xiong ZQ, McNamara JO (2008) Zinc-mediated transactivation of TrkB potentiates the hippocampal mossy fiber-CA3 pyramid synapse. *Neuron* 57: 546-558

Hubbard SR (2004) Juxtamembrane autoinhibition in receptor tyrosine kinases. *Nat Rev Mol Cell Biol* 5: 464-471

Hubbard SR, Wei L, Ellis L, Hendrickson WA (1994) Crystal structure of the tyrosine kinase domain of the human insulin receptor. *Nature* 372: 746-754

Ishii N, Tada M, Hamou MF, Janzer RC, Meagher-Villemure K, Wiestler OD, Tribolet N, Van Meir EG (1999) Cells with TP53 mutations in low grade astrocytic tumors evolve clonally to malignancy and are an unfavorable prognostic factor. *Oncogene* 18: 5870-5878

Iwakura Y, Nawa H, Sora I, Chao MV (2008) Dopamine D1 receptor-induced signaling through TrkB receptors in striatal neurons. *J Biol Chem* 283: 15799-15806

Iwasaki Y, Nishiyama H, Suzuki K, Koizumi S (1997) Sequential cis/trans autophosphorylation in TrkB tyrosine kinase. *Biochemistry* 36: 2694-2700

James CD, Olson JJ (1996) Molecular genetics and molecular biology advances in brain tumors. *Curr Opin Oncol* 8: 188-195

Jin W, Yun C, Hobbie A, Martin MJ, Sorensen PH, Kim SJ (2007) Cellular transformation and activation of the phosphoinositide-3-kinase-Akt cascade by the ETV6-NTRK3 chimeric tyrosine kinase requires c-Src. *Cancer Res* 67: 3192-3200

Jones KA, Bossler AD, Bellizzi AM, Snow AN (2019) BCR-NTRK2 fusion in a low-grade glioma with distinctive morphology and unexpected aggressive behavior. *Cold Spring Harb Mol Case Stud* 5

Jura N, Zhang X, Endres NF, Seeliger MA, Schindler T, Kuriyan J (2011) Catalytic control in the EGF receptor and its connection to general kinase regulatory mechanisms. *Mol Cell* 42: 9-22

Kabouridis PS, Magee AI, Ley SC (1997) S-acylation of LCK protein tyrosine kinase is essential for its signalling function in T lymphocytes. *EMBO J* 16: 4983-4998

Kaplan DR, Hempstead BL, Martin-Zanca D, Chao MV, Parada LF (1991) The trk proto-oncogene product: a signal transducing receptor for nerve growth factor. *Science* 252: 554-558

Khotskaya YB, Holla VR, Farago AF, Mills Shaw KR, Meric-Bernstam F, Hong DS (2017) Targeting TRK family proteins in cancer. *Pharmacol Ther* 173: 58-66

Klein R, Jing SQ, Nanduri V, O'Rourke E, Barbacid M (1991a) The trk proto-oncogene encodes a receptor for nerve growth factor. *Cell* 65: 189-197.

Klein R, Nanduri V, Jing SA, Lamballe F, Tapley P, Bryant S, Cordon-Cardo C, Jones KR, Reichardt LF, Barbacid M (1991b) The trkB tyrosine protein kinase is a receptor for brain-derived neurotrophic factor and neurotrophin-3. *Cell* 66: 395-403

Klein R, Parada LF, Coulier F, Barbacid M (1989) trkB, a novel tyrosine protein kinase receptor expressed during mouse neural development. *EMBO J* 8: 3701-3709

Kornberg L, Earp HS, Parsons JT, Schaller M, Juliano RL (1992) Cell adhesion or integrin clustering increases phosphorylation of a focal adhesion-associated tyrosine kinase. *J Biol Chem* 267: 23439-23442

Laetsch TW, DuBois SG, Mascarenhas L, Turpin B, Federman N, Albert CM, Nagasubramanian R, Davis JL, Rudzinski E, Feraco AM *et al* (2018) Larotrectinib for paediatric solid tumours

harbouring NTRK gene fusions: phase 1 results from a multicentre, open-label, phase 1/2 study. *Lancet Oncol* 19: 705-714

Lai Y, Liu XH, Zeng Y, Zhang Y, Shen Y, Liu Y (2012) Interleukin-8 induces the endothelial cell migration through the Rac 1/RhoA-p38MAPK pathway. *Eur Rev Med Pharmacol Sci* 16: 630-638

Lawn S, Krishna N, Pisklakova A, Qu X, Fenstermacher DA, Fournier M, Vrionis FD, Tran N, Chan JA, Kenchappa RS *et al* (2015) Neurotrophin signaling via TrkB and TrkC receptors promotes the growth of brain tumor-initiating cells. *J Biol Chem* 290: 3814-3824

Lee FS, Chao MV (2001) Activation of Trk neurotrophin receptors in the absence of neurotrophins. *Proceedings of the National Academy of Sciences of the United States of America* 98: 3555-3560

Lemmon MA, Schlessinger J (2010) Cell signaling by receptor tyrosine kinases. *Cell* 141: 1117-1134

Levi-Montalcini R (1987) The nerve growth factor 35 years later. *Science* 237: 1154-1162

Levi-Montalcini R, Meyer H, Hamburger V (1954) In vitro experiments on the effects of mouse sarcomas 180 and 37 on the spinal and sympathetic ganglia of the chick embryo. *Cancer Res* 14: 49-57

Lois C, Hong EJ, Pease S, Brown EJ, Baltimore D (2002) Germline transmission and tissue-specific expression of transgenes delivered by lentiviral vectors. *Science* 295: 868-872

Ma YH, Mentlein R, Knerlich F, Kruse ML, Mehdorn HM, Held-Feindt J (2008) Expression of stem cell markers in human astrocytomas of different WHO grades. *J Neurooncol* 86: 31-45

Markl B, Hirschbuhl K, Dhillon C (2019) NTRK-Fusions - A new kid on the block. *Pathol Res Pract* 215: 152572

Martin-Zanca D, Hughes SH, Barbacid M (1986) A human oncogene formed by the fusion of truncated tropomyosin and protein tyrosine kinase sequences. *Nature* 319: 743-748

Martin-Zanca D, Oskam R, Mitra G, Copeland T, Barbacid M (1989) Molecular and biochemical characterization of the human trk proto-oncogene. *Molecular and cellular biology* 9: 24-33

McCubrey JA, Steelman LS, Chappell WH, Abrams SL, Wong EW, Chang F, Lehmann B, Terrian DM, Milella M, Tafuri A *et al* (2007) Roles of the Raf/MEK/ERK pathway in cell growth, malignant transformation and drug resistance. *Biochim Biophys Acta* 1773: 1263-1284

Middlemas DS, Lindberg RA, Hunter T (1991) trkB, a neural receptor protein-tyrosine kinase: evidence for a full-length and two truncated receptors. *Molecular and cellular biology* 11: 143-153

Mitra SK, Hanson DA, Schlaepfer DD (2005) Focal adhesion kinase: in command and control of cell motility. *Nat Rev Mol Cell Biol* 6: 56-68

Naegelin Y, Dingsdale H, Sauberli K, Schadelin S, Kappos L, Barde YA (2018) Measuring and Validating the Levels of Brain-Derived Neurotrophic Factor in Human Serum. *eNeuro* 5

Nagappan G, Woo NH, Lu B (2008) Ama"Zinc" Link between TrkB Transactivation and Synaptic Plasticity. *Neuron* 57: 477-479

Nakagawara A (2001) Trk receptor tyrosine kinases: a bridge between cancer and neural development. *Cancer Lett* 169: 107-114

Nakagawara A, Azar CG, Scavarda NJ, Brodeur GM (1994) Expression and function of TRK-B and BDNF in human neuroblastomas. *Molecular and cellular biology* 14: 759-767

Nikoletopoulou V, Lickert H, Frade JM, Rencurel C, Giallonardo P, Zhang L, Bibel M, Barde YA (2010) Neurotrophin receptors TrkA and TrkC cause neuronal death whereas TrkB does not. *Nature* 467: 59-63

Okamura R, Boichard A, Kato S, Sicklick JK, Bazhenova L, Kurzrock R (2018) Analysis of NTRK Alterations in Pan-Cancer Adult and Pediatric Malignancies: Implications for NTRK-Targeted Therapeutics. *JCO Precis Oncol* 2018

Pacenta HL, Macy ME (2018) Entrectinib and other ALK/TRK inhibitors for the treatment of neuroblastoma. *Drug Des Devel Ther* 12: 3549-3561

Parsons JT (2003) Focal adhesion kinase: the first ten years. *J Cell Sci* 116: 1409-1416

Parsons JT, Horwitz AR, Schwartz MA (2010) Cell adhesion: integrating cytoskeletal dynamics and cellular tension. *Nat Rev Mol Cell Biol* 11: 633-643

Passiglia F, Caparica R, Giovannetti E, Giallombardo M, Listi A, Diana P, Cirrincione G, Caglevic C, Raez LE, Russo A *et al* (2016) The potential of neurotrophic tyrosine kinase (NTRK) inhibitors for treating lung cancer. *Expert Opin Investig Drugs* 25: 385-392

Ponten J, Macintyre EH (1968) Long term culture of normal and neoplastic human glia. *Acta Pathol Microbiol Scand* 74: 465-486

Puehringer D, Orel N, Luningschror P, Subramanian N, Herrmann T, Chao MV, Sendtner M (2013) EGF transactivation of Trk receptors regulates the migration of newborn cortical neurons. *Nat Neurosci* 16: 407-415

Pulciani S, Santos E, Lauver AV, Long LK, Aaronson SA, Barbacid M (1982) Oncogenes in solid human tumours. *Nature* 300: 539-542

Rajagopal R, Chao MV (2006) A role for Fyn in Trk receptor transactivation by G-protein-coupled receptor signaling. *Mol Cell Neurosci* 33: 36-46

Rajagopal R, Chen ZY, Lee FS, Chao MV (2004) Transactivation of Trk neurotrophin receptors by G-protein-coupled receptor ligands occurs on intracellular membranes. *J Neurosci* 24: 6650-6658

Rathod R, Havlicek S, Frank N, Blum R, Sendtner M (2012) Laminin induced local axonal translation of beta-actin mRNA is impaired in SMN-deficient motoneurons. *Histochemistry and cell biology* 138: 737-748

Reichert JM, Valge-Archer VE (2007) Development trends for monoclonal antibody cancer therapeutics. *Nat Rev Drug Discov* 6: 349-356

Roberts PJ, Der CJ (2007) Targeting the Raf-MEK-ERK mitogen-activated protein kinase cascade for the treatment of cancer. *Oncogene* 26: 3291-3310

Rose CR, Blum R, Pichler B, Lepier A, Kafitz KW, Konnerth A (2003) Truncated TrkB-T1 mediates neurotrophin-evoked calcium signalling in glia cells. *Nature* 426: 74-78

Rudzinski ER, Lockwood CM, Stohr BA, Vargas SO, Sheridan R, Black JO, Rajaram V, Laetsch TW, Davis JL (2018) Pan-Trk Immunohistochemistry Identifies NTRK Rearrangements in Pediatric Mesenchymal Tumors. *Am J Surg Pathol* 42: 927-935

Sasi M, Vignoli B, Canossa M, Blum R (2017) Neurobiology of local and intercellular BDNF signaling. *Pflügers Archiv : European journal of physiology* 469: 593-610

Scott LJ (2019) Larotrectinib: First Global Approval. *Drugs* 79: 201-206

Shah K, Rossie S (2018) Tale of the Good and the Bad Cdk5: Remodeling of the Actin Cytoskeleton in the Brain. *Mol Neurobiol* 55: 3426-3438

Shawver LK, Slamon D, Ullrich A (2002) Smart drugs: tyrosine kinase inhibitors in cancer therapy. *Cancer Cell* 1: 117-123

Solomon JP, Benayed R, Hechtman JF, Ladanyi M (2019) Identifying patients with NTRK fusion cancer. *Ann Oncol* 30: viii16-viii22

Solomon JP, Hechtman JF (2019) Detection of NTRK Fusions: Merits and Limitations of Current Diagnostic Platforms. *Cancer Res* 79: 3163-3168

Solomon JP, Linkov I, Rosado A, Mullaney K, Rosen EY, Frosina D, Jungbluth AA, Zehir A, Benayed R, Drilon A *et al* (2020) NTRK fusion detection across multiple assays and 33,997 cases: diagnostic implications and pitfalls. *Mod Pathol* 33: 38-46

Stransky N, Cerami E, Schalm S, Kim JL, Lengauer C (2014) The landscape of kinase fusions in cancer. *Nature Communications* 5

Su HP, Rickert K, Burlein C, Narayan K, Bukhtiyarova M, Hurzy DM, Stump CA, Zhang X, Reid J, Krasowska-Zoladek A *et al* (2017) Structural characterization of nonactive site, TrkA-selective kinase inhibitors. *Proceedings of the National Academy of Sciences of the United States of America* 114: E297-E306

Tanaka K, Okugawa Y, Toiyama Y, Inoue Y, Saigusa S, Kawamura M, Araki T, Uchida K, Mohri Y, Kusunoki M (2014) Brain-derived neurotrophic factor (BDNF)-induced tropomyosin-related kinase B (Trk B) signaling is a potential therapeutic target for peritoneal carcinomatosis arising from colorectal cancer. *Plos One* 9: e96410

Tapley P, Lamballe F, Barbacid M (1992) K252a is a selective inhibitor of the tyrosine protein kinase activity of the trk family of oncogenes and neurotrophin receptors. *Oncogene* 7: 371-381

Thoenen H (1995) Neurotrophins and neuronal plasticity. *Science* 270: 593-598

Ultsch MH, Wiesmann C, Simmons LC, Henrich J, Yang M, Reilly D, Bass SH, de Vos AM (1999) Crystal structures of the neurotrophin-binding domain of TrkA, TrkB and TrkC. *J Mol Biol* 290: 149-159

Vaishnavi A, Le AT, Doebele RC (2015) TRKing down an old oncogene in a new era of targeted therapy. *Cancer Discov* 5: 25-34

Wadhwa S, Nag TC, Jindal A, Kushwaha R, Mahapatra AK, Sarkar C (2003) Expression of the neurotrophin receptors Trk A and Trk B in adult human astrocytoma and glioblastoma. *J Biosci* 28: 181-188

Wai DH, Knezevich SR, Lucas T, Jansen B, Kay RJ, Sorensen PH (2000) The ETV6-NTRK3 gene fusion encodes a chimeric protein tyrosine kinase that transforms NIH3T3 cells. *Oncogene* 19: 906-915

Wang T, Wei JJ, Sabatini DM, Lander ES (2014) Genetic screens in human cells using the CRISPR-Cas9 system. *Science* 343: 80-84

Wang X, Prager BC, Wu Q, Kim LJY, Gimple RC, Shi Y, Yang K, Morton AR, Zhou W, Zhu Z *et al* (2018) Reciprocal Signaling between Glioblastoma Stem Cells and Differentiated Tumor Cells Promotes Malignant Progression. *Cell Stem Cell* 22: 514-528 e515

Watson FL, Porcionatto MA, Bhattacharyya A, Stiles CD, Segal RA (1999) TrkA glycosylation regulates receptor localization and activity. *Journal of neurobiology* 39: 323-336

Webb DJ, Donais K, Whitmore LA, Thomas SM, Turner CE, Parsons JT, Horwitz AF (2004) FAK-Src signalling through paxillin, ERK and MLCK regulates adhesion disassembly. *Nat Cell Biol* 6: 154-161

Wehrman T, He X, Raab B, Dukipatti A, Blau H, Garcia KC (2007) Structural and mechanistic insights into nerve growth factor interactions with the TrkA and p75 receptors. *Neuron* 53: 25-38

Westhoff MA, Serrels B, Fincham VJ, Frame MC, Carragher NO (2004) SRC-mediated phosphorylation of focal adhesion kinase couples actin and adhesion dynamics to survival signaling. *Molecular and cellular biology* 24: 8113-8133

Wiese S, Jablonka S, Holtmann B, Orel N, Rajagopal R, Chao MV, Sendtner M (2007) Adenosine receptor A2A-R contributes to motoneuron survival by transactivating the tyrosine kinase receptor TrkB. *Proceedings of the National Academy of Sciences of the United States of America* 104: 17210-17215

Wiesmann C, Ultsch MH, Bass SH, de Vos AM (1999) Crystal structure of nerve growth factor in complex with the ligand-binding domain of the TrkA receptor. *Nature* 401: 184-188

Wu G, Diaz AK, Paugh BS, Rankin SL, Ju B, Li Y, Zhu X, Qu C, Chen X, Zhang J *et al* (2014) The genomic landscape of diffuse intrinsic pontine glioma and pediatric non-brainstem high-grade glioma. *Nat Genet* 46: 444-450

Yamashiro DJ, Liu XG, Lee CP, Nakagawara A, Ikegaki N, McGregor LM, Baylin SB, Brodeur GM (1997) Expression and function of Trk-C in favourable human neuroblastomas. *Eur J Cancer* 33: 2054-2057

Zhang M, Song T, Yang L, Chen R, Wu L, Yang Z, Fang J (2008) Nestin and CD133: valuable stem cell-specific markers for determining clinical outcome of glioma patients. *J Exp Clin Cancer Res* 27: 85

Zufferey R, Nagy D, Mandel RJ, Naldini L, Trono D (1997) Multiply attenuated lentiviral vector achieves efficient gene delivery in vivo. *Nature biotechnology* 15: 871-875

6 Appendix

6.1 List of tables

6.2 List of figures

6.3 Abbreviations

μg	microgram
μl	microliter
μm	micrometer
μM	micromoles
BDNF	brain-derived neurotrophic factor
DNA	deoxyribonucleic acid
dNTP	deoxyribose nucleoside triphosphate
ICD	intracellular domain
mM	millimoles
ng	nanogram
nM	nanomoles
NTRK	Neurotrophin tyrosine receptor kinase
PCR	polymerase chain reaction
RGB	red/green/blue
RNA	ribonucleic acid
RT	reverse transcriptase
TKD	Tyrosine receptor kinase domain
TKI	Tyrosine kinase inhibitor
Trk A/B/C	Tropomysin receptor kinase A/B/C
RTK	Receptor tyrosine kinase

6.4 Affidavit / *Eidesstattliche Erklärung gemäß ASPO vom 05.08. 2009 § 23 Abs. 10*

<div align="center">Affidavit</div>

I hereby confirm that my thesis entitled **"Intracellular self-activation of the TrkB kinase domain causes FAK phosphorylation and disrupts actin filopodia dynamics"** is the result of my own work. I did not receive any help or support from commercial consultants. All sources and/or and materials applied are listed and specified in the thesis.

Furthermore, I confirm that this thesis has not yet been submitted as part of another examination process neither in identical nor in similar form.

Place, Date	Signature

<div align="center">Eidesstattliche Erklärung</div>

Hiermit erkläre ich an Eides statt, dass ich die Dissertation mit dem Titel **„Intrazelluläre Selbstaktivierung der TrkB Kinase induziert FAK Phosphorylierung und verändert die Dynamik von Aktinfilopodien"** eigenständig, d.h. insbesondere selbstständig und ohne Hilfe eines kommerziellen Promotionspartners angefertigt und keine anderen als die von mir angegebenen Quellen und Hilfsmittel verwendet zu haben.

Ich erkläre außerdem, dass die Dissertation weder in gleicher noch in ähnlicher Form bereits in einem anderen Prüfungsverfahren vorgelegen hat.

Ort, Datum	Unterschrift

6.5 Acknowledgments

First and foremost, my heartfelt gratitude goes to my supervisor, **PD Dr. Robert Blum**, who provided me with the opportunity to work on this fascinating project. Thank you for your patience, your always reassuring and enthusiastic attitude, invaluable guidance and fruitful suggestions during our endless discussions and meetings. Thank you for letting me follow my passion for cancer research, something that has blossomed during the course of my doctoral work. Your constant support to let me explore different directions, will forever give me hope and strength in my future endeavors. I hope I will be lucky again in the future to have such an encouraging boss. Thank you also for all those insightful stories on history, politics, theatre and art. You are a true mentor, in every sense of the word.

Next, I would like to thank **Prof. Svenja Meierjohann** and **PD Dr. Kurt Bommert** for their support as members of my thesis committee. Thank you for your active participation in our annual meetings, for your feedback on my progress, and for providing useful insights. Thank you Kurt, for giving me your cas9-Tet-pCW plasmid, this helped immensely as we finally had a great tool to express the TrkB mutants under controlled expression levels.

A special thank you to my project collaborators, **Prof. Carmen Villmann**, **Dr. Jochen Kuper**, **Camelia Monoranu**, **Gisela Wohlleben** and **Dr. Bülent Polat**. Thank you for helping out with your technical expertise, profound knowledge and willingness to share cell lines and patient tissues. This project would not have come this far without your support. Thank you to **Prof. Dr. Michael Sendtner** for graciously accepting me into the institute and allowing me to see my PhD to completion. Thank you **Hilde** for packaging my innumerable lentiviral vectors.

A big thank you to AG Blum, **Michi**, **Corinna**, **Cora**, **Manju** and **Dennis,** thank you for always patiently answering my endless queries, helping out in the lab and for always making me feel like I belong. Thanks to **Elena**, **Gülberk**, **Annemarie**, **Niels** and Michi, for all your help with cloning and for making the lab space such an enjoyable work environment. I miss our epic AG Blum game evenings and dinners in the city. Dennis, I hope you take all my drunk stories to the grave and I hope everyone is as lucky as me to find such a supportive lab mate turned friend for life. Thanks to my friends at the institute, **Nina**, **Hanaa**, **Patrick**, **Orlando**, **Simon**, **Thomas**, and **Elisabete**. I will always remember all our discussions in the kitchen, at the BBQ parties and the monthly beers, where I laughed till I had tears in my eyes. Nina, I look forward to many more road trip adventures with you. Thank you all for proving that science can also be fun.

The **Graduate School of Life Sciences** team, including **Dr. Stephan Schröder-Köhne**, **Dr. Gabriele Blum-Oehler**, **Dr. Franz-Xaver Kober**, **Jennifer Heilig**, **Katrin Lichosik**, **Felizitas Berninger**, **Sebastian Michel**, **Juliane Fiebig** and **Mona Müller**, has been instrumental in running and coordinating many of the aspects of the doctoral program. Many thanks to Gabi, for always obliging me despite her very busy schedule. Thank you to each of you for all your efforts in helping to make my doctoral phase a smooth, fulfilling, and enriching one. Thank you also for the financial support provided by the GSLS through my doctoral fellowship which gave me the opportunity to attend several conferences and pursue side projects.

To my family in Germany, **Prat**, **Alok**, **Cheek**, **Ayesha**, and **Yasir**, for always feeding this forever hungry human and for being with me, every step of the way, in this difficult yet fulfilling journey. **Andrea**, **Khusbhu** and **Vini**, many thanks for inviting me to all those super fun house parties and festivities. To my friends back home who are like my sisters, **Deborah**, **Uma**, **Sayali** and **Asawari**, thank you for being by my side for the last 10 years. Not to forget my IBB family, **Snehal**, **Monika**, **Gauri**, **Shalaka** and **Urvashi**, for being strong, independent women and for always inspiring me.

Lastly, none of this could have been possible without the unconditional love and endless support from my family. To my father, **Ranjan Gupta**, a scientist himself, for always guiding me on the right path. To my mother, **Vivien Gupta**, for letting me pursue all my dreams and for all those life lessons along the way. To my brother, **Reuben**, for always having my back since the day I landed on this planet. To **Dudu** for being a true feminist and the best grandpa a girl could have wished for, I still miss you and think of you every day. To **Dumma** and **Maja**, the strongest and most evergreen ladies I know. To my next closest family, the Das family in Sydney, **Sujata**, **Ujjal**, **Aveek** and **Rohan**, for always believing in me and for showing me glimpses of the world down under, I cherish memories of all our adventurous trips. To my **Saša**, for your patience, support and care and for teaching me to love again, piece of my heart will forever belong to you. Thank you all, for always being supportive, even on those bleak days when I didn't think I would make it to this point. I'm lucky to have you all.

ROHINI GUPTA

PHD STUDENT | UNIVERSITY HOSPITAL WÜRZBURG, GERMANY

CURRENT POSITION

**PhD student – GSLS Fellow
April 2016 - present**
(expected **Dr.rer.nat**: Jan 2021)
Institute of Clinical
Neurobiology, University
Hospital Würzburg, Germany
Würzburg, Germany

Thesis – Intracellular self-activation of the TrkB kinase domain causes FAK phosphorylation and disrupts actin filopodia dynamics

Topic – Neurobiology and neuro-oncology

CONTACT

Weingarten Str. 21,
97072 Würzburg, Germany
DoB – 01.09.1990 – Pune, India
Tel: +49 (0)931 201 44031
(office)
Mob: +49 1520 9018 426
gupta.rohini90@gmail.com
E_Gupta_R@ukw.de

WORK EXPERIENCE

PROJECT INTERN (Industry)
Syngene Int Ltd, Bangalore, India
Feb – Aug 2015
R&D Dept. – cloning, protein purification, ELISA.

EDUCATION

5 YEAR INTEGRATED **MASTER'S IN BIOTECHNOLOGY**
Institute of Bioinformatics and Biotechnology (IBB), University of Pune, Pune, India
Jul 2009 – May 2014
CGPA – 5.18/6.00 (**86.33%**)

AWARDS

- Poster prize (1st prize – 1000€), 12th -13th Apr 2019, IZKF Würzburg, Retreat at Kloster Banz, Germany
- GSLS PhD Fellowship, Apr 2016 – Mar 2019, Graduate School of Life Sciences (GSLS), University of Würzburg, Würzburg, Germany
- Indian Academy of Sciences (IAS) Summer Research Fellow, Aug – Sep 2014, IISER, Kolkata, India

RESEARCH EXPERIENCE

- **IAS Summer Fellowship** – 'Infectivity of mouse hepatitis virus in microglial cell line in vitro' (Aug 2014 – Sep 2014)
  Advisor: Dr. Jayasri Das Sarma, IISER, Kolkata, India
- **Master's Thesis** – 'Effect of Fragile X Mental Retardation Protein (FMRP) on the steady state levels of micro RNAs and regulation of protein synthesis' (Dec 2013 – May 2014)
  Advisor: Dr. Ravi S Muddashetty, NCBS-InStem, Bengaluru, India

LANGUAGES/SKILLS

German B1 Goethe-Zertifikat – 87.75% (Feb 2016) - Goethe Institute, Pune, India.
English native speaker;
Marathi, Hindi and **Bengali** native speaker.

Computer: MS Office, Fiji-ImageJ, Adobe Photoshop, GraphPad, OriginPro, Typo3, HTML, C+

COMMITTEES

Doctoral Researchers Council, GSLS, University of Würzburg, Würzburg, Germany
Jun 2018 – Aug 2019
Elected member of a team of doctoral student representatives – organising various scientific and non-scientific events for the GSLS

13th International GSLS Student Symposium - Eureka, Würzburg, Germany
10th-11th Oct 2018
Organizing committee (Homepage team, Poster session team)

12th GSLS Retreat, Jugendherberge Bad Kissingen, Germany
28th-29th Sep 2018
Organizing team

- **Bachelor's Thesis** – 'Evaluation of copra meal as a potential feedstock for production of biodiesel by *Aspergillus terreus IBB M1*' (Jun 2011 – Jul 2012)
  Advisor: Prof. Ameeta RaviKumar, IBB, University of Pune, India

EXPERTISE

SDS PAGE, Western Blot analysis, Immuno-cytochemistry, Immuno-precipitation, primary and secondary cell culture, analyzing human glioblastoma, confocal microscopy, live cell imaging, site directed mutagenesis, qPCR, migration assays, RNA and DNA isolation, PCR, primer designing, lentiviral plasmid cloning in bacteria, lentiviral transfection and transduction, ELISA, Luciferase assay, Single cell oil extraction, trans-esterification, thin layer chromatography, submerged and solid state fermentation.
FELASA-B: Lab-Animal training course certified, Oct 2017, Humboldt Universität, Berlin, Germany

CONFERENCES

Poster presentations (of PhD topic) at –
- 50th Society for Neuroscience (SfN), Neuroscience 2019, Chicago, USA 19th-23rd Oct 2019
- 11th Federation of European Neuroscience Societies (FENS) , Forum of Neuroscience, Berlin, Germany 7th-11th Jul 2018
- 12th Göttingen Meeting of the German Neuroscience Society (NWG), Göttingen, Germany 22nd-25th Mar 2017
- Eureka – 11th and 12th International GSLS Student Symposium, Würzburg, Germany 12th-13th Oct 2016 and 11th-12th Oct 2017

WORKSHOPS

- **Project Management** – Dr. Detlef Bittner – 24th Sep 2019, Würzburg, Germany
  Definition of project and project management; Phase model project management; Project structure; Time and resource planning; Project documentation; Communication plan; Monitoring and controlling projects
- **Introduction to Biotech Industries** – Dr. Christian Grote-Westrick – 22nd Nov 2018, Würzburg, Germany
  Good Manufacturing Practice (EU-GMP); Regulatory affairs; Technical documentation for medical devices; Quality control and

HOBBIES

Adventure sports (skydiving, bungee jumping, scuba diving), swimming, dancing, globe-trotting and reading fiction.

REFERENCE

PD Dr. Robert Blum
Principal Investigator,
Institut für Klinische
Neurobiologie,
Universitätsklinikum Würzburg
Versbacher Str. 5, E4,
97078 Würzburg, Germany
Tel: +49 (0)931 201 44031
(office)
Blum_R@ukw.de

assurance; Risk management, Lean management; Contract manufacturing; Audit Simulation.

- **Analyzing your Market Potential as a Scientist** – Robert Zaal – 27th Mar 2018, Würzburg, Germany
  Personal SWOT analysis; Analyzing and marketing your skills as a scientist in Industry.

- **GSLS Mentoring Life Sciences Program** – Jun 2018 – Jul 2019, Würzburg, Germany
  Women in Academia and Industry; Career development; One-on-one Mentor – Mentee relationship; CV and career counselling. *Mentor:* Dr. Petra Arndt, GCP Inspector, Paul-Ehrlich-Institut, Frankfurt am Main, Germany

PUBLICATIONS

Constitutively active TrkB kinase signalling reduces actin filopodia dynamics and cell migration
bioRxiv preprint (first posted online Sep 12, 2020)
https://doi.org/10.1101/2020.09.11.292565
Rohini Gupta, Melanie Bauer, Gisela Wohlleben, Vanessa Luzak, Vanessa Wegat, Dennis Segebarth, Elena Bady, Georg Langlhofer, Britta Wachter, Steven Havlicek, Patrick Lüningschrör, Carmen Villmann, Bülent Polat, Camelia M. Monoranu, Jochen Kuper, Robert Blum

On the objectivity, reliability, and validity of deep learning enabled bioimage analyses
eLife 2020, (published online - Oct 19, 2020)
https://doi.org/10.7554/eLife.59780
Dennis Segebarth, Matthias Griebel, Nikolai Stein, Cora R. von Collenberg, Corinna Martin, Dominik Fiedler, Lucas B. Comeras, Anupam Sah, Victoria Schoeffler, Theresa Lüffe, Alexander Dürr, **Rohini Gupta**, Manju Sasi, Christina Lillesaar, Maren D. Lange, Ramon O. Tasan, Nicolas Singewald, Hans-Christian Pape, Christoph M. Flath, Robert Blum

Fungal production of single cell oil using untreated copra cake and evaluation of its fuel properties for biodiesel
J. Microbiol. Biotechnol.2014, (published online - Oct 23, 2014)
https://doi.org/10.4014/jmb.1407.07074
Mahesh Khot, **Rohini Gupta**, Kadambari Barve, Smita Zinjarde, Sanjay Govindwar, Ameeta RaviKumar